MODEL OF WOVEN ELECTRODE DESIGNED FOR LONG-TERM CAPTURE OF ELECTROCARDIOGRAPH

by

Peter Brehm

B.S. Electrical Engineering, University of Colorado Boulder, 2012

M.S. Electrical Engineering, University of Colorado Boulder, 2017

A thesis submitted to the

Faculty of the Graduate School of the

University of Colorado in partial fulfillment

of the requirement for the degree of

Master of Science

Department of Aerospace Engineering Sciences

2022

Committee Members:

Anderson, Allison

Clark, Torin

Nabity, James

Brehm, Peter (M.S. Aerospace Engineering Department)

Model of Woven Electrode Designed for Long-Term Capture of Electrocardiograph

Thesis directed by Professor Dr. Allison Anderson

Abstract

There is a growing demand to continuously monitor the ECG over longer periods of time. This demand comes from all areas of life; from tracking sickness for improved treatment and prevention to optimizing performance for athletes and workers in dangerous environments. To meet this demand, wearable devices are designed to monitor health status continuously and autonomously. This is called wellness monitoring, and it has been shown to improve quality of life by reducing reliance on reactive treatments. When wellness monitoring is applied to ECG systems, the existing solutions have a variety of limitations oriented around the limits of traditional electrodes. Conductive textile electrodes offer an alternative to traditional electrodes but they come with their own challenges. One of the key challenges with textile electrodes is that it is not well understood how a given set of manufacturing parameters influence the ECG measurement. The current ways of relating manufacturing parameters to ECG measurements rely on physical trial-and-error methodologies which inhibit design cycle iterations.

This research presents a novel model of the ECG system, which ties the electrical behavior of woven textile electrodes to their manufacturing parameters. Specifically, this research investigates how the yarn type, weave pattern, and patch area of a woven electrode are related to the circuit parameters in the skin-electrode interface model. A parameterized model of the ECG system was constructed which depends on the circuit parameter of the skin-electrode interface as well as the circuit parameters of the associated circuitry. Through this relationship, the circuit parameters corresponding to woven electrodes were fit using an optimizer that minimizes the differences between a simulated and measured waveform.

The manufacturing parameters for 16 sets of woven electrodes were related to their electrical behavior. A yarn type with lower resistivity creates an electrode with lower skin-electrode impedance but higher variance. The Silver yarn electrodes have a variance of as much as 12MΩ. The larger the surface area of a woven electrode patch, the larger the capacitance, and the lower the impedance. The Area type electrodes increased in area from 0.5 in^2 up to 5 in^2 and their impedance decreased by 5MΩ, with one exception. The performance of the model was validated through a Leave One Out Cross Validation scheme which demonstrated a good model fit across 6 human subjects for 2 minutes of data collection.

This equivalent model demonstrated for the first time the relationship between woven electrode manufacturing parameters and their electrical circuit parameters. By using this model, woven electrodes can be better designed for optimal ECG capture capability. Furthermore, ECG circuitry can be customized to accommodate the variation between different types of electrodes. This work builds from previous work on textile sensor development and enables future work to target even better textile sensor design.

Dedications

This work is dedicated to my father, Steven Brehm, as well as the millions of people worldwide who have been affected by cardiovascular disease. My father has struggled with cardiovascular disease for over a decade and a half and continues the struggle today. I learned as a teenager when my father needed triple-bypass surgery, the complications associated with reactively treating a heart attack. Aside from the physical toll on the body, and the unending medical bills, there is a significant emotional cost on the individual and their loved ones. The concept of proactive healthcare has the potential to extend the quality of life for countless people. My father has endured despite this illness, and it is my hope that someday healthcare technology can prevent situations like this from occurring.

Acknowledgments

I have been supported by many people throughout this Master's program. I would like to acknowledge my wife Danielle, my Parents and friends and last but not least, my advisor Allison Anderson.

Danielle has been with me throughout this process and helped emotionally by keeping my morale high and my motivation strong. She has supported me in little ways like picking up extra chores around the house, and big ways like being a sounding board for my crazy ideas. Thank you, Dani, for always being there for me!

My parents and friends have supported me by being patient and understanding. I work full time and when I decided to go back to school, my time to socialize and connect with others was dramatically reduced. They were always willing to listen and offer an outside perspective. Thank you!

Professor Dr. Allison Anderson, thank you for accepting me as your grad student and guiding me through the Master's program. Your passion for human space flight is contagious and I am so grateful to have you as a mentor. I appreciate your patience and dedication to keeping me focused despite my bad habits. Thank you for your continued support, your positive attitude, and your wealth of advice.

Contents

Tables

Figures

I. Introduction and Motivation

The measurement of the body's physiological status through biometrics is a critical healthcare function, ranging from monitoring the sick and elderly, to tracking the performance of astronauts and athletes. Specifically, the electrocardiograph (ECG), which measures electrical impulses from the heart, is one of the most well-used methods today of capturing biometric activity to indicate health status. For example, the ECG is instrumental in monitoring cardiovascular disease (CVD) (Y Du 2017). CVD was the number one cause of death in the United States in 2019 and 2020 and was the single leading disease worldwide (Y Du 2017; Kochanek, Xu, and Arias 2020). Clinically, ECG signals are used to identify cardiac abnormalities and diagnose potential heart problems thus preventing more serious health issues from arising (John G. et al. 2010).

Since the first human ECG measurement in 1895, biometric capture technology has evolved dramatically. While modern healthcare technology is continually finding new ways to diagnose and monitor the health and status of individuals, many chronic diseases are still difficult or impossible to cure. Proactive healthcare through *wellness monitoring* may be an effective way to prevent these challenging ailments. Wellness monitoring is the concept of using wearable devices coupled with automated data analysis to passively and continuously monitor individualized health status over time (Giovanni 2021). This enables proactive intervention which can prevent costly or detrimental healthcare problems from developing. In the above example, CVDs are among the leading causes of prolonged disability and early mortality, which makes the timely diagnosis of early symptoms a recurrent critical issue (Nikolova-Hadzhigenova 2019). Early diagnosis and prevention of CVD enabled by long-term monitoring can not only save lives but also carries

significant financial benefits as an alternative to costly detection and treatment (Y Du 2017).

Monitoring the heart continuously has additional utility beyond addressing chronic illnesses. The human body's normal heart rate is impacted by sleep, emotion, exercise, fever, and many other stimuli (John G. et al. 2010; Arquilla, Webb, and Anderson, n.d.; Arquilla 2021b; Huff et al. 2022; Cobarrubias 2020). The list of applications for heart data is ever growing. For example, athletes regularly monitor their own heart rate data to track their health and performance during exercise (Cobarrubias 2020). These applications are an extension of wellness monitoring into human performance optimization. Another application of continuously monitor ECG is psychophysiological monitoring which connects metrics such as heart rate variability (HRV) to psychological state (Arquilla 2021b; 2021a). This can be as simple as diagnosing sleep related issues such as drowsiness or sleep apnea (Löfhede, Seoane, and Thordstein 2012) and can even be leveraged to monitor behavioral health objectively and continuously when coupled with advanced psychological state detection algorithms (Arquilla 2021a; Arquilla, Webb, and Anderson, n.d.).

One key feature of assessing ECG in these applications is that the long-term capture of physiological data occurs outside the hospital setting, which creates a demand for personal health monitoring systems. With the miniaturization of electronics and improvements in affordability, personal health monitoring is becoming more accessible and ubiquitous (An and Stylios 2018; Heikenfeld et al. 2018). Wearable devices are one form of personal health monitoring technology which has the potential to meet this demand and not only increase user convenience but also decrease the dependence on large and bulky hospital equipment (Yokus and Jur 2016). Wearable devices reduce high hospitalization expenses and improve

the quality of life for those who have chronic diseases and need to be monitored continuously (Yokus and Jur 2016).

One of the key challenges for monitoring the heart with wearable devices is the inability to obtain the full ECG waveform. Fundamentally, the ECG is a graph of the voltage generated by the heart with each contractile action of segments of cardiac muscle (John G. et al. 2010). This is important because the ECG waveform provides insight into the electrical status of the heart's state. The electrical impulses of the ECG correspond to the different chambers of the heart muscle. By noting changes in the waveform, it is possible to confidently infer what is occurring in the heart's nerves and muscle tissue. These elements of the wave form have additional utility in human performance optimization and psychophysiology. Today there are a growing number of commercial devices available to the general public such as Fitbits and Apple watches which provide limited cardiovascular performance data. Critically, these devices largely utilize photoplethysmography, a technique which observes blood flow in the skin, to detect heart rate peaks and subsequently to infer general heart status (Heikenfeld et al. 2018; Taji et al. 2014; Arquilla, Webb, and Anderson 2021). This method does not measure cardiac electrical signals and therefore does not capture the complete ECG waveform which contains valuable smaller peak information (Taji et al. 2014). As such, many HRV metrics which depend on distortions in the ECG waveform or subject-specific assessment of cardiac status cannot be calculated since it only measures the largest peak of the wave. Subsequently the reliance on this method limits the identification of pathologies from those which would be revealed via the full ECG waveform (Arquilla, Webb, and Anderson, n.d.).

Providing information of the full ECG waveform during chronic daily use outside of a clinical setting has been a technical challenge for implementing cardiac wellness monitoring (Arquilla, Webb, and Anderson 2021; Schauss 2022). The

challenge is associated with the traditional method of collecting the ECG waveform. Traditionally the ECG waveform is captured by applying adhesive electrodes with electrolyte gel to the skin surface. Those electrodes are connected to electrical circuitry which then captures and records the bioelectric signals generated by the body. Modern systems that capture ECG continuously rely on this sensor technology, despite the fact that it was not developed for persistent wearable formats (Bystricky et al. 2016). The Holter monitor, shown in Figure 1, is the current gold-standard device for clinically relevant monitoring. It is a battery-operated wearable device that uses traditional adhesive gel electrodes. It is worn during day-to-day operation because some specific cardiac events are difficult to observe in the clinical setting. Certain events such as arrhythmias (abnormal heart rhythms) may occur infrequently or only under certain conditions, such as stress or activity. These monitors are usually accompanied by instructions to keep a log of activity and symptoms during the observation period. The information captured by the monitor and the log will then be reviewed by a doctor afterwards. The results can be used to determine if an abnormal heart condition is present or if a treatment for a known condition is working properly. The key challenge of this method, is that the adhesive gel electrodes have several limitations; they must be applied fresh on specific locations, are consumable, dry out over time, and can irritate the skin with chronic use [2], (Taji et al. 2014). Every reapplication of adhesive electrodes, has the potential to introduce placement and measurement errors which reduces the diagnostic capability of the ECG. Some of these characteristics are tolerable in settings where a fresh supply of replacement electrodes can be properly reapplied, but monitoring for long periods outside of those environments is often not feasible with traditional electrodes (Yoo and Hoi-Jun Yoo 2011).

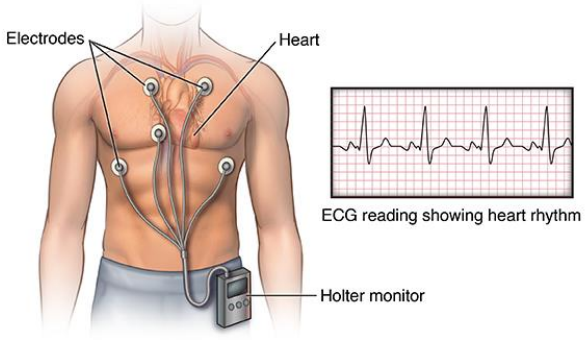

Figure 1: Holter monitor on the body with corresponding ECG waveform reading

One such application of key interest is in human spaceflight, where long term monitoring of the complete ECG waveforms is used to comprehensively monitor astronaut health (Huff et al. 2022). During Extravehicular Activities (EVAs) in particular, when astronauts are under severe physical and mental stress, monitoring the ECG waveform is used both for research and for risk mitigation (Johnston, Dietlein, and Berry 1975). During the Apollo missions a bioinstrumentation system was used to record the ECG of the astronauts (Johnston, Dietlein, and Berry 1975). According to the *Biomedical Results of Apollo* report, the electrode harness originally utilized adhesive taped Ag/AgCl electrodes filled with electrolyte paste. Several changes were made to the harness during the Apollo Program as a result of inflight problems, testing and operational changes. The electrode attachment technique was designed to maintain long-term body contact but attachment was difficult to maintain without discomfort and skin damage (Johnston, Dietlein, and Berry 1975). Despite the challenges with the ECG, they were able to capture arrhythmias of Apollo astronauts (Anzai, Frey, and Nogami 2014). As a specific case during Apollo 15, the waveform of astronaut James Irwin was observed to have bigeminal premature ventricular contraction (PVCs) and atrial premature contractions (APCs), which is believed to be the result of a deficiency in potassium electrolytes due to dehydration from fluid loss and over exertion (Johnston, Dietlein, and Berry 1975; Anzai, Frey, and Nogami 2014). This

observation would not have been possible with a modern blood flow monitor, since the shape of the waveform, not just the peak timing, had changed. Since the Apollo era, atrial and ventricular premature contractions, short-duration atrial fibrillation, and non-sustained ventricular tachycardia have all been reported during spaceflight missions (Huff et al. 2022; Anzai, Frey, and Nogami 2014).

ECG monitoring has been included as part of the autogenic feedback training exercise (AFTE) from NASA Ames Research center as a method of biofeedback to aid in autogenic therapy for spaceflight stress (Arquilla et al. 2020). Both the hazardous environment of space and the heavy tasking placed upon astronauts means that their body is under tremendous chronic stress (Arquilla 2021a; Anzai, Frey, and Nogami 2014). However full-time monitoring from ground support teams is not always be possible, especially during the communication constraints of long-duration or deep space missions. Furthermore, measurements at prescribed intervals allow for opportunities to miss potential cardiac events. Despite selecting for healthy participants, monitoring the heart health of astronauts continuously ensures wellness and prevents illness from arising during a mission. Additionally utilizing the ECG continuously would improve our understanding of the human bodies adaptation in deep space which is valuable for scientific research (Anzai, Frey, and Nogami 2014). In long-term spaceflight operations, traditional disposable electrodes are not a feasible option, due to the high cost of launch masses, limited volume allocated for consumables, and limited astronaut time for tasking. As an estimate for using the traditional electrodes on a long-duration mission, assuming a crew of 5, on a 16-month trip to Mars, consuming three ECG electrodes per day per crew member; the required added launch mass is approximately 41kg from 8200 disposable adhesive electrodes. This also assumes the shelf life for traditional ECG electrodes is at least 16 months.

To address these needs for long term ECG monitoring, novel sensors are currently being develop which improve upon the shortcomings of the traditional adhesive sensors. Conductive textile electrodes are one relatively new technology of interest (Paradiso and De Rossi 2006) and in this research *woven textile electrodes* specifically are presented as a potential solution. Textile electrodes are usually made of conductive yarns by weaving, knitting or embroidering processes; or by coating non-conductive fabrics with conductive polymers (An and Stylios 2018). The do not use gel electrolyte thus they are reusable, do not "dry out" or degrade over time, and can be integrated into larger garments (Arquilla, Webb, and Anderson 2020a). Additionally, they do not use adhesive to adhere to the body, ensuring they do not irritate the skin on remove and reapplication (Bystricky et al. 2016). Textile electrodes are more biocompatible, comfortable, and convenient to wear for long-durations than adhesive electrodes. These benefits though, are also their primary challenge. Without a gel electrolyte they have higher skin impedance and without adhesive they are more susceptible to motion related noise. Textile electrodes have the potential to fill the gaps left by other solutions by being a long-duration hands-off solutions without recurring consumable mass (Arquilla, Webb, and Anderson 2020a) but they do not come without drawbacks.

While conductive textiles are appealing in many regards, there is a limited understanding of how to optimize performance to overcome their drawbacks. Characterizing the higher impedance of the skin interface of conductive textiles has been difficult. This is because there are many factors which contribute to impedance beyond the electrode's physical characteristics, such as human subject characteristics, as well as fit and placement (Cobarrubias 2020). Typically, textile electrodes are evaluated through iterative fabrication and testing cycles (Schauss 2022). This is because it is unclear which manufacturing parameters correspond to a textile's electrical behavior and no predictive comprehensive model exists. More

precisely, for a given set of textile electrodes their electrical properties are unknown until measuring them after they have already been manufactured. This repetitive fabrication methodology is inefficient and limits their development. In order to use textile electrodes for chronic ECG applications, it is necessary to obtain a better understanding of their electrical behavior and how it relates to design and manufacturing (Taji et al. 2014). An equivalent model which relates the electrical behavior of textile electrodes to the manufacturing parameters would provide this understanding and would be instrumental in designing better integrated solutions for wellness monitoring. While there does exist a skin-electrode interface model from literature, it is used to generally describe the electrical behavior of electrodes on skin using classical circuit parameters (Medrano et al. 2007). No prior work has related the interface model to textile electrode manufacturing design parameters.

When approaching healthcare from the proactive perspective of wellness monitoring, the demand for continuously monitoring the full ECG waveform is apparent. The introduction of wearable technology solutions combine today's advances in electronics and communication technology with innovative cardiac recording capabilities resulting in a giant leap in the development of ambulatory monitoring (Nikolova-Hadzhigenova 2019). Commercially available wearable devices are functional, but they fall short by failing to capture the full ECG waveform. The traditional method of capturing the full ECG does not work well in continuous applications outside the clinical setting. Textile electrodes have the potential to capture the full ECG waveform for long periods of time while being low profile, consistent, comfortable, and reusable. In order to realize this potential and design these electrodes consistently, a generalized equivalent model is needed to characterize their behavior.

Objective

The engineering objective of this paper is to close a development gap for manufacturing textile electrodes by providing an *equivalent model*. Generally speaking, an equivalent model is a mathematical representation of a system which describes how the system will behave for a given set of conditions and inputs. In this case the equivalent model is a transfer function which describes the ECG system and the conditions are the various types of electrodes determined by their design parameters. This research builds a model which simulates woven electrode behavior, by relating electrical signal generated internal to the body, to the electrical signal measured by the ECG system. The ECG system contains the manufacturing design parameters of the electrodes described in terms of their skin-electrode interface circuit parameters. The model describes how the shape and amplitude of an ECG waveform changes when captured with a specific electrode. This model ties the ECG waveform to the manufacturing design parameters enabling faster optimization of long-term usage textile electrode designs.

After completing the engineering objective two hypotheses will be investigated.

- Hypothesis 1: The traditional skin-electrode interface model can describe the electrical behavior of woven textile electrodes
- Hypothesis 2: The circuit parameters of the skin-electrode interface model can be related to the manufacturing parameters of woven textile electrodes.

For hypothesis 1, the skin-electrode interface model is a circuit model described in Figure 6 with parameterized circuit elements, that describes how an electrical signal travels across the skin and into the ECG device. The "behavior of an electrode" refers to how the shape and amplitude of an ECG waveform changes when captured with that specific electrode relative to another electrode. This hypothesis investigates if the traditional skin-electrode model is sufficient to describe the interface or if a new circuit architecture is be needed. For hypothesis 2 the manufacturing design parameters refer specifically to yarn type, weave pattern,

and surface area. This hypothesis investigates the relationship between the circuit parameters of the skin-electrode interface model and the manufacturing parameters of woven electrodes. To investigate this parameter space, woven electrodes were previously manufactured by Dr. Katya Arquilla (Arquilla 2021b; Arquilla, Webb, and Anderson 2021; 2020a). The electrodes were used by Dr. Arquilla to collect human subject data (Arquilla 2021b; Arquilla, Webb, and Anderson 2021; 2020a). This dataset provides the base content which is used to fit parameters in the equivalent model.

In this thesis, a parametric model is built using measured ECG waveforms from a large set of woven electrode types, spanning several manufacturing parameters. Once the engineering objective is complete the electrical parameters, which have been found for a specific set of woven electrodes, can be related to the manufacturing parameters of woven textiles in general. This relation would aid in the design and manufacturing of future conductive textile electrodes for ECG devices and long-term monitoring solutions.

Chapter II will review the existing literature on the ECG and textile electrodes. A description is given of the ECG waveform and how it is measured. The analog circuitry of the ECG system is described at the functional level. Then the existing traditional adhesive electrodes are described and compared against the novel woven textile electrodes. The parametric skin-electrode interface model is described. Finally, a table which provides a comprehensive comparison between textile and traditional electrodes is provided summarizing the discussion of chapter 2.

Chapter III will build a parameterized transfer function of the full ECG system. The simplifying assumptions are stated and the overall methodology is described. The specific parameters for an adhesive electrode are collected from literature, and used to compute the in-body waveforms for all 10 subjects. A parametric transfer function of the ECG system is used to simulate the ECG waveform for a specific

textile. The circuit parameters corresponding to each electrode are numerically fit by comparing the measured and simulated waveforms across subjects.

Chapter IV contains the results, which will look at the relationship between the specific circuit parameters of the fit transfer function model and the corresponding manufacturing parameters of the unique textile electrodes. A description of the validation and the results of the parameter fit are presented here. The results describe the electrical parameters of electrode sets, and a comparison of the in-body waveform and simulated waveform used per subject.

Chapter V contains the discussion and conclusion. The discussion section will describe how well the electrical parameters of the model transform an input waveform into an output waveform. The discussion is also where the correlation between electrical and manufacturing parameters occurs and which parameters of the model are most influential for designing future textile electrodes. The concluding remarks provide guidance for the next steps in designing woven textile electrodes and suggestions and observations regarding improvements to the model.

II. Literature Review

This chapter reviews the existing literature associated with the ECG waveform, the circuitry that captures it and specifically the electrodes that contact the skin. The properties of traditional adhesive electrodes are described and compared against the properties of conductive textile electrodes. The woven textile electrodes currently under investigation are included in the literature review comparison. The standard skin-electrode interface model is reviewed, as well as previous methods for modeling the ECG system as a transfer function. A method of determining the values of the components in the skin-electrode interface model. Finally, a summary table is provided which compares the pros and cons of the two electrode types side-by-side.

The Electrocardiograph

In 1895 Willem Einthoven invented the first practical electrocardiograph and later received the Nobel prize for his work. The ECG device has seen many iterations and optimizations but fundamentally the electrophysiological processes that was used then is the same as what is used today. The human body biologically generates electrical signals called biopotentials as a result of electrochemical activity of excitable cells (John G. et al. 2010). The ECG describes the electrical signals specifically across the heart muscle as they periodically vary over time (Y Du 2017; John G. et al. 2010). This paper focuses mainly on the electrodes used to capture the ECG waveform so a brief description of the underlying mechanisms responsible for the ECG and the shape of the ECG waveform is presented here.

The ECG waveform is a graph of voltage versus time describing the electrical depolarization and repolarization of specific chambers of the heart during the cardiac cycle (Tereshchenko and Josephson 2015). The electrical impulses, also known as action potentials, are initially generated by pace making nerve cells [14]. These impulses travel across the heart along the His-Purkinje nerve fibers causing the adjacent muscle fibers to contract (John G. et al. 2010; Tereshchenko and

Josephson 2015). The summation of all the electrical activity in the heart at any given time can be approximately represented by an equivalent electric dipole at the center of the heart [6]. This dipole moment is defined by a vector quantity containing the overall magnitude and direction of the electrical charges within the heart at a specific instant. As the heart beats the overall electric field changes thereby causing a change in the magnitude and orientation of the equivalent dipole vector. By simplifying the complex electrophysiology of the heart into a single dipole vector, the status of the heart can be quantifiably characterized [6]. The electric potentials at the heart then travel outwards through the conductive tissues and salty extracellular fluids of the thoracic cavity, to the surface layers of the skin where it then is transduced into electrical current by an electrode [14].

There are 5 main components to an ECG waveform annotated by the order they appear chronologically with the letters "PQRST" (Hurst 1998). The P wave is the leading peak which represents the depolarization of the atrial chamber of the heart (Gangemi 1995). The Q R and S peaks form a single complex which contains the most visually prominent peak, the R-peak. The QRS complex is a combination of the Q trough, R-peak, and S trough. This wave corresponds to the depolarization of the ventricles and the repolarization of the atria (Gangemi 1995). Lastly is the T wave which represents the repolarization of the ventricles (Gangemi 1995). Of note, since the repolarization of the atria occurs at the same time as the depolarization of the ventricles in the QRS complex, the atrial repolarization is not clearly detected by the ECG since the tissue mass of the ventricles is much larger than that of the atria (Gangemi 1995). The ECG waveform and its associated peaks are labeled in Figure 2.

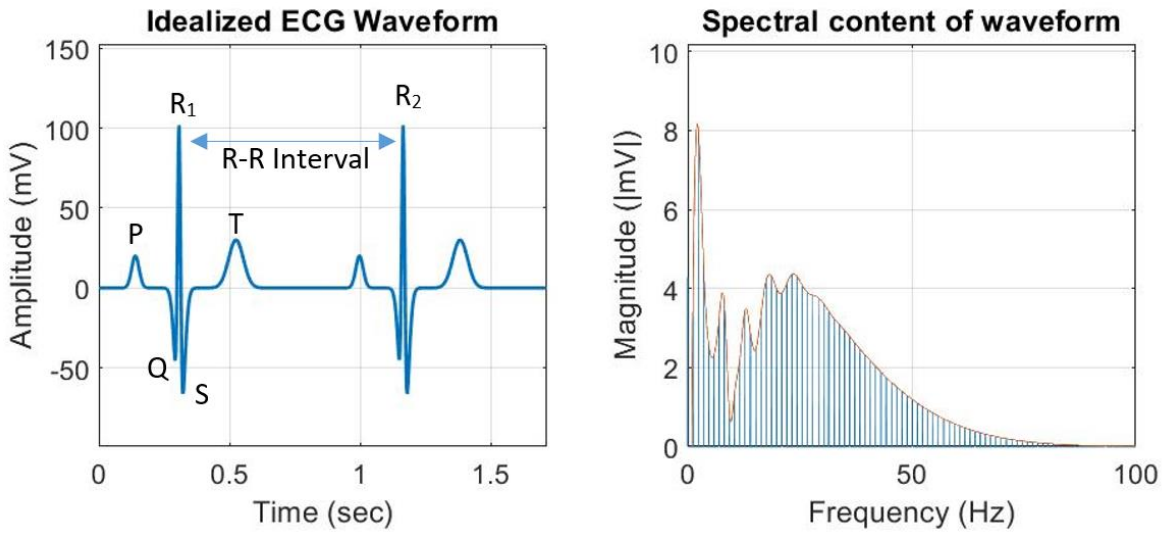

Figure 2: Idealized ECG waveform of a heart in ideal sinus rhythm in the time domain (Left) and frequency domain (right).

Some popular metrics from the ECG are the R-R Interval, the peak amplitudes and shapes, the heart rate (HR), and various descriptions of Heart Rate Variability (HRV). The spacing between two adjacent R peaks is called the R-R Interval. The average spacing over time is the subjects heart rate. Heart rate variability is a measure of the fluctuations in successive R-R interval over time. In addition to the metrics between adjacent waveforms there are metrics within an individual waveform. For example: The P-R interval, Q-T interval and S-T interval measures of the time between the corresponding peaks of a given waveform. Metrics such as these, as well as the relative amplitudes of the individual peaks, can help a doctor diagnose if the heart is healthy and performing as expected or if there are symptoms of cardiac problem.

The ECG waveform typically measured at the skin has a voltage range of 0.5mV to 5 mV, depending on human subject factors (John G. et al. 2010). The smaller peaks similarly vary in width and amplitude but the R-peak is typically the largest. The waveform's frequency content ranges from 1Hz to 100Hz depending on the subject and their activity level (Y Du 2017; Tereshchenko and Josephson 2015). The cardiac cells have a resting electric potential of approximately -85mV [14]. These

electrical parameters are detected by precise circuitry and precise placement of electrodes. The circuitry used to capture the ECG waveform will be discussed next.

The ECG Circuitry

The fundamental ECG circuitry is designed to measure the voltage difference between two electrodes at the surface of the body. Starting at the electrode and working outwards from the body towards the computer display, the main functional buildings blocks, shown in Figure 3, are: the sensing electrode, the amplifier's protection circuit, the lead selector, the amplifier stage (Amp), the filter stage, the isolation circuit, and the analog to digital converter (ADC) (John G. et al. 2010). After the signal is digitized, it can be post processed, saved in memory, and/or displayed directly for analysis.

The specific ECG system used by Arquilla et al. for data collection was the BIOPAC MP160 ECG hardware suite ("MP System Hardware Guide" 2015). This includes the BIONOMADIX wireless ECG transmitter. The BIONOMADIX is a portable device which connects to the electrodes and digitizes the signal before wirelessly relaying it back to the BIOPAC for further processing and display. The BIONOMADIX transmitter performs the general functions described below.

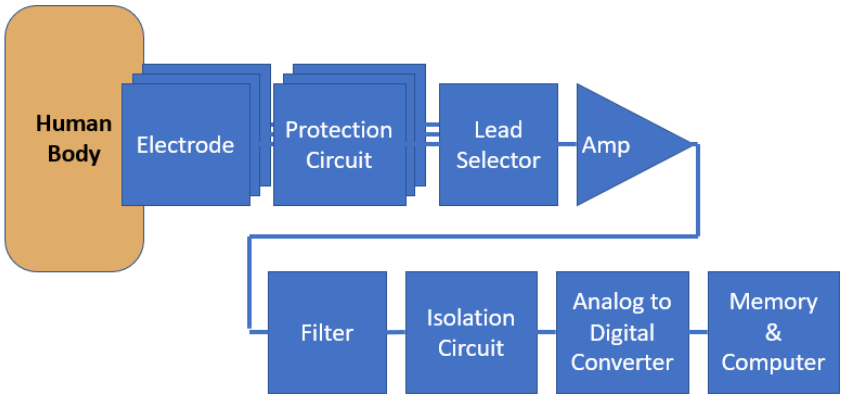

Figure 3: Functional Block Diagram of a typical ECG system (Y Du 2017; John G. et al. 2010).

The electrodes will be discussed in depth later, so the first block to be discussed is the amplifier's protection circuit. The electrode can be thought of as the

transducers that convert flowing ions to flowing electrons (Y Du 2017). The protection circuit (PC) prevents damage to the rest of the circuit in case a high voltages appear across the input electrodes (John G. et al. 2010). Traditionally this is intended to protect the ECG device in case of the application of defibrillation, but for long term use, wearable devices would also need this function to protect against electrostatic discharge and events similarly harmful to electronics.

The next block is the lead selector (LS). Since voltage is a differential measurement, pairs of electrodes are needed to make a measurement. Each electrode pair forms a lead. This circuitry is responsible for determining which lead (electrode pair) is measured at a given instance in time. The lead selector will then connect those electrodes to the rest remainder of the circuit. In the next instance in time, the lead selector will again connect a pair of electrodes to the next stage of the ECG circuit.

The amplifier stage (Amp) is responsible for amplifying the ECG signal so that it is easier to capture and digitize. This stage has very high input impedance because ideally there should be as little current draw as possible since current distorts the electric field, and corrupts the signal (John G. et al. 2010). The specific voltage gain of the BIONOMADIX circuitry is 2000, or approximately 66 dB [22]. The differential input impedance of the BIONOMADIX amplifier is 2MΩ [22]. This stage also sets the signal to noise ratio (SNR) by amplifying both the signal and the background noise present at the electrodes. SNR is defined as the ratio of the power of a signal to the power of the noise (Arquilla, Webb, and Anderson 2020b). When the signal is less powerful than the noise, the SNR will be negative (units in decibel) indicating that the signal is not retrievable from the ambient noise. When SNR is positive, the signal strength is stronger than the noise, and can be retrieved. The specific SNR depends on how much noise is present.

The filter stage is perhaps the most important stage of the ECG circuitry because it is used to remove signals present which are not from the heart. A high

pass or DC filter (HPF) eliminates any DC offset developed between electrodes as well as ultra-low frequency signals (Y Du 2017). While a low pass filter (LPF) removes high frequency noise above the upper frequency components of the cardiac cycle (>100Hz) (Tereshchenko and Josephson 2015). A notch filter, or band stop filter (BSF), is used to block out specific signals known to be present such as the 60Hz interference from power lines. The last part of the filter stage is associated with rejecting the common mode interference; noise that is present across multiple electrodes. The specific filters in the BIONOMADIX circuitry are maximally flat Butterworth filters: a single pole high pass filter with cutoff frequency of 1Hz, a single pole low pass filter with cutoff frequency of 35Hz, and a notch filter centered at 60Hz with a 2Hz bandwidth ("MP System Hardware Guide" 2015).

Since filtering noise is a critical function, a brief detour to discuss noise sources is also provided here. Electrical noises affecting the signal quality mainly include intrinsic body noise, skin-electrode interface noise and environment noise. Intrinsic body-noise is the detection of the contraction or tension of non-cardiac muscles such as respiration, and is the dominant noise factor for long-term use (Y Du 2017). Skin-electrode interface noise is the result of physical motion of the electrode on the skin in the form of sliding, slipping or gaps between the skin and the electrode. This is also the result of poor skin to electrode contact. The quality of the skin (i.e., sweaty vs. dry) can also introduce interface noise in long-term measurements since it may change over time. Long term measurements also require consistent placement of the electrode on the skin, because a misplaced electrode would introduce another source of measurement variation. Environmental noise is electrical noise from external sources. It can consist of power line interference, impulse noise, electrostatic potentials, stray capacitance, and nearby electronic devices (Heikenfeld et al. 2018). Regardless of where the noise is coming from, the signal must be separated from the noise, and this is why the ECG system relies on the filter stage.

The isolation circuitry (IC) is designed to protect the patient in case the ECG system malfunctions (John G. et al. 2010). It prevents harmful currents from coming back into the body. Traditionally this is because medical equipment is usually connected to high power lines, such as the 120V wall outlet. In the BIONOMADIX this block is moved after the digitization step, and is realized by means of radio isolation.

The analog to digital converter (ADC) is the device responsible for converting the continuous analog signal of the heart to a discrete time signal (John G. et al. 2010). The ADC does this by sampling the continuous signal at a frequency called the Nyquist rate. The Nyquist sampling rate is at least two times the highest frequency component of the waveform so that aliasing does not occur [2]. Once digitized the ECG data is stored in memory where it can be retrieved for further post process analysis and display. For the BIONOMADIX transmitter, the sampling rate was 2kHz.

These are the main building blocks for an ECG measurement circuit. The last ECG building block to be discussed is the electrode itself.

The Electrode

Electrodes are the focus of this modeling effort, so greater detail will be spent discussing the existing literature associated with their characteristics and parameters. Specific attention will be given to the exact woven electrode types which were used to collect the ECG data for this thesis. Generally, an electrode is the component of the ECG device which makes contact with the skin. It measures the voltage potential across two points on the body, by converting the flow of ions underneath the skin to flowing electrons in the wires (John G. et al. 2010). The first characteristic of ECG electrodes, regardless of type, is the location of the electrode's placement on the skin of the body. Electrode placement is critical to the repeatability and voltage magnitude of the ECG signal (Arquilla et al. 2020). As described in *Medical Instrumentation: Application and Design* by John G Webster:

"If the electrodes are located on different equal-potential lines of the electric field of the heart dipole, a non-zero voltage is measured. Different pairs of electrodes at different locations yield different voltages. Thus it is important to have certain standard positions for consistent evaluation of the ECG." (John G. et al. 2010).

Repeated ECG electrode placement on the body is non-trivial since slight variations in electrode placement can result in variation in the ECG waveform which can correspondingly lead to misdiagnoses and reduced trust in the monitoring system (Arquilla et al. 2020). There are several standards which have been adopted by the medical community starting with a three-electrode configuration and increasing electrode count to as many as twelve. According to a study performed by the Society of Cardiological Science and Technology in 2017, a repeated electrode placement tolerance of 19mm was deemed acceptable for making electrocardiograph measurements (Gregory et al. 2019). The three-electrode method used during data collection by Arquilla et al., 2020 is commonly called the three lead Einthoven's triangle (Y Du 2017). The three electrodes, forming three leads, is the Einthoven triangle, graphically described in Figure 4.

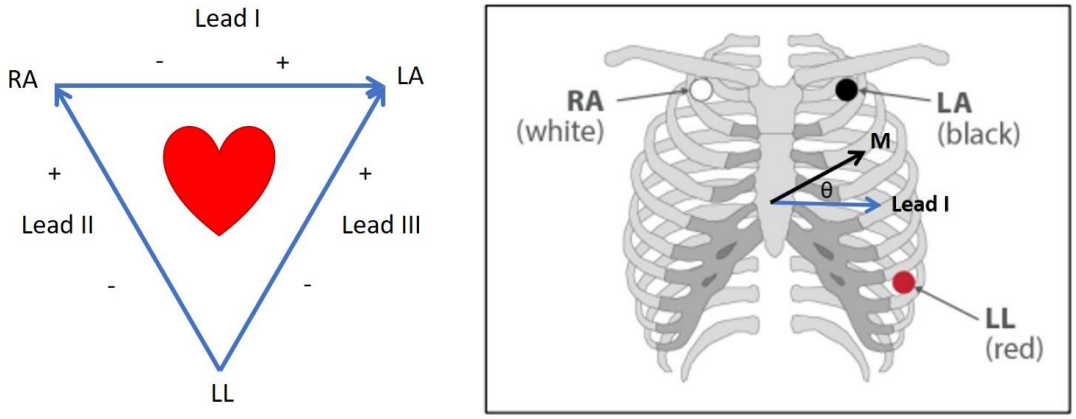

Figure 4: Einthoven's Triangle for 3 lead Electrocardiograph measurement

In order to understand the Einthoven triangle, some terminology is useful to describe how the measurements are made. As described earlier, a pair of electrodes placed on the body forms a *lead*. A lead vector is defined as the unit vector which describes the orientation of the electrode pair placement (John G. et al. 2010). A

cardiac vector is defined as the dipole moment representing the summation of all electrical activity in the heart at a given instant in time. For some cardiac vector, **M**, and some lead unit vector, **a**, the measured voltage V_a, the equation for which is shown in Eqn. 1, is simply the dot product between the two vectors, where θ is the angle between them:

$$V_a = \bar{\boldsymbol{a}} \cdot \bar{\boldsymbol{M}} = |\bar{\boldsymbol{M}}| * \cos(\theta) \quad (1)$$

For example, Voltage V_1 is the voltage measured by lead 1 between the Right Arm (RA) and Left Arm (LA) electrodes, V_2 is the voltage by lead 2 between the RA and Left Leg (LL) electrodes, and V_3 is the voltage measured by lead 3 between the LA and LL electrodes. Cardiologists use a standard notation describing the direction of the lead vectors such that lead 1 is 0 degrees, lead 2 is 60 degrees, and lead 3 is 120 degrees. This grants the ECG the ability to "view" the heart from several angles. Techniques with more electrodes are adding more angular diversity.

The electrodes themselves are placed to minimize noise contributions and maximize signals from the heart. The RA electrode is located under the right clavicle, the LA electrode is under the left clavicle, and the LL electrode is placed on the lower left abdomen within the rib cage frame between ribs. Admittedly there is a large variation in placement between population because there is a large variance in the anthropometry. Humans all vary significantly, for example in weight, BMI, fatty tissues, or physical size, therefore for long-term monitoring it is more important to have a consistent method of placement for a given person with repeated use than across people (subject to general placement constraints described previously).

Wet Electrodes vs. Dry Electrodes

After electrode placement, the next characteristic of interest is the electrode type. There are many different types but generally electrodes are divided into two categories in the literature, "wet" and "dry" (Heikenfeld et al. 2018; Arquilla, Webb,

and Anderson 2020a; Yoo and Hoi-Jun Yoo 2011). Wet electrodes are accompanied by a gel or electrolyte solution which aids in measurement by reducing the electrical contact impedance (Heikenfeld et al. 2018), while dry electrodes do not use an additional electrolyte gel. The traditional adhesive electrode is considered "wet" while the novel conductive textile electrodes proposed in this research are "dry". The Wet/Dry terminology is a bit of a misnomer despite colloquial usage, because dry electrodes which are dry initially, quickly accumulate tiny amounts of skin moisture and perspiration making them functionally able to be modeled like "wet" electrodes (An and Stylios 2018). This is because the minute amount of moisture is functionally the same as a very thin layer of electrolyte which, from a modeling perspective, means the dry electrodes have the same functional model structure as wet electrodes after a given settling time (An and Stylios 2018; Geddes and Valentinuzzi 1973).

The most commonly used "wet" electrodes are silver/silver chloride (Ag/AgCl) gel-based adhesive electrodes. These electrodes are rigid metal cylinders with an adhesive sticker and an electrolyte gel section on one side and a protruding metal attachment point on the other side (Arquilla, Webb, and Anderson 2021). The adhesive sticker ensures constant skin contact while the gel electrolyte ensures a low electrical impedance. They have many benefits such as being non polarizable, generating low noise, and being tolerant to motion but they have limitations in long term monitoring applications (An and Stylios 2018; Taji et al. 2014; Y Du 2017; Arquilla, Webb, and Anderson 2020a). According to A Searle and L Kirkup the limitations associated with wet electrodes are oriented around the gel electrolyte (Searle and Kirkup 2000). The reliance on an electrolyte leads to reduced signal quality as the gel dehydrates and the reapplication of gel may not be feasible (Arquilla, Webb, and Anderson 2021; Searle and Kirkup 2000). The application and removal of electrolyte gel is unpleasant for the subject and time consuming for the clinician (Searle and Kirkup 2000). Furthermore with chronic use, both the

adhesive and the electrolyte can cause skin irritation (Arquilla, Webb, and Anderson 2021; John G. et al. 2010).

"Dry" electrodes come in a variety of types, and the type discussed here is the dry textile electrode. Textile electrodes are swatches of fabric, either partially containing or entirely consisting of electrically conductive yarn. They are not inherently accompanied by adhesive or by electrolyte gel. Compared to traditional Ag/AgCl electrodes, textile electrodes have the advantage of being soft, flexible and breathable, allowing the wearer to feel more comfortable long term (An and Stylios 2018; Arquilla, Webb, and Anderson 2021). Furthermore, textile electrodes are reusable, and potentially integratable into familiar everyday clothing. On a Likert scale characterization of comfort Woven electrodes have been reported as "scratchier" than adhesive electrodes, while also rating less "clingy", "cold", and "sticky" (Arquilla, Webb, and Anderson 2021). Since textile electrodes do not use adhesive to adhere to the body, they do not irritate the skin on removal and reapplication. Additionally, since they do not use an added gel electrolyte, their performance does not degrade over time. These benefits, though, are also their primary challenge. Without adhesive they are susceptible to motion related noise from poor skin contact, and without added gel electrolyte, they have higher electrical skin impedances (Nikolova-Hadzhigenova 2019). To address problem of skin contact Arquilla et al. utilized a placement garment described in (Arquilla et al. 2020). This garment helps ensure repeatable placement of the textile electrodes on the body and applied a constant pressure against the skin.

There are some similarities between wet and dry electrodes. Both require some amount of stabilization time. This is likely due to human body factors, like skin temperature as well as skin moisture (An and Stylios 2018). Fortunately in long term monitoring applications, missing the first 5-10 minutes does not impose significant problems to a longer dataset (Yoo and Hoi-Jun Yoo 2011). Both

electrodes also utilize the same placement locations on the human body and are capable of capturing the complete ECG waveform.

Manufacturing Parameters of Textile Electrodes

Next the manufacturing parameters of textile electrodes will be discussed in more depth. Textile type is briefly mentioned because this paper focuses on woven fabric but it is worth mentioning that there are popular alternative textile solutions in the literature such as knit and embroidered electrodes. Within woven textile electrodes the three manufacturing design parameters of interest are yarn type, weave pattern, and surface area. It is also worth acknowledging that the manufacture of textiles in general includes design parameters beyond these three, but within the context of woven electrodes these parameters are the most relevant, and thus the focus of this thesis.

Textile Type: Weave, knit, embroidery

Textiles can be manufactured from different methods of converting yarn or thread into fabric. Woven textiles are created on a loom through the weaving process of interlacing threads perpendicularly according to a repeated pattern (Gustaf Hermann Oelsner 1915). Woven fabric has the main benefit of inextensibility and fixed thread contact with the body, which primarily means woven electrodes have a constant electrical impedance (Arquilla, Webb, and Anderson 2021). This also makes it easy to integrate electrically conductive yarns which have little to no stretch (Devendorf and Di Lauro 2019). Mechanically, woven fabric does not remain pressed against the skin, unless an additional supporting structure is present such as a foam backing or an adjustable strap(Arquilla, Webb, and Anderson 2021). For manufacturing conductive textiles integrated into larger garments, woven fabrics are attractive because they more easily accommodate multiple yarns and yarn types.

When compared to woven fabrics, knitted fabrics are created from the process of repeatedly intermeshing loops of yarn. Knitted fabrics are more flexible,

stretchable, and take up the curvature of the body when worn (An and Stylios 2018). The elastic nature does still struggle to conform to concave surfaces of the body; for example, between pectorals or underneath collar bones. Since knits are traditionally formed from looping a single yarn, it is challenging to incorporate various yarn types during manufacture, and therefore it is more challenging to integrate knit electrodes into a non-conductive garment. Another trade-off with knit fabric is that the electrical properties change when stretching (Yokus and Jur 2016). Changes in shape and stitch contact density due to stretching correspondingly influence their electrical impedance, which adds a dimension of variation to the measurement and distorts the original signal. This additional variation associated with stretching is difficult to separate from the original signal. For the purposes of monitoring ECGs an electrode which changes shape or size, as is the case with knitting, would correspondingly change resistance and require more complex circuitry or postprocessing.

Embroidery is the process of sewing a patch or design into an existing fabric. Unlike woven and knit electrodes, the embroidered electrodes are always added after the base fabric has been manufactured (Bystricky et al. 2016). Embroidered patches are highly customizable and easy to fabricate, but also require the additional step during fabrication (Bystricky et al. 2016; Kannaian, Neelaveni, and Thilagavathi 2013). Usually, embroidery is added to a woven base material, so they tend to also be inelastic, and experience similar characteristics as the base weave. Since embroidered patches are so customizable, there are more patterns and textures that can be explored than with knit and woven fabrics, but this comes at the cost of added complexity. The largest limitation of embroidered electrodes is that not all conductive threads can be used in sewing machines during the additional manufacturing step. Furthermore embroidery machines are more expensive than basic sewing machines, which makes embroidered electrodes a less cost-effective option (Arquilla, Webb, and Anderson 2020a).

It has been difficult to conclusively determine which type of textile structure performs best in ECG recording because it involves many factors, such as the geometry of the fibers and yarns, the stitch density, contact area, the manufacturing process as well as the conductive material type (An and Stylios 2018). In this research, woven electrodes were chosen because conductive elements can be integrated seamlessly and exist in stable, inelastic structures that have constant resistance (Arquilla, Webb, and Anderson 2021).

Yarn Type

When manufacturing a woven textile, yarn type is one of the first design choices to consider – both for the base yarn and the conductive elements. This section will focus on the conductive elements and how the decision of yarn type impacts the manufacturability and long-term function of an electrode. Electrical conductivity in textiles can occur via the thread material itself (e.g., spun steel thread) or the thread can be non-conductive (e.g., nylon thread) and a conductive coating can be applied (e.g., silver-coated nylon). There are various methods of applying a conductive coating to a base yarn such as chemical deposition, or simply screen printing. One of the main demands of textile electrodes is that they are reusable. This means over day-to-day use the garment will absorb sweat from the wearer and collect dirt from the environment so machine washability is a priority which is addressed through yarn type.

For conductive threads one popular choice is steel spun thread. The thread is spun from stranded stainless-steel fibers so it is electrically conductive throughout its cross section. This resembles a structure of a spun staple fiber yarn where individual short lengths of steel fiber are given structure through the application of a spin or twist (Arquilla, Webb, and Anderson 2021). Using conductive threads can be more simple to manufacture but limits design freedom to the fabric stitch pattern (Arquilla, Webb, and Anderson 2021). Some conductive threads are very strong and inelastic which tend to degrade manufacturing machines faster than regular thread

(Bystricky et al. 2016). Stainless steel is generally corrosion resistance but it can and will rust in certain conditions. When considering washability, electrodes constructed with stainless steel threads have shown no significant degradation in performance, but time-to-failure tests have not yet been conducted (Arquilla, Webb, and Anderson 2020a).

Screen printing is the process of applying a conductive coating to a fabric through a shaped screen. Chemical plating is the process of applying a conductive coating to a thread before it becomes a fabric. Conductive inks and pastes used in screen printing tend be expensive to purchase, and the curing process takes more time to be test-ready(Arquilla, Webb, and Anderson 2020a). With screen printing there is a risk of cracking, degrading signal quality, which is not a concern for conductive yarns or chemical plated threads. Silver-coated nylon is a popular chemical plated option which consists of several filaments of nylon, which are each chemically coated in silver nanoparticles and spun together. Compared to steel, silver is more biocompatible because it is antibacterial (Vojtech et al. 2013) and has a lower resistivity. Silver electrodes have performed better in detection of the P, Q and T peaks than spun steel thread electrodes (Arquilla, Webb, and Anderson 2021). Silver coated nylon has also been washed and measured after washing and shown no significant degradation in performance, but time-to-failure tests have not yet been conducted (Arquilla, Webb, and Anderson 2020a).

Weave Pattern

Within the category of woven fabrics there is an infinite variety of woven patterns which can be manufactured. Fundamentally weaving is a process of interlacing some length of yarn perpendicularly across another length of yarn (K. et al. 2012). The order and method in which this interlacing process occurs will determine the pattern, mechanical structure and functional surface area of the electrode (Arquilla, Webb, and Anderson 2021). To understand a weave pattern, it is helpful to first define some terminology commonly used in literature.

Warp and weft are the vertical and horizonal yarn lengths respectively. Warp threads are pulled taught by a loom, and a weft thread will alternatingly pass over and under the warp threads according to a predefined pattern (Gustaf Hermann Oelsner 1915). An anchor is an instance where the weft crosses over the warp. A float is an instance when a weft thread repeatedly passes beneath a warp thread. The number of warp threads that are passed between anchors is called the float count. An anchor offset is shift in anchor position in adjacent weft thread patterns. A simplified example of two patterns and their corresponding cross section are shown in Figure 5.

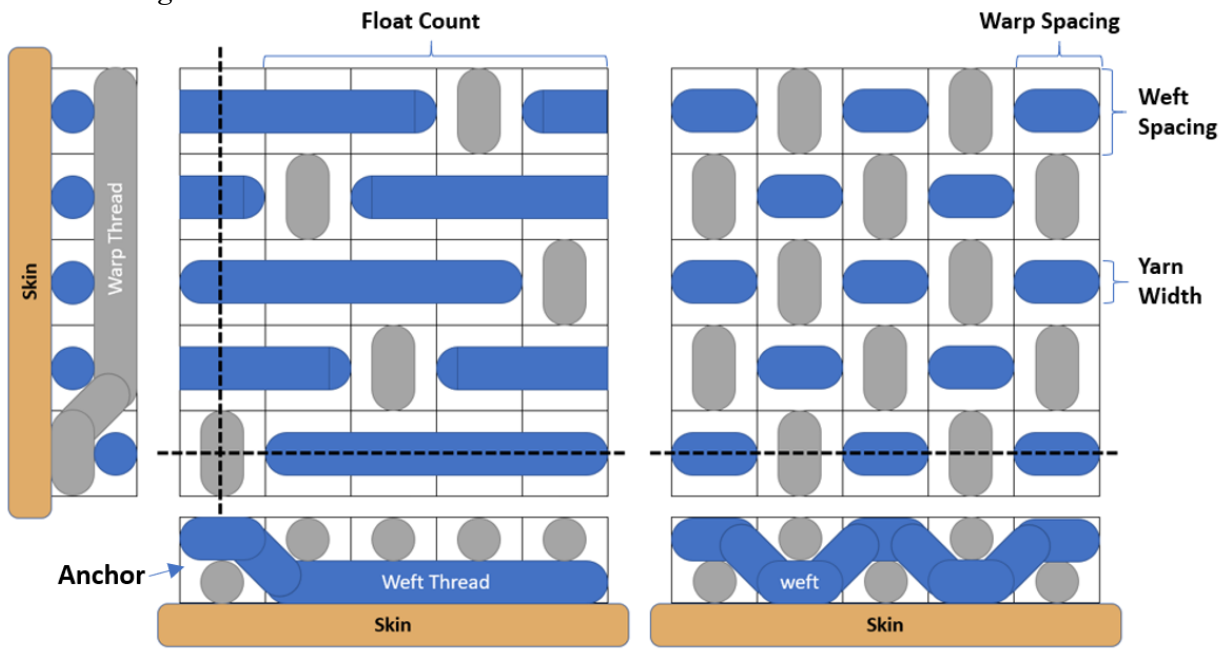

Figure 5: Example patterns with skin cross section, left: ¼ Sateen pattern, right: 1/1 Plain weave pattern. The left has more conductive contact area with the skin because less weft length is spent transitioning over and under the warp threads.

The pattern on the left represents a 1/4 sateen weave structure with a one anchor offset. The pattern on the right shows a plain weave structure, where the weft yarns alternate over and under the warp yarns. The vertical warp threads, spaced horizontally, are pulled tight by the loom which determines the warp thread spacing. The weft thread is passed horizontally by a shuttle and then pushed vertically up against the fell of the cloth determining the weft thread spacing. The

weft and warp thread spacing determine how tight or loose the overall fabric will be, and the overall thread density. The more frequently anchoring occurs, as in a plain weave, the tighter the fabric pattern will be. When anchoring occurs less frequently, as in the Sateen pattern, the fabric is softer and "puffier" because the weft threads are able to float (Arquilla, Webb, and Anderson 2021). This creates textiles which are not simple flat 2D surfaces but have some additional depth and texture.

In this example, consider now that the weft yarn (blue) is conductive while the warp yarn (gray) is not. Any given pattern will determine how much conductive yarn contacts the skin. Instances of anchoring will create more gaps in the electrode surface area which reduces the skin-electrode surface area but also stabilizes the yarn reducing motion. Fewer anchor points mean longer floats, which increase surface area but looser fibers are prone to picking up noise from motion artifacts and are also less durable and more likely to snag. Yarn thickness, as well as thread density (weft and warp spacing) are also related to the conductive contact area. In one report, the measured skin-electrode impedance is positively related to the yarn diameter and negatively related to the stitch density (An and Stylios 2018). In the cross section view it is easier to see how a pattern with fewer anchors would result in an electrode with a larger contact surface area with the skin.

Patch Surface Area

The last manufacturing parameter in woven textile electrodes is the electrode patch area. A patch is a swatch of woven textile fabric used as an electrode in the ECG. The patch area is simply the surface area of the shape of the textile electrode. In the ideal example from Figure 5, the patch is a 5 by 5 unit square, with an overall patch area of 25 units^2. In reality, the intended electrode design may differ from the as-built electrode size due to imprecise manufacturing processes. Furthermore, the as-built electrode area is different than the conductive surface area. The *conductive surface area* is defined as the functional surface area made by

conductive yarn which contacts the skin. Since the woven patch is a 3-dimensional structure of both conductive and non-conductive yarns, the conductive surface area is a smaller percentage of the area of the patch. The conductive surface area depends on both the pattern and area of the patch. It is therefore necessary to characterize the functional surface area of an electrode because the impedance of the skin-electrode interface is inversely proportional to the conductive contact surface area (Nikolova-Hadzhigenova 2019). A smaller area patch will have a higher skin-electrode impedance and introduce more high-frequency noise than larger patches (An and Stylios 2018; Nikolova-Hadzhigenova 2019). While a larger patch will capture more muscle signals and introduce more muscle contraction noise (An and Stylios 2018; Arquilla, Webb, and Anderson 2021). The conductive contact area affects the skin-electrode interface and correspondingly its impedance which strongly affects the acquired ECG signal (Taji et al. 2014).

In the idealized example from Figure 5 both patterns have a square patch area of 25 units^2 but they do not have the same functional conductive surface area. As a first order approximation, the conductive area is the summation of all the smaller blue areas. Using this approximation, the plain weave has a conductive surface area of 22% of the patch area. The 1/4 Sateen pattern is comparatively better but still only about 36% of the patch area. There are many assumptions imbedded in this example approximation, but the purpose is to illustrate how weave pattern and patch area can dramatically impact the functional conductive surface area of a particular woven textile electrode.

Skin-Electrode Interface Model

To capture the behavior of the textile electrode, a circuit model and a discussion of the parameters needed to describe an electrode's electrical behavior is presented. When biopotentials are recorded from the surface of the skin, the conductive interface between the electrode and the skin is modeled using a circuit model called the *skin-electrode interface model* (John G. et al. 2010). This model, shown in Figure

6, characterizes the skin, the electrode, and the interface between them using passive circuit elements.

Starting with the heart and working outwards toward the electrode, the ECG signal must pass through several layers of tissue. The innermost is the thoracic cavity and subcutaneous tissue, next is the dermis which is the thickest layer of the skin, and finally the outermost layer is the epidermis. The skin therefore should not be viewed as an information source but instead as an information barrier (Heikenfeld et al. 2018). According to J. Heikenfeld et al.

> "Electrical impedance is largely determined by the roughness of the skin which introduces pockets of air that can result in higher impedance. Wet electrodes reduce that resistance by closing the air gaps with electrolyte. The stratum corneum (SC) is electrically insulating with a resistance that is significantly higher than that of the underlying layers of the epidermis. The impedance can vary strongly depending on the activity and density of sweat glands, and the local thickness and composition of the stratum corneum. The entire epidermis including the SC can be treated equivalently with a parallel resistor/capacitor which is chosen according to the body location and electrodes." (Heikenfeld et al. 2018).

From the literature review there are two standard skin-electrode models describing the behavior of the skin interface. A "single-time" constant model developed by Swanson and Webster (John G. et al. 2010) contains a single stage parallel R/C pair. The single stage model attempts to combine the skin and electrode into one stage, but exhibits less accurate modeling results and therefore was not chosen in this analysis (Taji et al. 2014). A double time model developed by Neuman (An and Stylios 2018) uses two stages of parallel resistor capacitor pairs to represent the electrode interface. The double time model, shown in Figure 6, exhibits more accurate modeling results for traditional electrodes and was therefore chosen as a baseline for this analysis effort. It is the goal of Hypothesis 1 to

determine if woven textile electrode behavior can be described by the double-time skin electrode model or if a different architecture is needed.

Some models include a voltage dependent voltage source to represent the current transform occurring at the skin interface. The signal is conducted through the body's extracellular fluid by the flow of ions, meaning the charge carrier is Na+ or K+ ions. On the other side of the skin, the signal is conducted by the flow of electrons and current is measured in Amperes. The skin interface is where this current transforms from flowing ions to flowing electrons. For the purposes of the equivalent model the "raw signal" does not need to be replicated in ionic current units, and so this element has been excluded from the model.

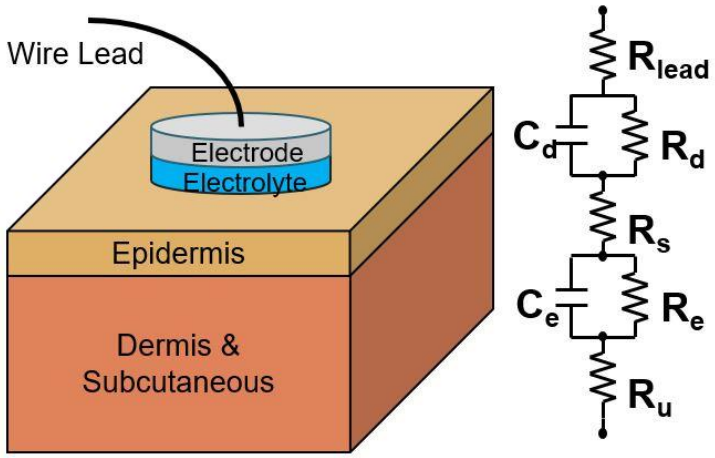

Figure 6: Double Time circuit model of the skin-electrode interface (Heikenfeld et al. 2018; Yokus and Jur 2016; John G. et al. 2010; Löfhede, Seoane, and Thordstein 2012; Yoo and Hoi-Jun Yoo 2011; Medrano et al. 2007; Assambo et al. 2007)

According to the skin-electrode model, the cumulative impedance, Z_E, can be represented as a complex function of frequency where $j^2 = -1$ and ω is frequency. Before describing each term, Z_E can be reorganized to a ratio of polynomials for ease of use in further analysis. The equations for the polynomial coefficients are shown in Table 1. To simplify the equation, let $s = jw$ and substitute the terms for

polynomial coefficients. This notation is useful for frequency domain analysis as a transfer function which will be described in more detail in the next section.

$$Z_E = R_{lead} + \frac{R_d}{1 + j\omega R_d C_d} + R_s + \frac{R_e}{1 + j\omega R_e C_e} + R_u = \frac{b_2 s^2 + b_1 s^1 + b_0}{a_2 s^2 + a_1 s^1 + a_0} \quad (2)$$

Table 1: Coefficients for the impedance of the Skin-Electrode Interface Model

$b_2 = (R_{lead} + R_s + R_u) * R_d C_d R_e C_e$	$a_2 = R_d C_d R_e C_e$
$b_1 = (R_{lead} + R_s + R_u) * (R_e C_e + R_d C_d) + R_d R_e C_e + R_e R_d C_d$	$a_1 = R_e C_e + R_d C_d$
$b_0 = R_{lead} + R_s + R_u + R_d + R_e$	$a_0 = 1$

In this model: R_u represents the resistance of the dermis and subcutaneous layers, R_e represents the resistance of the epidermis layer, C_e represents the capacitance induced by the nonconductive stratum corneum layer, R_s represents the resistance of the sweat or electrolyte depending on the electrode type, R_d represents the charge transfer resistance in the conductive electrode, C_d represents the capacitance across the electrode-electrolyte interface, and R_{Lead} represents the resistance of the connection to the wire leads traveling to the ECG input circuitry (An and Stylios 2018). The thoracic volume conductor, is considered a purely passive medium containing no electric sources or sinks and generate negligible DC potentials (John G. et al. 2010). Several papers have applied the double time model to textile electrodes, but this paper will explore how well that assumption holds.

The components of the model which capture the skin's behavior are R_e, C_e, and R_u. The electrical properties of skin have great variation and depend upon many factors including, but not limited to, hydration, hairiness, thickness (%body fat), surface area and location on the body (An and Stylios 2018). This model shows that the impedance of electrodes is fundamentally frequency-dependent; As the frequency increases, the impedance decreases which is consistent with the capacitive behavior of the skin-electrode interface (An and Stylios 2018). For a 1 cm^2 patch of skin, the skin impedance (R_e || C_e + R_u) reduces from approximately 200kΩ at 1Hz to 200 Ω at 1 MHz (John G. et al. 2010).

The components of the model which capture the electrode's behavior are R_d, C_d, R_s, and R_{lead}. The electrical properties of the electrode depend upon many factors including, but not limited to, the conductor metallic composition, conductor geometry, the presence/type of electrolyte, and conductive skin surface area. Similar to skin, electrodes display a fundamentally capacitive reactance. The lead wire resistance, R_{Lead}, is simply the DC resistance of the wire connecting the electrode to the ECG circuitry and on the order of 0.1- to 3Ωs depending on lead wire length.

The specific values R_d, C_d, and R_s, are difficult to identify for a given textile electrode. It is possible to measure overall impedance Z_E at various frequencies and determine the specific parameters retroactively, but currently there is not a method of predicting these circuit parameters prior to fabrication from the manufacturing parameters. It is for this reason that the goal of Hypothesis 2 is to search for a relationship between the parameters of the skin electrode impedance model and the manufacturing parameters (Yarn Type, Patch Area, and Weave Pattern).

Transfer Functions

When it comes to creating a computational model, a transfer function is a type of model which is described generally as a mathematical function which theoretically relates the systems outputs to each possible input (Girod, Rabenstein, and Stenger 2001). This is an incredibly broad analysis tool because the transfer function captures everything in between the input and output, and it describes mathematically how the input becomes the output. A transfer function can relate any combination of inputs to outputs, such as single inputs to single outputs (SISO), and multiple inputs to multiple outputs (MIMO) (Girod, Rabenstein, and Stenger 2001). When this concept is applied to the ECG system the electrical potential generated by the body is the input to the system. The measured waveform displayed on the computer screen is the output of the system (John G. et al. 2010). The ECG system is a discrete time periodic system because the input is a repetitive continuous signal, and the output is discreetly sampled in time by the ADC. For

time periodic systems, as is the case with the ECG, the frequency domain is often a useful basis for analysis with many papers presenting the ECG system as a function of frequency (An and Stylios 2018; Taji et al. 2014; Yoo and Hoi-Jun Yoo 2011; Tereshchenko and Josephson 2015; Rahul, Sora, and Sharma 2019). A transfer function in the frequency domain maps the frequency components of the input to the frequency components of the output. The Fast Fourier Transform (FFT) is one method used to convert signals from the time domain to the frequency domain (Rahul, Sora, and Sharma 2019). The general form of this type of transfer function, *TF(jw)*, described in Eqn. (3), equals the ratio of the systems output, V_{out}, to the systems input, V_{in}.

$$\frac{FFT\{v_{out}(t)\}}{FFT\{v_{in}(t)\}} = \frac{V_{out}(jw)}{V_{in}(jw)} = TF(jw) \quad (3)$$

From circuit theory, a frequency dependent transfer function is also described as a ratio of two polynomials with coefficients (Thomas, Rosa, and Toussaint 2009). The generalized frequency dependent transfer function is defined below by Eqn. (4) (John G. et al. 2010; Thomas, Rosa, and Toussaint 2009). The transfer function depends on the circuit parameters of the system it describes. The circuit parameters are represented here by the A and B coefficients. These terms are weights assigned to the power of each frequency. Here the subscripts n and m indicate the highest order term used to define the system and s=jw is used to simplify the expression.

$$TF\left(jw, A_{0,1,\ldots,n}, B_{0,1,\ldots,m}\right) = \frac{B_m(jw)^m + \cdots B_1(jw)^1 + B_0}{A_n(jw)^n + \cdots A_1(jw)^1 + A_0} = \frac{B_m(s)^m + \cdots B_1(s)^1 + B_0}{A_n(s)^n + \cdots A_1(s)^1 + A_0} \quad (4)$$

Previous literature has used transfer functions to model various ECG systems (Oleksy and Tkacz 2010; Terada et al. 2021; Nakamura, Kato, and Ueno 2018; Wang and Lin 2021; Ozkan et al. 2020; Maji and Burke 2018). The focus of those efforts is mostly oriented around improving the traditional methods of ECG collection not on evaluating the electrode type as a function of its manufacturing parameters. Some examples consist of: Evaluating traditional electrode placement

of the 5-lead versus 12-lead methods (Oleksy and Tkacz 2010), Evaluating various circuit topologies for de-noising and amplifying the waveform (Terada et al. 2021; Wang and Lin 2021; Nakamura, Kato, and Ueno 2018), and evaluating filtering in order to improve diagnostic capability (Maji and Burke 2018). One noteworthy paper by Ozkan et al. presented a transfer function of a wearable 3-lead ECG system designed for long-term data capture using textile electrodes (Ozkan et al. 2020). The paper offered a larger scope of work describing the whole wearable ECG system as a part of the Internet of Things (IoT). Their transfer function model described custom low-power circuitry as well as the textile electrodes but did not distinguish the specific contribution of the electrodes from the rest of the system (Ozkan et al. 2020). No work relating manufacturing parameters of textile electrodes to their electrical properties through a transfer function was found in the literature.

Summary

A summary of the literature review discussing electrode types is compiled in Table 2 below. The table shows the various electrode types and compares them side by side. Overall, the literature describes various types of textiles electrodes and justifies their adoption for long-term ECG monitoring. In the literature there exist equivalent models of the generalized skin-electrode interface, and transfer functions of various ECG systems, but none of them focus on the relationship between a textile electrodes electrical behavior and its manufacturing parameters. At the core of this research is the aim to build an equivalent model of a woven electrode from first principles, which is able to relate the manufacturing parameters of yarn type, weave pattern and patch area, to the circuit parameters in the skin-electrode interface model. This specific relationship is missing from the literature.

Table 2: Summary of Electrode Types and their Pros and Cons of Electrodes

Parameter	Electrode Types			
	Traditional Adhesive Gel	Textile Electrodes		
		Weave	Embroidered	Knit
Comfort	Cold, clingy, sticky (Arquilla, Webb, and Anderson 2021)	Scratchy(Arquilla, Webb, and Anderson 2021), Soft flexible Breathable (An and Stylios 2018)	Soft flexible Breathable (An and Stylios 2018)	Soft flexible Breathable (An and Stylios 2018)
Stability	Electrolyte dries over time (Yokus and Jur 2016; Arquilla, Webb, and Anderson 2021; Yoo and Hoi-Jun Yoo 2011)	Minutes, Stable over time (An and Stylios 2018; Yoo and Hoi-Jun Yoo 2011)	Stable over time (Yoo and Hoi-Jun Yoo 2011)	Minutes, Stable over time (An and Stylios 2018; Yoo and Hoi-Jun Yoo 2011)
Reusability	Disposable (Taji et al. 2014)	Washable (Arquilla, Webb, and Anderson 2020a)	Washable (Bystricky et al. 2016; Ankhili et al. 2019)	Washable (Bystricky et al. 2016)
Mechanical Skin Contact	Adhesive (Taji et al. 2014)	Additional mechanism required (Arquilla, Webb, and Anderson 2020a)	Additional mechanism required (Bystricky et al. 2016; Ankhili et al. 2019)	Additional mechanism required (Bystricky et al. 2016)
Impedance (ohms)	3k – 50k (Yoo and Hoi-Jun Yoo 2011)	Constant (Arquilla, Webb, and Anderson 2021; 2020a), 100k – 1M (An and Stylios 2018; Sriraam et al. 2019)	Constant (Arquilla, Webb, and Anderson 2021),	Variable (Yokus and Jur 2016; Arquilla, Webb, and Anderson 2021), 100k – 1M (An and Stylios 2018; Sriraam et al. 2019)
Signal Quality	Resist motion artifacts, Clean (Taji et al. 2014)	Vulnerable noise and false peaks (Arquilla, Webb, and Anderson 2021)	Vulnerable noise and false peaks (Bystricky et al. 2016)	Vulnerable noise and false peaks (Bystricky et al. 2016)
Ease of use	Requires Skin prep (Taji et al. 2014)	Light weight, Convenient (Nikolova-Hadzhigenova 2019)	Light weight, Convenient (Nikolova-Hadzhigenova 2019)	Light weight, Convenient (Nikolova-Hadzhigenova 2019)
Manufacture	Familiar, inexpensive	Easily integrated into clothing (Yokus and Jur 2016; Arquilla, Webb, and Anderson 2021)	Easily integrated into clothing (Ankhili et al. 2019)	Easily integrated into clothing (Yokus and Jur 2016)

Biocompatible	Toxicological Skin Irritation (Nikolova-Hadzhigenova 2019; Yokus and Jur 2016; Arquilla, Webb, and Anderson 2021; Taji et al. 2014; Yoo and Hoi-Jun Yoo 2011)	Low irritation (An and Stylios 2018)	Low irritation (Ankhili et al. 2019)	Low irritation (An and Stylios 2018)
Mechanical	Rigid (Arquilla, Webb, and Anderson 2020a)	Flexible inextensible(Arquilla, Webb, and Anderson 2021)	Flexible inextensible(Arquilla, Webb, and Anderson 2021)	Elastic (Arquilla, Webb, and Anderson 2021)
Application	Clinical Recording (Yoo and Hoi-Jun Yoo 2011)	Long-Term Monitoring (Yokus and Jur 2016)	Long-Term Monitoring (Yokus and Jur 2016; Bystricky et al. 2016; Paradiso and De Rossi 2006)	Long-Term Monitoring (Yokus and Jur 2016; Bystricky et al. 2016; Paradiso and De Rossi 2006)

III. Equivalent Model

This chapter describes the model of the ECG system and how it is used to relate the manufacturing parameters of woven electrodes to their circuit parameters. First, the knowns, unknowns, and assumptions are defined. The set of manufactured woven electrodes are described as well as the corresponding ECG data collected previously in a human subject experiment. The equivalent model of the ECG system is explained as a parameterized transfer function in the frequency domain. The average measured waveforms are computed, and used to generate simulated waveform. The circuit parameters of the transfer function are fit by minimizing the difference between measured and simulated waveforms. Lastly the bode plot of the adhesive ECG system is provided to visualize the performance of the model across frequency.

Method of Analysis

First, we will define the knowns and unknowns. The block diagram describing the model of the ECG system as a transfer function relating inputs to outputs is shown in Figure 7. The heart produces an electrical in-body signal. This is the input waveform which is initially unknown. With the electrodes, we are able to collect a measured signal from a person on the skin's surface. This is the output waveform, which is known. The transfer function that relates the in-body signal to the measured signal depends on the parameters in the skin-electrode interface model, and the parameters of circuit model (Taji et al. 2014). All the circuitry elements are either assumed or known, and for an adhesive electrode, the skin-electrode interface parameters are known. For woven electrodes, however, the transfer functions parameters are unknown. The method of analysis will systematically solve for the unknown terms. To do this, we must describe some properties of transfer functions.

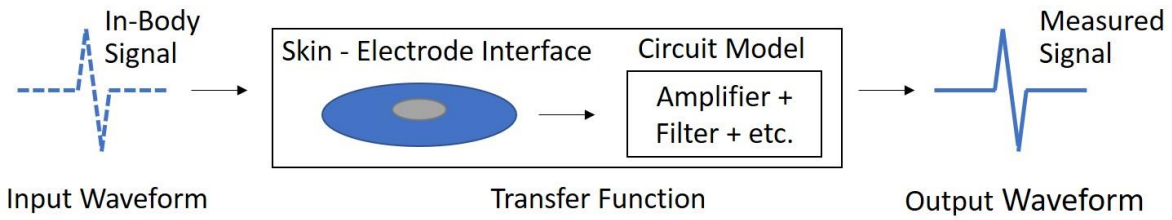

Figure 7: Notional block diagram of ECG system. $V_{out} = V_{in} * TF$
The in-body signal is an input to the transfer function, which produces a measured output signal.

This transfer function can be thought of as a three-variable system; The input, the output and the function relating them $\frac{V_{out}(s)}{V_{in}(s)} = TF(s)$ as seen in Eqn. (3). If two of the three are known it always is possible to numerically solve for the third. In our case, when the input signal is unknown, a known output signal can be propagated backwards through the known inverse transfer function to produce the input signal, $V_{in}(s) = V_{out}(s) * TF^{-1}(s)$. This will be done with data for the adhesive electrode to derive an in-body signal for each person. Similarly, when the output signal is unknown, a known input signal, such as the in-body signal, can be forward propagated through a transfer function to produce an output signal. Another way to say this is that the model is producing a simulated output waveform which would result, given the current set of parameters of the transfer function. This is useful because the parameters of transfer function can be tuned to define the shape of the resulting output waveform. When the transfer function is unknown, as is the case for the textile electrodes, the transfer function parameters can be solved by numerically fitting the output waveform with a known measured waveform. Finally, the simulated output waveforms for the textile electrodes will be analyzed to assess the relationship between the manufacturing parameters for each electrode set and corresponding skin-electrode interface parameters. The manufacturing parameters of interest are weave pattern, electrode surface area, and thread type.

Initial Assumptions

This research uses an existing textile electrode data set. Woven conductive electrodes were designed, fabricated, and used to capture human subject data by Arquilla et al. contained in references (Arquilla 2021a; Arquilla, Webb, and

Anderson, n.d.; 2021; 2020a; 2020b). Sixteen sets of conductive woven electrodes were built for a 3-lead ECG configuration. The electrodes were intentionally manufactured to investigate experimentally the manufacturing design parameters of previously stated. The woven electrodes, described in Table 3, vary in surface area (8 sizes), weave pattern (4 types), and yarn type (2 types). The conductive electrodes were integrated into a fabric structure of non-conductive cotton thread with a foam backing and a metal snap. In addition to the woven textile electrodes, a traditional adhesive electrode was captured with 5cm diameter Ag/AgCl electrodes. In total, 170 distinct data sets were collected, each lasting approximately 2 minutes (Arquilla, Webb, and Anderson 2021). Permission was given to use these datasets for this modeling effort. The electrodes were used in conjunction with the BIOPAC MP160 ECG hardware suite described in the literature review ("MP System Hardware Guide" 2015). The full description of data collection procedure is outlined by Arquilla et al. in "Detection of the Complete ECG Waveform with Woven Textile Electrodes" (Arquilla, Webb, and Anderson 2021).

Table 3: Electrode Manufacturing parameters

ID	Label	Design Area (in)	As Built Area (in)	Yarn Type	Pattern
1	Area1	1.00 x 1.00	0.50 x 1.00	Steel Spun	1/15 Sateen
2	Area2	1.33 x 1.33	0.50 x 1.33	Steel Spun	1/15 Sateen
3	Area3	1.66 x 1.66	1.00 x 1.66	Steel Spun	1/15 Sateen
4	Area4	2.00 x 2.00	1.00 x 2.00	Steel Spun	1/15 Sateen
5	Area5	2.33 x 2.33	1.00 x 2.33	Steel Spun	1/15 Sateen
6	Area6	2.66 x 2.66	1.50 x 2.66	Steel Spun	1/15 Sateen
7	Area7	3.00 x 3.00	1.50 x 3.00	Steel Spun	1/15 Sateen
8	Area8	3.33 x 3.33	1.50 x 3.33	Steel Spun	1/15 Sateen
9	1Si	1.33 x 1.33	0.66 x 1.33	Silver Nylon	1/15 Sateen
10	2Si	1.33 x 1.33	0.66 x 1.33	Silver Nylon	Broken Twill
11	3Si	1.33 x 1.33	0.66 x 1.33	Silver Nylon	Twill
12	4Si	1.33 x 1.33	0.66 x 1.33	Silver Nylon	Birds Eye
13	1St	1.33 x 1.33	0.66 x 1.33	Steel Spun	1/15 Sateen
14	2St	1.33 x 1.33	0.66 x 1.33	Steel Spun	Broken Twill
15	3St	1.33 x 1.33	0.66 x 1.33	Steel Spun	Twill

16	4St	1.33 x 1.33	0.66 x 1.33	Steel Spun	Birds Eye
17	Adh	3.04 in^2 *	3.04 in^2 *	N/A*	N/A*

* The 5 cm diameter adhesive electrode has the following electrical circuit parameters: Re = 35.2k Ω, Ce = 0.9μF, Rd = 29.5k Ω, Cd = 5.8 μF, and Ru/2+Rs+Rlead = 3.6k Ω (Assambo et al. 2007).

The weave patterns designed by Arquilla et al. are presented in Figure 8 and electrode sizes presented in Figure 9 (Arquilla, Webb, and Anderson 2021). Each pixel represents a unit square equal to the intended warp and weft spacing. Black pixels represent an anchor and white pixels represent the float of the weft yarn. The weft threads are conductive while the warp threads are non-conductive.

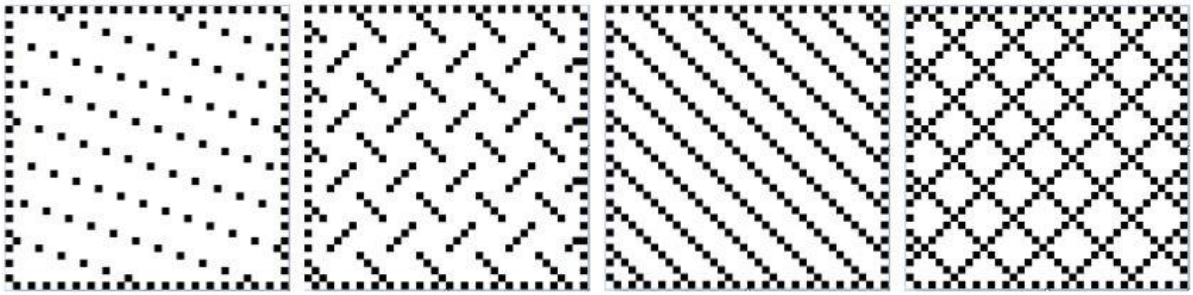

Figure 8: Pattern Types of woven electrodes. From Left to Right; 1/15 Sateen, Broken Twill, Twill, and Birdseye. Patterns not to scale.

With these pixel patterns the difference between manufactured area and the functionally conductive area can be found. Since only the weft yarn is conductive the black pixels represent anchor points where the electrode is not electrically conductive. The ratio of conductive area to manufactured area is given by the Eqn. (5) below. This ratio will be used to compute the functional surface area of a woven electrode from the manufactured surface area.

$$Conductive\ Ratio = \frac{total\ pixel - black\ pixel}{total\ pixel} \quad (5)$$

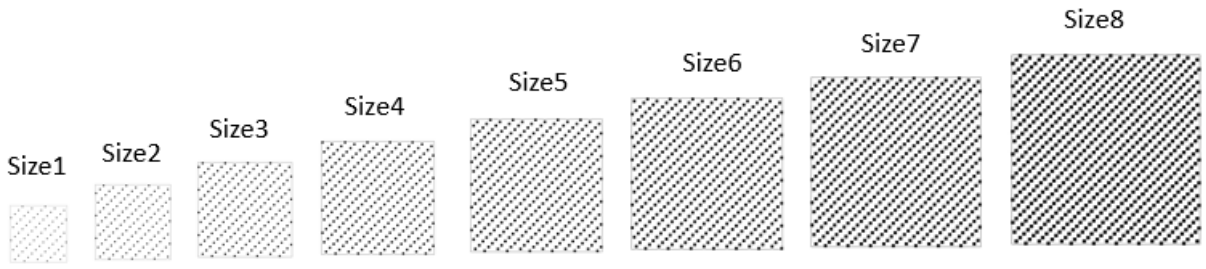

Figure 9: Relative Patch Surface Areas by design of the woven electrode. Smallest to largest from left to right.

It is worth noting a distinction between the manufactured dimensions and the designed dimensions in Table 3. All electrodes were designed to be square but during manufacturing were distorted into rectangles. This occurred due to inconsistencies in the manufacturing process of packing the weft during fabrication due to the manually intensive nature of developing these electrodes. This deviation is not the focus of this research and so the "as built" areas will be used for analysis, not the designed areas since it most accurately represents the system from which the model parameters will be derived.

The simplifying assumptions are broken into general categories: human subject, electrode, circuitry, and ECG waveform. It is outside the scope of this analysis to investigate how anthropometric characteristics effect the ECG waveform or the skin-electrode impedance. Therefore, constant values for skin properties are used across human subjects. Next, it is assumed the method of applying the electrodes to the subject was consistent. Regarding the circuitry, it is assumed the BIONOMADIX components from BIOPAC are operating as intended on the ECG waveform, and therefore can be treated as idealized components. Finally, the main method of computing input and output waveforms is done with the average waveform derived from the human subjects. The two minutes of data collection began after subjects wore the electrodes for approximately 5 minutes. Therefore it is assumed that any transient effect of the electrode being applied to the skin on the waveform had reached steady state (An and Stylios 2018). Comparing average waveforms, would reduce any other influences of outside factors while allowing the

effect of the electrode to remain. These simplifying assumptions are described in the list below.

1) Human Subject Assumptions: Skin characteristic are constant and standardized across all 170 datasets. Specifically, R_e, C_e, and R_u, are all constant throughout the analysis. Evaluation of the following characteristics is out of scope.
    a. Skin thickness (% body fat, BMI)
    b. Hairiness – smoothness versus roughness
    c. Hydration – skin moisture versus dryness
2) Electrode Assumptions: Consistent application method during testing.
    a. Consistent location placement per subject per electrode.
    b. Consistent skin pressure per subject per electrode
    c. The circuit parameters for the adhesive electrode are known (Assambo et al. 2007).
    d. Manufacturing parameters of the woven electrodes are known (Arquilla, Webb, and Anderson 2021).
3) Circuitry assumptions: Idealized BIOPAC components
    a. Circuitry remained the same for all 170 measurements.
    b. The protection circuit (PC), lead selector (LS), and isolation circuit (IC), all have negligible loss compared to gain and are excluded from the TF.
    c. The filters are assumed to be a standard 2nd order low pass, high pass and notch filters with cutoffs outside the band of the ECG waveform.
    d. The amplifier provides flat gain across in-band frequency.
4) Waveform Assumptions: The electrodes have reached steady state.
    a. The Average ECG waveform is sufficient to compare electrode's effect
    b. The Average in-body ECG Waveform is the same across datasets

Parameterized Transfer Function

The skin-electrode interface model is built from the simplified block diagram shown in Figure 3. In order to build the full ECG system another beneficial

property of transfer functions can be leveraged, the cascade. Since the transfer function relates the input to the output, sequential transfer functions can be cascaded since the output of one becomes the input to the next one. The main benefit of representing the model in this way is that sequential blocks are simply multiplied together. Using this property, the transfer function of the ECG system up to the ADC is described in Eqn. . In this equation the ECG system described from Figure 3, is defined with all its functional blocks cascaded together. The subscripts describe each block from left to right: Protection Circuitry (PC), Lead Selector (LS), Amplifier, Filter, and Isolation Circuit (IC).

$$TF_{ECG} = TF_{electrode} * TF_{PC} * TF_{LS} * TF_{AMP} * TF_{Filter} * TF_{IC} \quad (6)$$

Transfer functions PC, LS, and IC can be dropped from this analysis per assumption 3b which leaves three transfer functions for which we need to solve, The electrode, the amplifier, and the filter.

The electrode block contains the skin-electrode interface model. To build the transfer function, a pair of electrodes which connect to the differential input of an amplifier form the circuit shown in Figure 10. The input and the output voltages need to be related in terms of all intermediate circuit parameters.

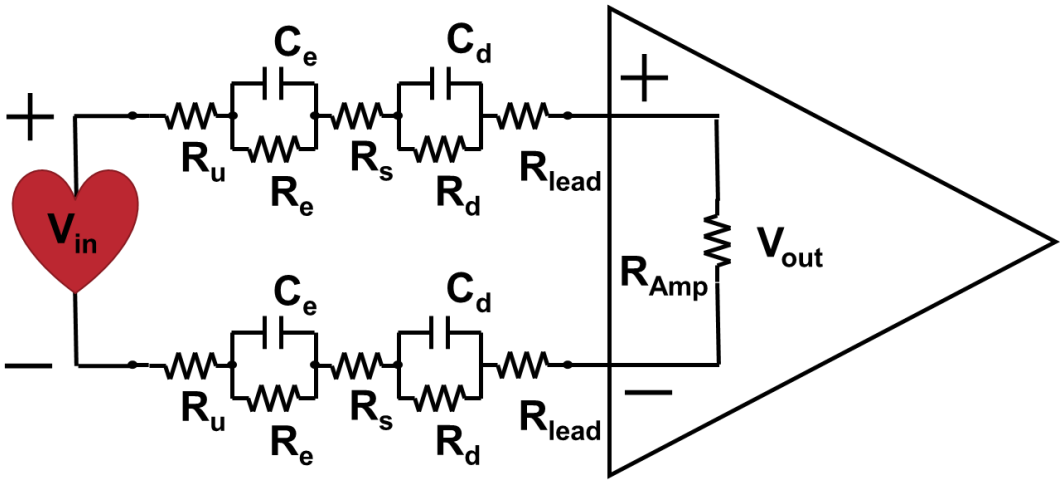

Figure 10: Electrode Circuit diagram with skin-electrode interface model

For simplicity, the circuit is condensed into a smaller form where Z_e is the cumulative impedance from the skin electrode interface model. The representation in Figure 11 shows the simplifier circuit with the input and output voltages. The circuit resembles a voltage divider.

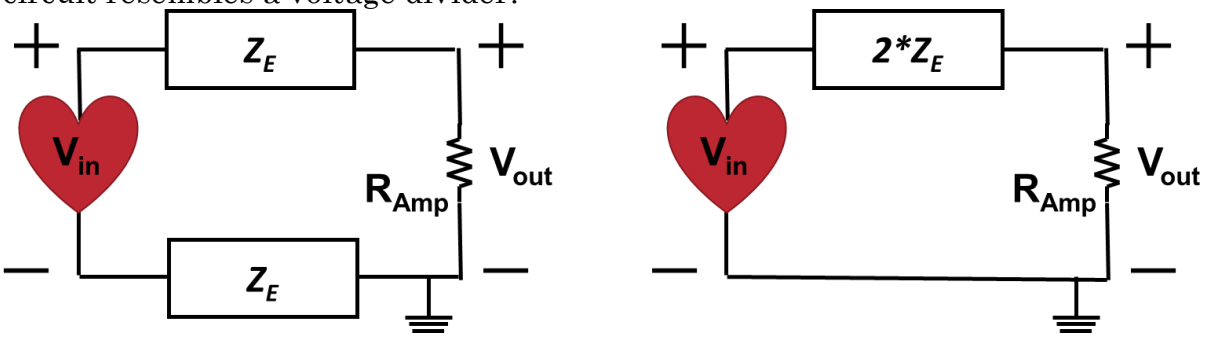

Figure 11: ECG Circuit model of Electrode interface for a single lead (Left), Simplified circuit model (right)

Using Kirchoff's current law, the input can be related to the output by equating the current flowing around the loop (Thomas, Rosa, and Toussaint 2009). Equation (7) below shows the fundamental current balance relating the input and output voltages with the circuit's parameters. The input impedance to the amplifier is R_{amp}. The frequency dependent impedance from the skin-electrode interface model in equation (2) is Z_E. Recall that Z_E is a function of s, R_{lead}, C_d, R_d, R_s, C_e, R_e, and R_u given by Table 1.

$$\frac{V_{in} - V_{out}}{2 * Z_E} = \frac{V_{out} - 0}{R_{Amp}} \tag{7}$$

By rearranging this equation such that voltage is on one side and impedance is on the other, it is possible to put this equation into transfer function notation. The transfer function for this is shown below in Eqn. (8). The transfer function depend on the A and B coefficients which themselves are dependent on R_{lead}, C_d, R_d, R_s, C_e, R_e, R_u and R_{amp} given in Table 4. These terms represent the electrical properties of the electrode, and the skin.

$$TF_{Electrode}(s, A_{0,1,2}, B_{0,1,2}) = \frac{V_{out}}{V_{in}} = \frac{R_{Amp}/2}{Z_E + R_{Amp}/2} = \frac{A_2 s^2 + A_1 s^1 + A_0}{B_2 s^2 + B_1 s^1 + B_0} \tag{8}$$

Table 4: Coefficients for electrode transfer function in terms of skin-electrode impedance coefficients

$B_2 = (R_{lead} + R_s + R_u) * R_d C_d R_e C_e + A_2$	$A_2 = \frac{R_{Amp}}{2} * R_d C_d R_e C_e$
$B_1 = (R_{lead} + R_s + R_u) * (R_e C_e + R_d C_d) + R_d R_e (C_e + C_d) + A_1$	$A_1 = \frac{R_{Amp}}{2} * (R_e C_e + R_d C_d)$
$B_0 = R_{lead} + R_s + R_u + R_d + R_e + A_0$	$A_0 = \frac{R_{Amp}}{2} * 1$

The next step is to create the transfer functions of the amplifier and filter. The amplifier and filter block parameters, (gain and cut off frequencies) are collected from the BIOPAC hardware guide ("MP System Hardware Guide" 2015). The idealized TF of the amplifier is a linear voltage gain of 2000, or 66dB from the BIOPAC circuitry, and assumed to be flat across frequency, (TF_{Amp} = 2000/1) ("MP System Hardware Guide" 2015). The filter consists of three sub filters whose order, and gain flatness are known from simplifying assumptions. The filter transfer functions are assumed to be a 2nd order high pass, low pass and notch filters cascaded together shown below in Equation (9). Here ω_H is the high pass cut off frequency, 1Hz, ω_L is the low pass cutoff frequency, 35Hz, and ω_N is the notch frequency, 60Hz, d is the damping factor, 1, and b is the notch bandwidth, 2Hz.

$$TF_{Filter} = TF_{HPF} * TF_{LPF} * TF_{BSF} = \frac{1}{1 + 2d\omega_H + {\omega_H}^2} * \frac{{\omega_L}^2}{1 + 2d\omega_L + {\omega_L}^2} * \frac{1 + {\omega_N}^2}{1 + b + {\omega_N}^2} \quad (9)$$

The transfer functions of the electrode, filter, and amplifier cascaded together form the transfer function of the full ECG system show in Equation (10) as dependent on knowns and unknowns. The entire system depends on the parameter terms given in Table 5 which are known from literature or assumed in the simplifying assumptions. In the instances where the adhesive electrode is used, the C_d, R_d, and R_s terms are known, but for all the remaining electrodes these terms are unknown.

$$TF_{ECG}(knowns, unknowns) = TF_{electrode} * TF_{AMP} * TF_{Filter} \quad (10)$$

Table 5: Parameters of the full ECG System, with constant and variable terms identified

Knowns										
R_{lead}	C_e	R_e	R_u	R_{amp}	*Gain*	ω_H	ω_L	ω_N	*d*	*b*
10Ω	0.9uF	35.2kΩ	2.6kΩ	2.6kΩ	66dB	1Hz	35Hz	60Hz	1	2Hz
Unknowns										
s, C_d, R_d, Rs										

The complete ECG transfer function model shown in Eqn. (10) is built in MATLAB (all code in Appendix A), using the function `tf([num],[den])`. Here each block is built individually. For the electrode's transfer function [num] is a 1x3 matrix with the A coefficients in the numerator, and [den] is a 1x3 matrix with the B coefficients in the denominator and s is implicitly defined. The inverse transfer function is formed by inverting the numerator and denominator inputs. The same applies to the transfer functions for the filter and amplifier. This is a generalized function in variable form. For simplicity, when the parameters of the transfer function are set for a specific electrode type, the transfer function will be referred to as that electrode's transfer function. As an example, the skin-electrode interface parameters for a standard adhesive electrode are known. By plugging in these known values for the terms C_d, R_d, and R_s, the adhesive electrode's transfer function is the transfer function describing the ECG system when adhesive electrodes are used. Similarly, the adhesive waveform refers to the ECG waveform that was captured with the adhesive ECG system.

Average ECG Waveform

To characterize the effect of the electrode on the ECG system, an average ECG waveform was generated from the 2 minutes of ECG data per subject per electrode. By computing the average waveform, the ECG signal as augmented by the electrode remains while the effects of noise artifacts and human subject variation are reduced. Further this allows this method to be robust to differences collected across different data collection trials. The average ECG waveform is

defined in this paper as the mean PQRST waveform produced during the 2-minute collection. This is extracted by finding the R-peaks of each ECG waveform, aligning them in time based on R-peak prominence, and then taking the average. The peaks are found using the function `findpeaks()` in conjunction with the function `isoutlier()`. These two functions will ensure only high-quality R-peaks are identified and minimized the number of errant waveforms retained (e.g., a motion artifact incorrectly identified as an R-peak). Figure 12 shows two example datasets, the left with minimal noise, and the right with a significant noise artefact. It can be seen that the motion artefact is not retained for analysis, and thus does not distort the average waveform. The corresponding average waveforms are shown as well as the frequency spectrum of the ECG data. This process is performed for each of the 170 datasets. The averaged ECG waveform was passed forward and backward through the various transfer functions. It is also used to evaluate the fit of the transfer function parameters by comparing the average waveform to the simulated waveform produced with the fit parameters.

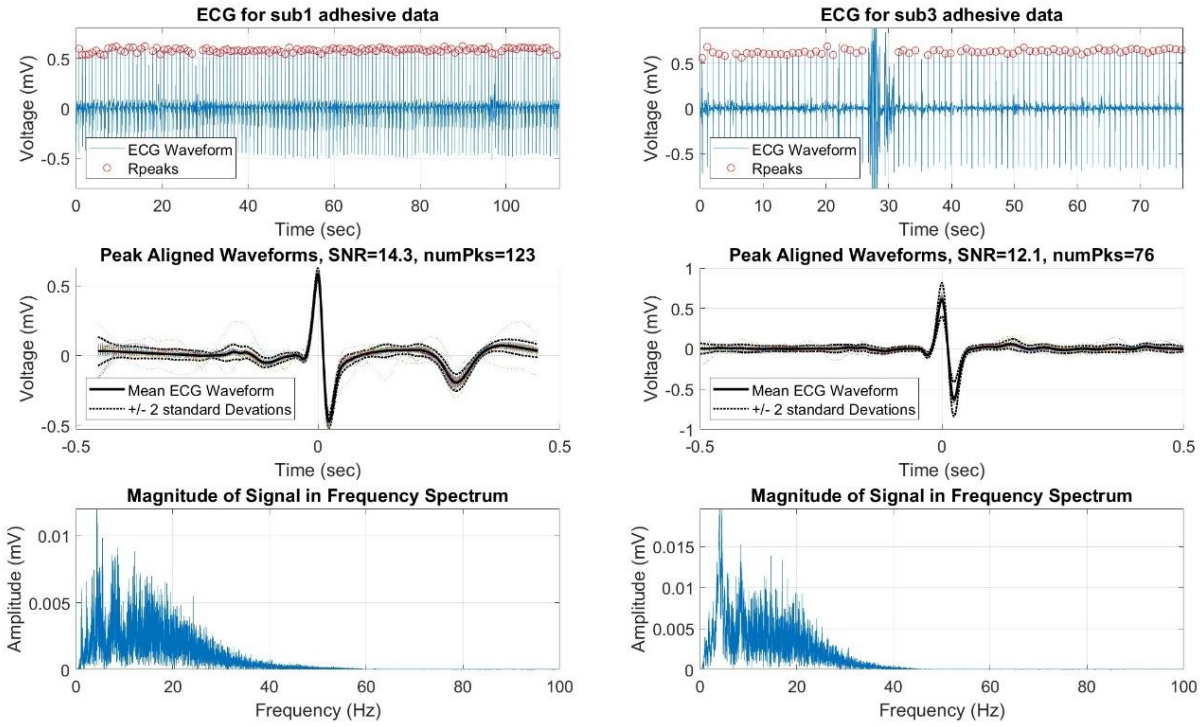

Figure 12: Measured ECG data from 2 human subjects with adhesive electrodes, (Left: Subject1, Right: Subject 3), (Top: Raw Data, Middle: Average Waveform, Bottom: ECG Spectrum)

After calculating the average waveform, to ensure high quality waveforms were used, the signal to noise ratio was computed. In Figure 12 subject 1's waveform (the left column) has a SNR = 14.3 and was computed from 123 R-peaks, while subject 3's waveform (right column) has SNR = 12.1 and was computed from 76 R-peaks. Any average waveform with SNR < 0 or fewer than 30 R-peaks, was excluded from consideration. Of the 170 datasets, none of the adhesive datasets were eliminated. It was found that four subjects only had two or fewer average signals that met these criteria (out of the 16 data sets collected per subject). With these criteria, four subjects, ID3, 5, 7 and 10 from Arquilla et al., were removed from this analysis. This means that 170 minus 64 equals 106 datasets, which were used for analysis. Of the 6 remaining subjects, an additional 24 did not meet the criteria so were not used for fitting, but were included in the analysis of results

In-Body Signal

With the adhesive transfer function and measured waveform identified, the raw signal can be found. In MATLAB the tool to simulate a time domain response from a frequency domain transfer function is `lsim(sys,U,T)`. This function performs either operation: $V_{out} = TF * V_{in}$ or $V_{in} = TF^{-1} * V_{out}$. In this function, the sys variable needed for the lsim function is generated by the `tf()` function. U the amplitude vector of the mean waveform signal, and T is time vector of the mean waveform signal. The result is an amplitude vector of the same length as the U vector. Figure 13, shows the block diagram of identifying the raw in-body signal from the measured adhesive data and the adhesive transfer function. This raw signal is assumed to be the same for all measurements per human subject. By solving for the initially unknown in-body signal, it can then be used to solve for the transfer function parameters of woven electrodes.

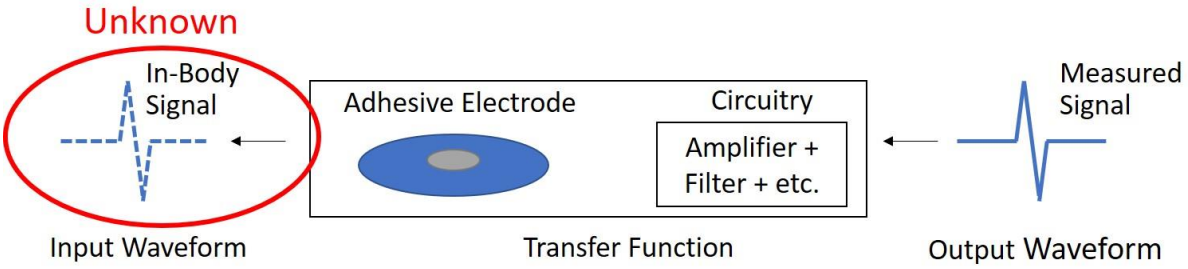

Figure 13: ECG system with adhesive electrode performing the function of: $V_{in} = TF^{-1} * V_{out}$

Textile Transfer Function,

This subsection describes the process of identifying the parameters of the textile transfer function and correspondingly the circuit parameters for a particular woven textile. The block diagram shown in Figure 14, depicts a woven electrode ECG system with, unknown parameters, producing some simulated output. The transfer function is unknown for a textile electrode, but with the input and output voltage waveforms, it is possible to solve for the transfer function through numerical iteration. The basic algorithm is to 1) start with a "guess" for the unknown parameters, 2) produce a simulated output using the known input signal,

3) compute an error term from the difference between measured and simulated data, 4) repeat this process by tuning the guessed parameters until the error term reaches a minimum. Once this state is reach, the circuit parameters are saved as the best fit for the particular measured textile type. An optimizer function iterates these steps automatically and returns the numerically solved values. Though the figure below indicates the woven electrode parameters are "unknown", it is possible to input any variables into the transfer function and create a corresponding simulated waveform. The iterative process keeps track of which set of parameters produced the most accurate simulated waveform, and thereby identifies the unknown terms.

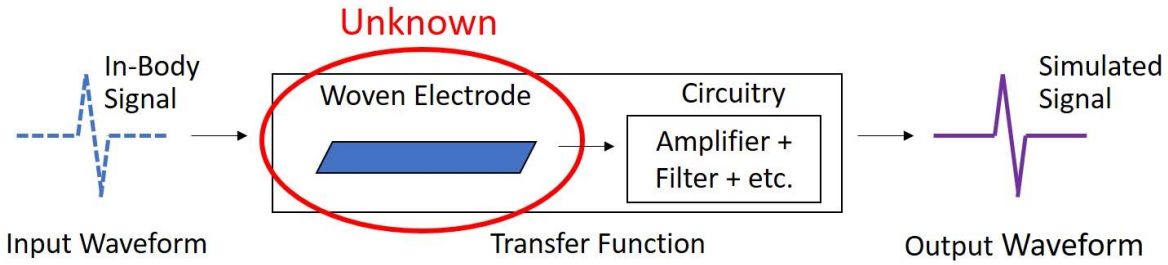

Figure 14: ECG system of Textile electrode implemented with the best fit circuit parameters producing the corresponding Simulated waveform

The key function used to tune the parameter is the MATLAB optimizer `fmincon(FUN,X0,BOUNDS)`. This function finds a constrained minimum of a provided function for multiple variables. The first input to fmincon, FUN, is the error function. The error function, shown in Eqn. (11), is the normalized sum of square differences between the measured and simulated waveforms. When the error is zero, then the simulated and measured waveforms are identical. The more different the two signals are from one another the larger the error. This function will identify the parameters which minimize the error term.

$$Normalized\ Error = \sum \left| \frac{V_{Measured} - V_{simulated}}{\max(V_{Measured})} \right|^2 \qquad (11)$$

The next input to fmincon, X0, is the starting parameters, or the initial guess. The parameters, C_d, R_d, and R_s of the interface model are tuned by the optimizer to minimize the normalized error. All the other values of the model are kept constant. The last input to fmincon, BOUNDS, is the upper and lower bounds of the tuning parameters. This sets limits around what specific values are allowed by the optimizer. When fitting the parameters, X0, is initially a random number between the bounds. The upper bounds for the tuning parameters are 1uF, 50 MΩ, and 50 MΩ, and the lower bounds are 1nF, 1kΩ, and 1kΩ for C_d, R_d, and R_s respectively. These bounds were set such that the optimizer could produce a result which did not hit the bound. The function fmincon returns the parameters which drive the error closest to zero, and correspondingly best fit the data.

Since the electrodes are the same between subjects, the transfer function parameters must also be the same. Therefore, by performing this process across all human subjects, a set of parameters which produces the overall lowest error represents the most accurate circuit model of the electrode. To fit the transfer function across subjects, the sum of the individual subject errors was minimized. This concepted is depicted below in the block diagram of Figure 15.

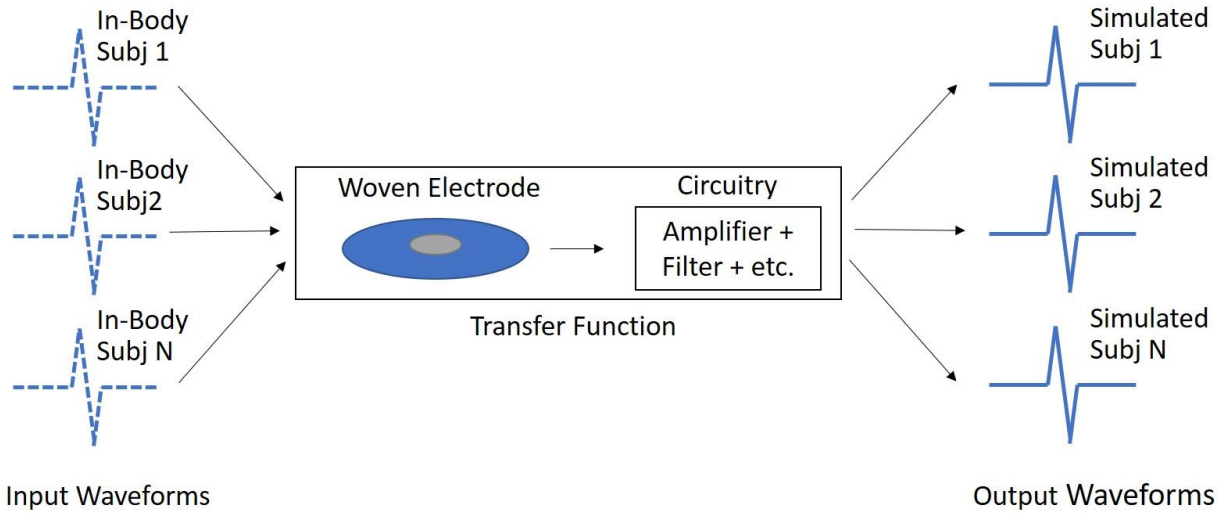

Figure 15: Transfer function model for a single Electrode fit across subjects

In other words, the errors of all 6 subjects are calculated with fmincon, and those individual errors are added together. The parameters which produce the lowest total error are selected as the parameters which best describe the particular textile. This process is repeated for each of the 16 woven electrode types. The circuit parameters, R_d, C_d, and R_s, fit across subjects are presented in the results in Table 6 along with the corresponding Z_E impedance expressed as magnitude and phase.

Frequency Response

A bode plot is a common method of graphing the frequency dependence of a transfer function. This plot relates in decibels how the output voltage is related to the input voltage across frequency. In Figure 16, the magnitude and phase of the adhesive ECG system is plotted against frequency. For this bode plot, magnitude indicates the gain or loss of the signal as it passes through the ECG system while phase indicates the delay of the signal as it passes through the ECG system.

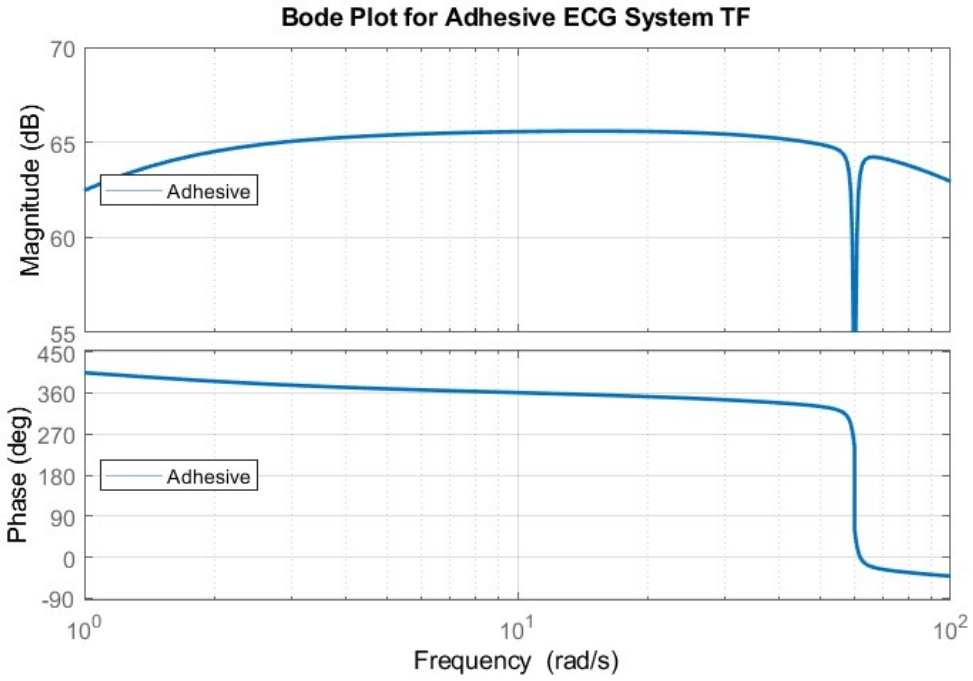

Figure 16: Bode Plot for Adhesive ECG system

The adhesive ECG system has a relatively flag magnitude across in-band frequency with the 66dB gain from the amplifier and approximately 0.5dB loss.

There is a clear notch cutout at 60Hz, and there is magnitude roll off at the lower and upper edges of the band from the filter. The phase of the adhesive system is similarly flat across frequency with a sharp transition at the notch. From this plot it is apparent that the in-band frequency is from about 2 Hz up to about 50 Hz. Since impedance is frequency dependent, for simplicity magnitude and phase in the results section will be shown at 25Hz. This frequency was chosen because it is roughly in the center of the ECG waveform's frequency content as shown in Figure 12 and the ECG systems response is relatively flat across at 25Hz as shown in Figure 16. The bode plots of all 16 woven electrode ECG systems are presented in Appendix C. The parameterized model of the ECG system has been presented. Next the results of fitting this model to woven textile data will be analyzed.

IV. Analysis of Results

In this chapter, the results of this research are presented and analyzed. First the fit circuit parameters from the skin-electrode interface model are given for each of the 16 types of woven electrodes. The measured versus simulated waveforms for the six best fits and six worst fits are show in Figure 17 and Figure 18, with the complete set of fit waveforms displayed in Appendix B. A brief analysis is provided of how each manufacturing parameter (yarn, pattern, area) is related to the fit circuit parameters. Last, the model is validated through a leave-1-out cross validation (LOOCV) scheme to confirm the models intended ability to predict waveforms.

The fit circuit parameters, C_d, R_d, and R_s of each electrode type and the corresponding impedances, Z_E, are shown in Table 6. These parameters were fit using the criteria of SNR > 0dB and number of peaks > 30, so not all 6 subjects were used to perform the fit. The skin-electrode impedance Z_E, from Eqn. (2), is calculated from the fit parameters and is expressed in phasor notation as a magnitude, A, and phase, θ, given by $Z_E = Ae^{i\theta}$. The magnitude of impedance represents the cumulative resistance experienced by a time varying signal. The phase of impedance represents the shift in degrees between the voltage across the skin-electrode interface and the electrical current through the interface. Since there is some capacitance there is a small amount of phase delay by the current following the voltage.

Table 6: Fit Circuit Parameters and corresponding Electrode Impedance at 25Hz using SNR and number of peaks criteria. Adhesive electrode parameters are included here for convenient comparison.

Label	Cd (nF)	Rd (MΩ)	Rs(MΩ)	$\lvert Z_E \rvert$ (MΩ)	$\angle Z_E$ (deg)
Adh	5800	0.0026	0.001	0.00935	-57.59
Area1	2.6	10.20	34.69	35.34	-3.79
Area2	4	19.93	13.17	13.39	-6.80
Area3	7.6	16.67	14.48	14.55	-3.30
Area4	5.1	10.90	13.50	13.70	-5.23
Area5	6.4	14.38	11.42	11.53	-4.94
Area6	4.1	22.04	12.46	12.67	-7.03

Area7	17.9	8.80	11.06	11.09	-1.87
Area8	7.1	5.40	8.49	8.69	-5.85
1Si	9	6.15	6.14	6.26	-6.47
2Si	4.5	44.46	18.28	18.38	-4.48
3Si	7.7	5.98	10.03	10.18	-4.62
4Si	6.1	8.81	13.99	14.15	-4.20
1St	3.1	21.71	17.65	17.96	-6.47
2St	8.9	49.98	15.11	15.14	-2.74
3St	6.5	49.99	13.74	13.80	-4.09
4St	9.7	21.34	17.89	17.93	-2.12

Note: This magnitude and phase are of the impedance of Z_E, in units of MΩ and degrees and are not the same metric as the magnitude and phase in the bode plot, which are in units of gain in dB and degrees.

Using these fit circuit parameters, the corresponding simulated waveforms are shown. The six best fit simulated waveforms which produced the lowest errors are shown below in Figure 17. Note the different Y-axis of each waveform. The amplitude of each ECG waveform is a product of each subject and the corresponding electrode used for collection. Subject 2 appears in four of the top six best fit waveforms. The normalized sum of squared differences (SSD) cost term is shown for each plot. Of note, the Area 4 electrode type occurs 3 times in the top 6 best fit cases.

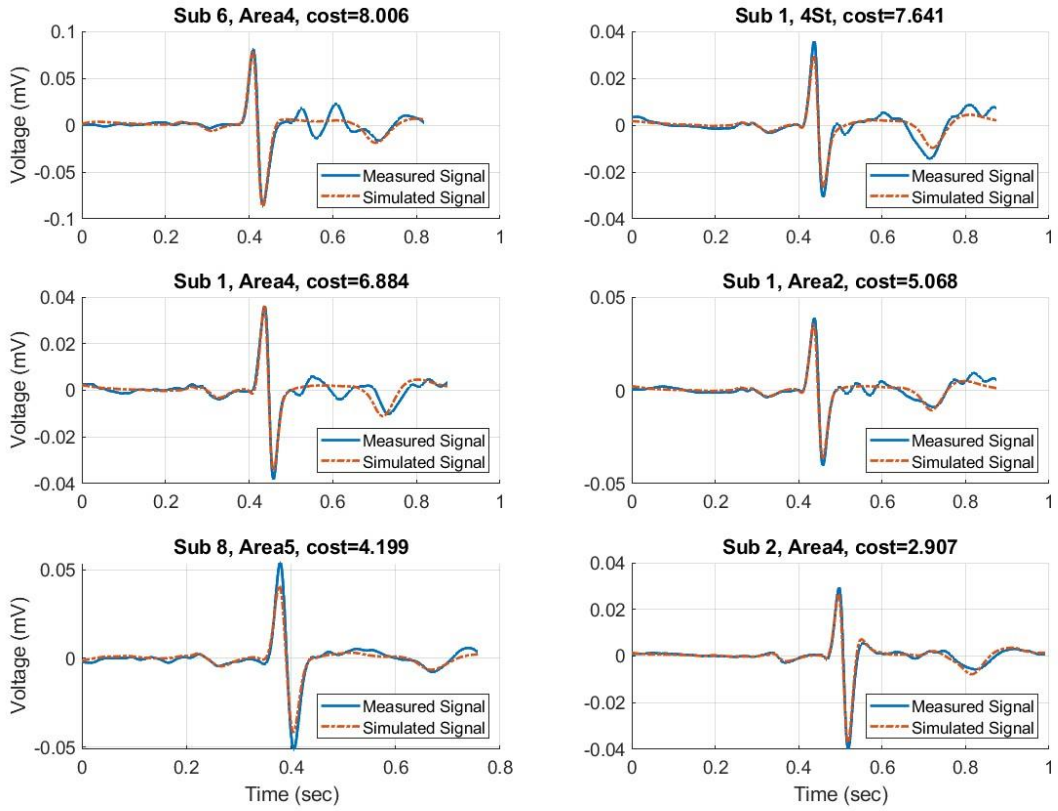

Figure 17: The 6 best fit simulated waveforms with their corresponding measured waveforms

The worst fit simulated waveforms which produced the highest errors are shown below in Figure 18. These errors are dominated by either an under amplification of the R-peak or a poor shape fit. The model optimizer attempts to produce the lowest error across subjects by using the normalized error function in Eqn. (11). The normalized cost function was chosen so that the model would not disproportionately favor or penalize ECG waveforms for having larger or smaller amplitudes respectively. Of the 96 electrode types, the Area 1 electrode type occurs twice in the top 6 worst cases, and 3 times in the top 10 worst cases. Silver threaded Broken Twill, (2Si) also appears twice in the top 6 worst cases.

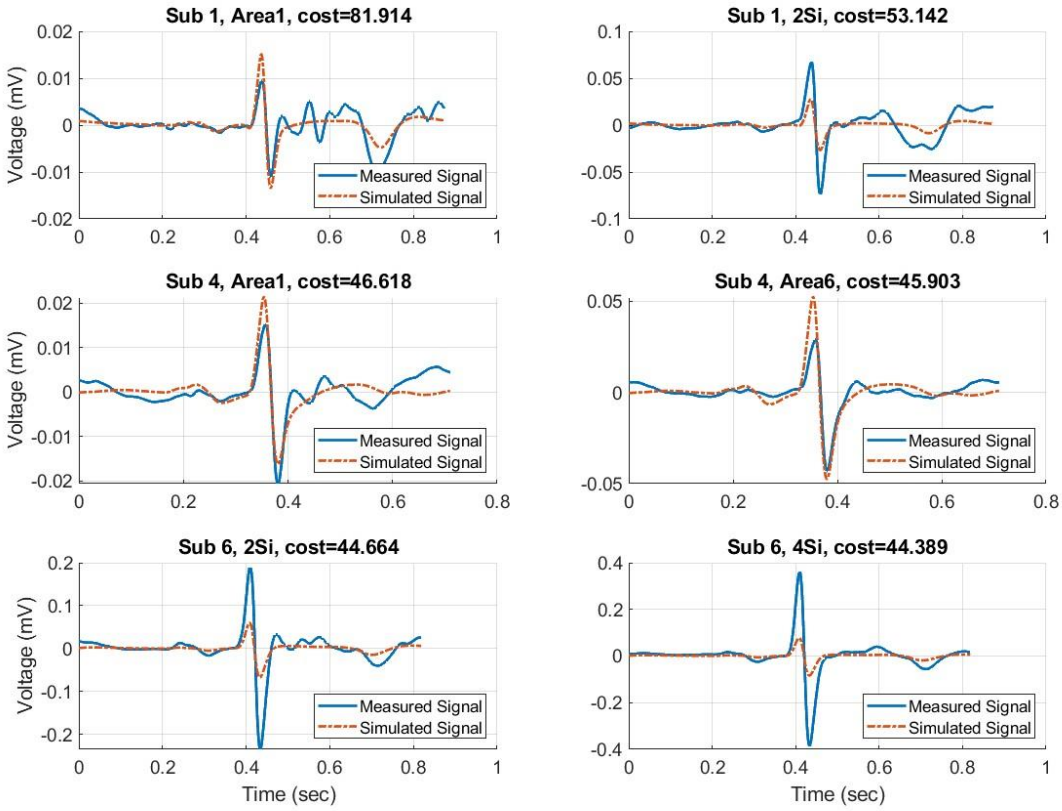

Figure 18: The 6 worst fit simulated waveforms with their corresponding measured waveforms

Area Analysis

The first analysis is of the manufacturing parameter of surface area. Another way to view the variation between the subjects of the measured waveforms is to plot the measured R-Peaks across the manufactured areas. Figure 19 shows the measured R-Peak magnitude of each mean ECG waveform for each subject specific to the Area type electrodes. Subject 9 clearly has the highest amplitude R-peaks followed by subject 6, while the rest of subjects have similar amplitude peaks. In this plot, despite the shifts in amplitude among subjects, there is a slight upward trend as area increases.

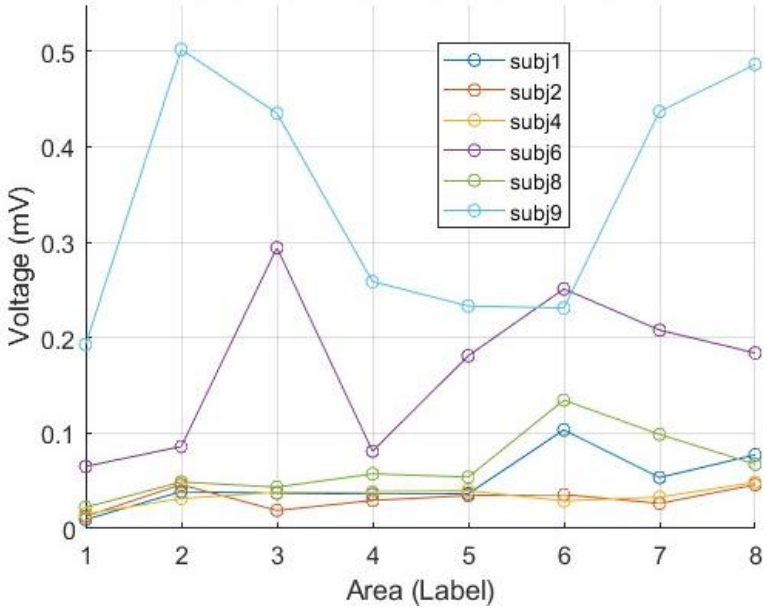

Figure 19: R-Peaks of Measured ECG Waveforms

Next the manufactured area is plotted against the circuit parameters. In Figure 20, and Figure 21, yarn type (Spun Steel) and pattern type (1/15 Sateen) are kept constant while area is swept from sizes 1 through size 8 as shown in Table 6. Here the as-manufactured areas are plotted against the skin-electrode interface impedance. Two sets of Z_e parameters are shown, when the parameters are fit using the SNR and number of peaks criteria as indicated in Table 6, and then when the parameters are fit for all 6 subjects regardless of their criteria. This was done to demonstrate the stability of the model predictive capability.

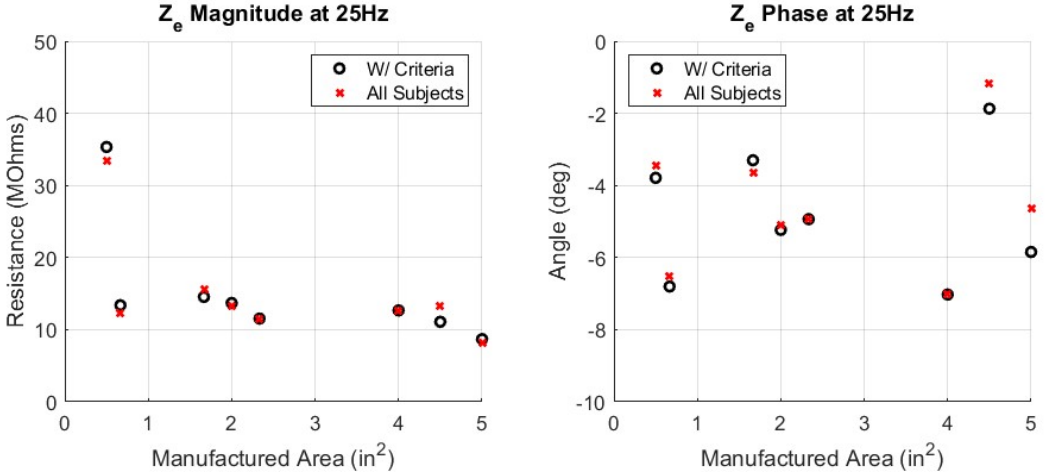

Figure 20: Surface Area Comparison versus impedance Ze;
Yarn = Spun Steel, Pattern = 1/15 Sateen, Magnitude (left) and Phase (right)

The first trend is that as area increases, the magnitude of the impedance decreases and phase stays relatively the same. The width and length of the eight electrodes manufactured for the area sweep should also be noted. Though it is true that area increases for each type, the warp dimension does not monotonically increase like the weft direction does. This inconsistency creates three subgroups among the eight area swept electrodes. The first group consists of Area 1 and 2 with side length 0.5 in. The second group is Area 3, 4 and 5 all with side length 1 in. The last group is area 6, 7, and 8 with side length 1.5 in. These groupings are apparent in the plot of the magnitude of the impedance. The span of impedances, excluding area 1, is approximately 5MΩ. Within each sub-group the trend of decreasing impedance is also valid. Though the change from Area 1 to Area 2 is much greater than the spans between other subgrouping.

The fit circuit parameters of the area sweep are shown in Figure 21. Two sets of parameters are shown. The first set uses the criteria and matches Table 6 data. The second set is from fitting the parameters when all 6 subjects are used. The general trends indicate that as the area of a woven electrode increases, the capacitance C_d increases, while the resistance R_s and R_d decrease. The series resistance term, R_s, appears to strongly dominate the magnitude of impedance Z_E. The capacitance values range from as low as 2.6nF with the lowest area up to 7.1nF at the largest area, with a notable exception of the area7 electrode having a capacitance of 17.9nF. The comparison of using the criteria versus using all subjects for fitting the circuit parameters was only performed on the area swept electrode types.

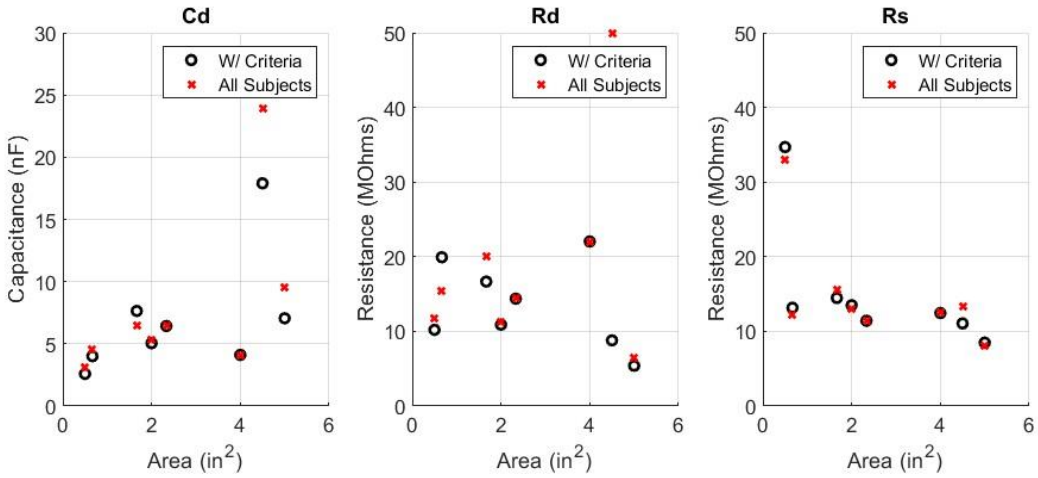

Figure 21: Surface Area Comparison versus Circuit Parameters; Yarn = Spun Steel, Pattern = 1/15 Sateen, Cd (left), Rd (middle) Rs (Right)

Yarn Analysis

The next design parameter comparison in Figure 22 and Figure 23 show yarn type and pattern type when manufactured area is constant. For these plots manufactured area is approximately 0.9 in² for all eight electrode types. Recall that the two yarn types, were silver coated nylon with a resistivity of 13 Ω/ft and spun steel with a resistivity of 28 Ω/ft. The first figure shows the magnitude and phase of the skin-electrode interface impedance. Of the 4 pairs of silver/steel electrode pairs, 3 of the silver electrodes (red) have a lower magnitude impedance than the steel electrodes (blue). With the Silver broken twill being the single case of higher impedance than Steel Broken twill. The span of impedances between steel and silver thread type pairs is greatest in the 1/15 Sateen pattern, at nearly 12MΩ. Whereas the span for the other 3 pairs is more consistently around 3MΩ. The phase of 3 out of 4 of the silver electrodes is more negative than the phase of the of the steel electrodes, but are nearly equivalent spanning a couple degrees or less. Of note, the electrodes labeled 1St and 1Si have similar phase, and the markers simply overlap in the figure. Silver impedance has a wider span than steel across patterns, with 2Si having the largest impedance, and 1Si having the smallest impedance. The span is of silver is 12MΩ while the span of steel is 4MΩ.

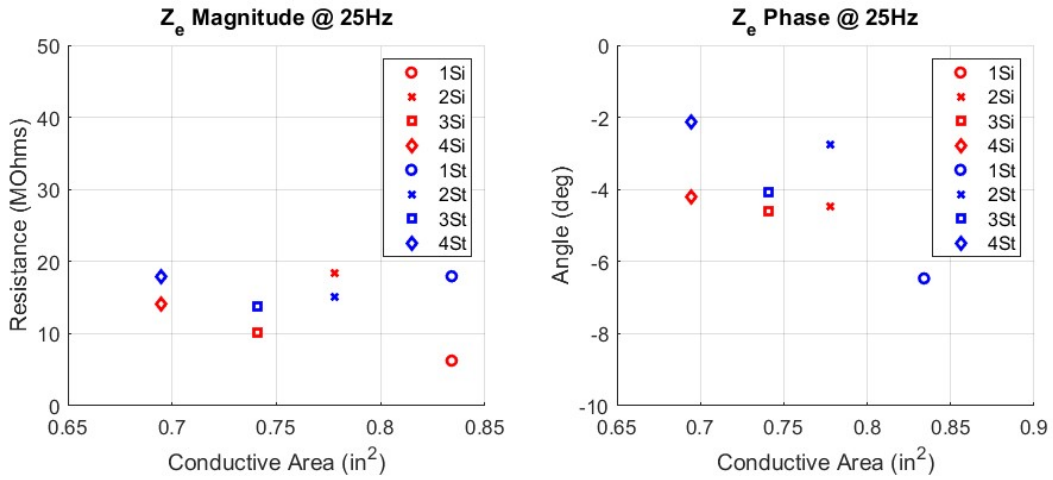

Figure 22: Pattern and Yarn type Comparison versus Impedance Ze, Manufactured Area = 0.9 in²; Magnitude (left), Phase (Right)

With the circuit parameters shown in Figure 23, capacitance does not appear to depend on yarn type since steel is more capacitive in half the pairs while silver is more capacitive in the other half. Unlike with impedance steel has a slightly wider span of capacitance with both the largest and smallest capacitance, for a span of 6nF compared to Silver's span of 4.5nF. For parallel resistance R_d all 4 pairs show silver yarn has a lower resistance than steel yarn. For the series resistance R_s 3 of the 4 pairs show that silver yarn has a lower resistance than steel yarn. Just like with the area sweep, R_s dominates the impedance, while steel has a span of about 4MΩ.

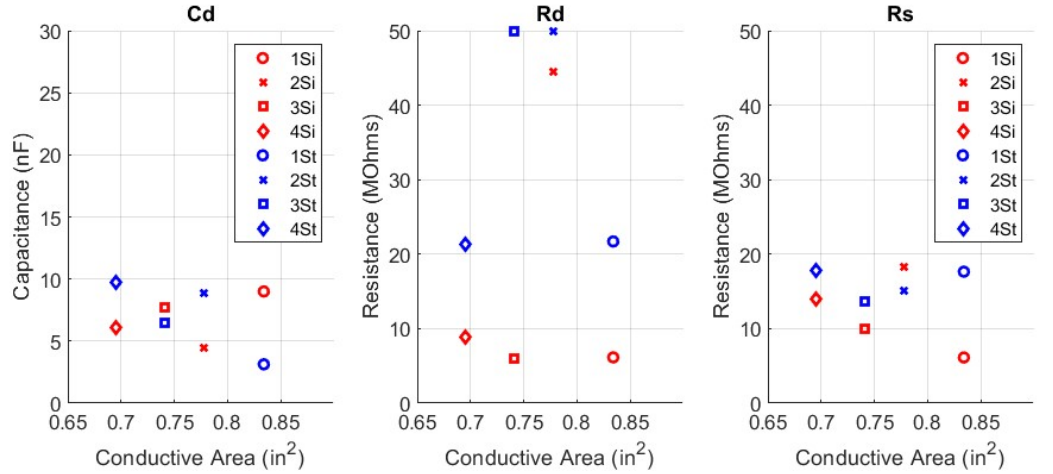

Figure 23. Pattern and Yarn type Comparison versus Circuit parameters, Manufactured Area = 0.889 in²; Cd(Left) Rd(middle), Rs(Right)

Pattern Analysis

For the pattern analysis the same figures from the yarn analysis are used. First, recall Figure 8 which shows the pixel patterns of the 4 pattern types and the distinction between an electrode's manufactured area and its conductive area. The manufactured area, 0.9 in^2, is scaled by the conductive ratio in Eqn. (5) for each pattern type. Table 7 below shows the conductive ratio for each of the pattern types and the corresponding conductive surface areas.

Table 7: Pattern type breakdown for functional conductive area, manufactured area = 0.889 in^2

Pattern	Anchor Count	Total Pixel	Conductive Ratio	Conductive Area (in^2)
1/15 Sateen	80	1296	0.938	0.824
Broken Twill	162	1296	0.875	0.768
Twill	216	1296	0.833	0.732
Birdseye	283	1296	0.781	0.686

In Figure 22 the four patterns are plotted by their conductive areas. The smallest area is birdseye with the diamond mark, next is twill with the square marker, then broken twill with the x marker, and the largest area is 1/15 sateen with the circle marker. In a similar fashion to the area sweep, when the pattern types are plotted by their areas, a slight downward sloping trend in impedance is visible. This trend is less apparent than in the area sweep because the relative areas a much closer together. The largest conductive area pattern is the silver 1/15 sateen, and it also has the lowest impedance at 6.3MΩ. Meanwhile the smallest conductive area pattern is steel birdseye, which has a relatively higher impedance of 18MΩ. The trends in phase are flat with area spanning only a couple degrees across pattern types. In Figure 23 R_s indicates a slight downward trend with conductive area that matches the impedance trend. The span in R_s is about 12MΩ from max to min. The capacitance shows a slight downward trend with conductive area. The highest capacitance is from steel birdseye, the pattern with the smallest conductive area. The smallest capacitance is from Steel 1/15 Sateen, the pattern with the largest conductive area.

Leave One Out Cross Validation

The goal of LOOCV is to evaluate how well the predictions made by the model match the observed data. The basic process is to sequentially exclude each subject during the fit optimization step. Then to use the fit parameters to simulate a waveform for the subject which was excluded. The root means squared error (RMSE), shown in Eqn. (12), between measured and simulated waveforms is calculated. Here n is the number of samples in the average ECG waveform. After every subject has been excluded once, and their RMS error is calculated, the square root of the average of the RMSEs is computed for each electrode type.

$$RMSE = \sqrt{\frac{\sum_n((V_{meas} - V_{sim})^2)}{n}}\,[mV] \qquad (12)$$

Below is which depicts the RMS errors. The right most column is the average of the RMS errors for each electrode type. The column for each subject lists the RMS error when that subject was excluded from the optimizer fit. Since the previous criteria was to only include subjects, whose mean waveforms exceeded an SNR greater than 0dB, not all other subjects were used in the fitting. As an example, for the Area 1 electrode type, subjects 8 and 9 did not produce waveforms with SNR > 0dB so they were not used for fitting the parameters. On t row only subjects 1, 2, 4 and 6 produced passing waveforms and therefore the LOOCV iterated across this subset of subjects to determine the fit parameters. The subject 1 column for the Area 1 row is the RMSE when the parameters were fit with subjects 2, 4, and 6. The subject 2 column is the RMSE when the parameters with fit with subjects 1, 4 and 6. The subject 8 column is the RMSE when the parameters were fit with subjects 1, 2, 4 and 6. To indicate this nuance the subjects not used for fitting are colored grey. These greyed cells further validate the predictive strength of the model. From this validation analysis it is apparent that across subjects, subject 9 is the poorest fit, and across electrode types, and subject 2 is the best fit subject across electrodes. The

four silver electrodes are the four poorest fits across subjects. The mean RMSE column indicates the cumulative quality of the fit terms across all subjects. This indicates an overall good fitting function.

Table 8: Leave One Subject Out Cross Validation Results

Label	RMSE of Excluded Subject (mV)						$\overline{RMSE}$
	1	2	4	6	8	9	
Area1	0.003	0.003	0.004	0.015	0.005	0.038	0.012
Area2	0.007	0.011	0.009	0.020	0.010	0.104	0.027
Area3	0.007	0.005	0.008	0.059	0.009	0.083	0.028
Area4	0.007	0.006	0.010	0.017	0.012	0.051	0.017
Area5	0.007	0.008	0.009	0.036	0.010	0.047	0.020
Area6	0.021	0.008	0.007	0.050	0.025	0.046	0.026
Area7	0.011	0.005	0.010	0.040	0.019	0.091	0.029
Area8	0.015	0.010	0.010	0.037	0.015	0.095	0.030
1Si	0.015	0.013	0.015	0.091	0.018	0.162	0.052
2Si	0.016	0.003	0.008	0.042	0.007	0.155	0.039
3Si	0.016	0.010	0.009	0.073	0.012	0.092	0.036
4Si	0.008	0.005	0.013	0.072	0.007	0.235	0.056
1St	0.018	0.004	0.006	0.021	0.021	0.046	0.019
2St	0.005	0.005	0.006	0.035	0.011	0.030	0.015
3St	0.003	0.003	0.005	0.037	0.006	0.023	0.013
4St	0.007	0.004	0.003	0.021	0.008	0.116	0.026

The specific parameters C_d R_d and R_s computed at each iteration of the LOOCV are shown in Appendix D. The mean and standard deviation of the circuit parameters are also recorded.

V. Discussion, and Conclusion

The primary contribution of this research is the development of the equivalent model of the ECG system. The engineering objective was to construct a computational model from first principals which could describe conductive woven electrodes. This objective was completed. The relationships between manufacturing

parameters and circuit performance have not been characterized for textile electrodes in prior work. Now new insights are possible regarding how the manufacturing parameters of woven electrodes impact their ability to capture ECG waveforms. The performance of the model was confirmed with a leave one out cross validation test.

The first insights come in the form of the two hypotheses which were investigated after the completion of the engineering objective. The first hypothesis considered if the circuit parameters of the skin-electrode interface model could explain the electrical behavior of woven textile electrodes. This was confirmed by the model's ability to accurately simulate ECG waveforms. The LOOCV scheme validated the model's predictive strength, even for subjects which were not used to fit the model's parameters. Because the model was built from first principles, a larger number of subjects, would only improve the model's ability to fit and simulate accurate waveforms.

The second hypothesis considered if the circuit parameters of the skin-electrode interface model could be related to the manufacturing parameters. By building a parameterized transfer function it is possible to peer inside the transfer function and observer how, and if, the circuit parameters are related to the manufacturing parameters. Furthermore, the robustness of the model ability to predict parameters was demonstrated by removing the conservative criteria of poor-quality waveforms. The resulting parameters remained relatively constant.

For each of the three manufacturing parameters, there are interesting conclusions to discuss. The effect of the surface area of the electrode behaved in a manner consistent with that of the equations for parallel plate capacitor and a volume resistance. The capacitance of a parallel plate capacitor is directly proportional to the area of the plates. The plates in this context are the conductive surface area of the electrodes. The resistance of a volume is inversely proportional to the surface area of that volume. The volume in this context is the conductive

thread. The main observation from the area analysis is that a larger area patch, will have a higher capacitance and a lower resistance. As such, the smaller patches will collect lower amplitude waveforms through signal attenuation and capture more high frequency noise. The larger patches will collect larger amplitude waveforms, due to less signal attenuation and collect more low frequency noise. These relations are consistent with hypothesis 2. The insights about electrode area producing larger amplitude waveforms have been experimentally observed by others (Yokus and Jur 2016; Arquilla, Webb, and Anderson 2021).

For Yarn type the two yarns have the same yarn diameter, but different resistivities. The resistance of a volume is directly proportional to the resistivity of that volume. Resistivity does not appear in the equations for capacitance, and correspondingly we do not see a big trend in capacitance or phase with yarn type. The main observation from the yarn analysis is that electrodes with lower resistivity yarn will have a lower resistance, and a lower Z_E impedance but unchanged capacitance. Lower resistivity means less signal attenuation for both the ECG waveform and the noise. This is also confirmed by observing the relative spans of impedances between silver and steel yarns. Silver yarn has more varied impedance than steel, implying there may be more noise impacting the mean ECG measurement from silver electrodes which would be due to its lower resistivity. This is consistent with hypothesis 2. Arquilla et al. and others have made this observation through experimental measurements(Arquilla, Webb, and Anderson 2021; 2020a; Vojtech et al. 2013).

The effect of pattern type on the electrode was smaller than the other two effects. As with the area type, there is a downward trend in overall impedance as conductive area increases but because the conductive areas a closer together the trend less apparent. It appears the pattern types are not distinct enough from each other create clear trends in the circuit parameters. In turn, this means the pattern types did not cause a relative effect on the ECG waveform collection. The primary

method of analyzing the pattern types was through their conductive surface areas. Either the distinction between conductive surface area and patch area is not a viable discriminator, or the conductive areas of the patches were not different enough to compensate for the other factors such as yarn type or inter-subject variability. This manufacturing parameter confirmed hypothesis 2 but more investigation is definitely warranted regarding pattern type. Pattern type has been explored by Arquilla et al (Arquilla, Webb, and Anderson 2021).

While this model is built from the traditional skin-electrode interface model, the specific circuit architecture chosen to model this behavior has implications for the fit parameters. The three fit parameters form a parallel resistor/capacitor (RC) pair in series with another resistor. The series resistance seemed to strongly dominate the impedance term because all frequency content must travel through the series resistance. At these frequencies the parallel RC allows higher frequency content to bypass the Resistance R_d, in favor of the lower impedance C_d. Furthermore the R_s term traditionally applies to the electrolyte gel, but for woven textile electrodes there is no electrolyte gel. The closest approximation would be the minute amount of perspiration which accumulates between the skin and electrode. Another factor which is not currently captured in the model is skin pressure and fit. It is possible that the R_s term captures how much the woven electrode is pressed into the skin. This could indicate that in order to reduce impedance some amount of contact pressure is required. Now that the model exists, it is possible to begin tracking relationships between these various factors and their corresponding circuit parameters.

Future Work

There are many areas which should be explored for future work. They are divided into two categories; expanding the base data sets, and improving the model. The first category involves exploring various electrode types used to fit the parameters. This data directly impacts our understand of how to manufacture

better woven electrodes for long-duration monitoring. Future work should investigate the following areas:

- How fit and pressure for woven electrodes impacts ECG signal quality. This metric was "constant" but details beyond this were not captured. In worked performed by Schauss et al. the same woven electrodes manufactured by Dr. Arquilla were used to capture much higher quality data sets (less noise artifacts) (Schauss 2022). One of the main differences in this work is that a different foam backing and placing garment was used and correspondingly the fit pressure was increased. The data captured by Schauss, could be used to fit the model to produce the corresponding circuit parameters. This could help inform how fit and pressure impact the circuit parameters.
- How varied manufacturing parameters impact ECG signal quality either through more pattern types, more yarn types, or finer steps in area. These manufacturing parameters provide a starting point, but there remain a wide variety of pattern types, and conductive yarns which were not included (Arquilla, Webb, and Anderson 2020a; Gustaf Hermann Oelsner 1915). For example, how would an electrode with conductive warp and weft thread impact the ECG waveform? Inherent in woven textiles with only conductive weft thread, is a raster pattern. This raster is broken by conductive warp threads.
- How woven electrodes perform for longer durations. Since the goal is to replace systems like the Holtier monitor for chronic applications, ECG data should be collected for durations on the order of hours to days. This longer data set could be fed to the model for fitting of the corresponding circuit parameters. The model could also be used to evaluate if the electrodes performance changes over time.

The second category involves improving the model itself. A more accurate model will dive into the simplifying assumptions and explore how a more comprehensive

model can make better predictions. Future work should investigate the following areas to improve the model:

- How would better peak finding techniques used to isolate higher SNR waveforms impact the model's ability to produce accurate circuit parameters? In this work the untreated waveforms were used for analysis, but techniques such as De-noising, Daubechies Wavelet filtering, or Convolution filtering could be utilized as have been done in previous work (Cobarrubias 2020; Schauss 2022; Arquilla, Webb, and Anderson 2020a).
- How would higher order polynomials for the skin-electrode interface model. The double-time architecture was evaluated, but there are other skin-interface architectures which may provide even better fits. A generalized Nth order polynomial could also be investigated, though care should be taken to avoid fitting noise with higher order fits.
- How would decomposing the skin-electrode interface model even further to represent each individual thread width contacting the skin. This approach was suggested in (Terada et al. 2021)
- How would incorporating this model into other weave modeling software, such as AdaCAD (Friske, Wu, and Devendorf 2019), help reduce the delta between as designed and as manufactured textile electrodes?

Conclusion

This model represents, to our knowledge, the first validated computational model of woven textile electrodes. The overall trends for the yarn type and surface area design parameters align with the expectations, indicating that the model is appropriate and captures the electrical behavior of the woven electrodes. Simplifying assumptions were made which future work should explore. This work is the first to compare simulated and measured ECG waveforms collected with woven electrodes. This model is the first to identify the circuit parameters of the skin-electrode interface model using ECG data captured with woven electrodes.

Additionally, more varied pattern types should be explored to determine how they impact ECG data. By building a predictive model, it can now be used as a guide to design future woven electrodes for long term ECG capture. In summary, this research facilitates a path for future development of these novel sensors to enable long-term ECG monitoring for woven textile electrodes.

Bibliography

An, Xiang, and George Stylios. 2018. "A Hybrid Textile Electrode for Electrocardiogram (ECG) Measurements and MotionTracking." In . https://doi.org/10.3390/ma11101887.

Ankhili, Amale, Shahood Uz Zaman, Xuyuan Tao, Cedric Cochrane, Vladan Koncar, and David Coulon. 2019. "How to Connect Conductive Flexible Textile Tracks to Skin Electrocardiography Electrodes and Protect Them Against Washing." *IEEE Sensors Journal* 19 (24): 11995–2. https://doi.org/10.1109/JSEN.2019.2938333.

Anzai, Tagayasu, Mary Anne Frey, and Akihiko Nogami. 2014. "Cardiac Arrhythmias during Long-Duration Spaceflights." *Journal of Arrhythmia* 30 (3): 139–49. https://doi.org/10.1016/j.joa.2013.07.009.

Arquilla, Katya. 2021a. "Garment-Integrated Biosignal Sensors for Astronaut Health during Long-Duration Space Missions," 4.

———. 2021b. "Monitoring Behavioral Health in Extreme Operational Environments." Boulder, Colorado: University of Colorado at Boulder. https://www.proquest.com/docview/2532092922?pq-origsite=gscholar&fromopenview=true.

Arquilla, Katya, Sarah Leary, Andrea K. Webb, and Allie P. Anderson. 2020. "Wearable 3-Lead Electrocardiogram Placement Model for Fleet Sizing of Medical Devices." *Aerospace Medicine and Human Performance* 91 (11): 868–75. https://doi.org/10.3357/AMHP.5633.2020.

Arquilla, Katya, Andrea Webb, and Allison Anderson. 2020a. "Textile Electrocardiogram (ECG) Electrodes for Wearable Health Monitoring." *Sensors* 20 (4): 1013. https://doi.org/10.3390/s20041013.

Arquilla, Katya, Andrea K Webb, and Allison P. Anderson. 2020b. "Woven Electrocardiogram (ECG) Electrodes for Health Monitoring in Operational Environments." In *2020 42nd Annual International Conference of the IEEE Engineering in Medicine & Biology Society (EMBC)*, 4498–4501. Montreal, QC, Canada: IEEE. https://doi.org/10.1109/EMBC44109.2020.9176478.

Arquilla, Katya, Andrea K Webb, and Allison P Anderson. 2021. "Detection of the Complete ECG Waveform with Woven Textile Electrodes," 13.

———. n.d. "Utility of the Full ECG Waveform for Real-Time Stress Classification," 16.

Assambo, C, A Baba, R Dozio, and M J Burke. 2007. "Determination of the Parameters of the Skin-Electrode Impedance Model for ECG Measurement," February, 6.

Bystricky, Tomas, Daniela Moravcova, Petr Kaspar, Radek Soukup, and Ales Hamacek. 2016. "A Comparison of Embroidered and Woven Textile Electrodes for Continuous Measurement of ECG." In *2016 39th International Spring Seminar on Electronics Technology (ISSE)*, 7–11. Pilsen, Czech Republic: IEEE. https://doi.org/10.1109/ISSE.2016.7562871.

Cobarrubias, Elizabeth. 2020. "Design and Test Strategies for Biopotential Sensors in Smart Garments." PhD Thesis, North Carolina, United States: North

Carolina State University. https://www.proquest.com/docview/2491965630?pq-origsite=gscholar&fromopenview=true.

Devendorf, Laura, and Chad Di Lauro. 2019. "Adapting Double Weaving and Yarn Plying Techniques for Smart Textiles Applications." In *Proceedings of the Thirteenth International Conference on Tangible, Embedded, and Embodied Interaction*, 77–85. Tempe Arizona USA: ACM. https://doi.org/10.1145/3294109.3295625.

Friske, Mikhaila, Shanel Wu, and Laura Devendorf. 2019. "AdaCAD: Crafting Software For Smart Textiles Design." In *Proceedings of the 2019 CHI Conference on Human Factors in Computing Systems*, 1–13. Glasgow Scotland Uk: ACM. https://doi.org/10.1145/3290605.3300575.

Gangemi, Marcia A. 1995. "Pathophysiology of Heart Disease: A Collaborative Project of Medical Students and Faculty." *Cardiopulmonary Physical Therapy Journal* 6 (3): 31. https://doi.org/10.1097/01823246-199506030-00013.

Geddes, L. A., and M. E. Valentinuzzi. 1973. "Temporal Changes in Electrode Impedance While Recording the Electrocardiogram with 'Dry' Electrodes." *Annals of Biomedical Engineering* 1 (3): 356–67. https://doi.org/10.1007/BF02407675.

Giovanni, Elisabetta De. 2021. "System-Level Design of Adaptive Wearable Sensors for Health and Wellness Monitoring." PhD Thesis, Switzerland: EPFL. https://infoscience.epfl.ch/record/285631.

Girod, Bernd, Rudolf Rabenstein, and Alexander Stenger. 2001. *Signals and Systems*. 2nd Ed. p. 50: Wiley. https://www.wiley.com/en-us/Signals+and+Systems-p-9780471988007.

Gregory, Pete, Stephen Lodge, Tim Kilner, and Suzy Paget. 2019. "Accuracy of ECG Chest Electrode Placements by Paramedics: An Observational Study." *British Paramedic Journal* 4 (3): 51–52. https://doi.org/10.29045/14784726.2019.12.4.3.51.

Gustaf Hermann Oelsner. 1915. *A Handbook of Weaves*. The Macmillan Company (Forgotten Books).

Heikenfeld, J., A. Jajack, J. Rogers, P. Gutruf, L. Tian, T. Pan, R. Li, et al. 2018. "Wearable Sensors: Modalities, Challenges, and Prospects." *Lab on a Chip* 18 (2): 217–48. https://doi.org/10.1039/C7LC00914C.

Huff, Janice L., Ianik Plante, Steve R. Blattnig, Ryan B. Norman, Mark P. Little, Amit Khera, Lisa C. Simonsen, and Zarana S. Patel. 2022. "Cardiovascular Disease Risk Modeling for Astronauts: Making the Leap From Earth to Space." *Frontiers in Cardiovascular Medicine* 9 (May): 873597. https://doi.org/10.3389/fcvm.2022.873597.

Hurst, J Willis. 1998. "Naming of the Waves in the ECG, With a Brief Account of Their Genesis." *American Heart Association*, Circulation, 98 (18): 6. https://doi.org/10.1161/01.CIR.98.18.1937.

John G., Webster, John W. Clark, Michael R. Neuman, Walter H. Olson, Robert A. Peura, and Frank P. Primiano Jr. 2010. *Medical Instrumentation: Application and Design 4th Edition*. 4th ed. John Wiley & Sons, Inc.

Johnston, Richard, S., Lawrence F. Dietlein, and Charles A. Berry. 1975. "Biomedical Results of Apollo." NASA-SP-368. Biomedical Results of Apollo. National Aeronautics and Space Administration. https://ntrs.nasa.gov/citations/19760005580.

K., B., Jiri Militky, Rajesh Mishra, and Dana Kremenakov. 2012. "Modeling of Woven Fabrics Geometry and Properties." In *Woven Fabrics*, edited by Han-Yong Jeon. InTech. https://doi.org/10.5772/38723.

Kannaian, T, R Neelaveni, and G Thilagavathi. 2013. "Design and Development of Embroidered Textile Electrodes for Continuous Measurement of Electrocardiogram Signals." *Journal of Industrial Textiles* 42 (3): 303–18. https://doi.org/10.1177/1528083712438069.

Kochanek, Kenneth D, Jiaquan Xu, and Elizabeth Arias. 2020. "Mortality in the United States, 2019." Data Brief 395. NCHS Mortality in the US. Maryland: CDC. https://www.cdc.gov/nchs/data/databriefs/db395-H.pdf.

Löfhede, Johan, Fernando Seoane, and Magnus Thordstein. 2012. "Textile Electrodes for EEG Recording — A Pilot Study." *Sensors* 12 (12): 16907–19. https://doi.org/10.3390/s121216907.

Maji, Soumyajyoti, and Martin J. Burke. 2018. "Effect of Electrode Impedance on the Transient Response of ECG Recording Amplifiers." In *2018 IEEE International Symposium on Medical Measurements and Applications (MeMeA)*, 1–6. Rome: IEEE. https://doi.org/10.1109/MeMeA.2018.8438732.

Medrano, G., A. Ubl, N. Zimmermann, T. Gries, and S. Leonhardt. 2007. "Skin Electrode Impedance of Textile Electrodes for Bioimpedance Spectroscopy." In *13th International Conference on Electrical Bioimpedance and the 8th Conference on Electrical Impedance Tomography*, edited by Hermann Scharfetter and Robert Merwa, 17:260–63. IFMBE Proceedings. Berlin, Heidelberg: Springer Berlin Heidelberg. https://doi.org/10.1007/978-3-540-73841-1_69.

"MP System Hardware Guide." 2015. BIOPAC Systems, Inc. www.biopac.com.

Nakamura, Hajime, Yuki Kato, and Akinori Ueno. 2018. "Design and Validation of Front-End Voltage Follower for Capacitive Electrocardiogram Measurement Using Bootstrapping Technique." In *2018 40th Annual International Conference of the IEEE Engineering in Medicine and Biology Society (EMBC)*, 5780–83. Honolulu, HI: IEEE. https://doi.org/10.1109/EMBC.2018.8513499.

Nikolova-Hadzhigenova, Elena Simeonova. 2019. "Application of Textile Electrodes in Medical Telemetry." In *2019 X National Conference with International Participation (ELECTRONICA)*, 1–4. Sofia, Bulgaria: IEEE. https://doi.org/10.1109/ELECTRONICA.2019.8825637.

Oleksy, Wojciech, and Ewaryst Tkacz. 2010. "Investigation Of A Transfer Function Between Standard 12-Lead ECG And EASI ECG," 7.

Ozkan, Haydar, Orhan Ozhan, Yasemin Karadana, Muhammed Gulcu, Samet Macit, and Fasahath Husain. 2020. “A Portable Wearable Tele-ECG Monitoring System.” *IEEE Transactions on Instrumentation and Measurement* 69 (1): 173–82. https://doi.org/10.1109/TIM.2019.2895484.

Paradiso, Rita, and Danilo De Rossi. 2006. “Advances in Textile Technologies for Unobtrusive Monitoring of Vital Parameters and Movements.” In *2006 International Conference of the IEEE Engineering in Medicine and Biology Society*, 392–95. New York, NY: IEEE. https://doi.org/10.1109/IEMBS.2006.259307.

Rahul, Jagdeep, Marpe Sora, and Lakhan Dev Sharma. 2019. “An Overview on Biomedical Signal Analysis” 7 (5): 5.

Schauss, Gabriella. 2022. “Wearable Textile Electrocardiogram Sport Bra for Real Time Health Monitoring.” Boulder, Colorado: University of Colorado at Boulder. https://www.proquest.com/docview/2678689414/abstract/1858A9CA7113445BPQ/1?accountid=14503.

Searle, A, and L Kirkup. 2000. “A Direct Comparison of Wet, Dry and Insulating Bioelectric Recording Electrodes.” *Physiological Measurement* 21 (2): 271–83. https://doi.org/10.1088/0967-3334/21/2/307.

Sriraam, N., Avvaru Srinivasulu, V S Prakash, and Sarthak Sahoo. 2019. “A Smart Textile Electrode Belt for ECG Recordings - A Pilot Study with Indian Population.” In *2019 2nd International Conference on Signal Processing and Communication (ICSPC)*, 267–70. Coimbatore, India: IEEE. https://doi.org/10.1109/ICSPC46172.2019.8976815.

Taji, Bahareh, Shervin Shirmohammadi, Voicu Groza, and Izmail Batkin. 2014. “Impact of Skin–Electrode Interface on Electrocardiogram Measurements Using Conductive Textile Electrodes.” *IEEE Transactions on Instrumentation and Measurement* 63 (6): 1412–22. https://doi.org/10.1109/TIM.2013.2289072.

Terada, Takamasa, Masahiro Toyoura, Takahide Sato, and Xiaoyang Mao. 2021. “Noise-Reducing Fabric Electrode for ECG Measurement.” *Sensors* 21 (13): 4305. https://doi.org/10.3390/s21134305.

Tereshchenko, Larisa G., and Mark E. Josephson. 2015. “Frequency Content and Characteristics of Ventricular Conduction.” *Journal of Electrocardiology* 48 (6): 933–37. https://doi.org/10.1016/j.jelectrocard.2015.08.034.

Thomas, Roland E., Albert J. Rosa, and Gregory J. Toussaint. 2009. *The Analysis & Design of Linear Circuits*. 6th Ed. Wiley.

Vojtech, Lukas, Radoslav Bortel, Marek Neruda, and Milos Kozak. 2013. “Wearable Textile Electrodes for ECG Measurement.” *Advances in Electrical and Electronic Engineering* 11 (5): 410–14. https://doi.org/10.15598/aeee.v11i5.889.

Wang, Ting-Wei, and Shien-Fong Lin. 2021. “Negative Impedance Capacitive Electrode for ECG Sensing Through Fabric Layer.” *IEEE Transactions on Instrumentation and Measurement* 70: 1–8. https://doi.org/10.1109/TIM.2020.3045187.

Y Du, Winncy. 2017. “Design of an ECG Sensor Circuitry for Cardiovascular Disease Diagnosis.” *International Journal of Biosensors & Bioelectronics* 2 (4). https://doi.org/10.15406/ijbsbe.2017.02.00032.

Yokus, Murat A., and Jesse S. Jur. 2016. “Fabric-Based Wearable Dry Electrodes for Body Surface Biopotential Recording.” *IEEE Transactions on Biomedical Engineering* 63 (2): 423–30. https://doi.org/10.1109/TBME.2015.2462312.

Yoo, J. and Hoi-Jun Yoo. 2011. “Fabric Circuit Board-Based Dry Electrode and Its Characteristics for Long-Term Physiological Signal Recording.” In *2011 Annual International Conference of the IEEE Engineering in Medicine and Biology Society*, 2497–2500. Boston, MA: IEEE. https://doi.org/10.1109/IEMBS.2011.6090692.

Appendix

Appendix contains content which to too unwieldy to place in the thesis but is supplementary information which was used for analysis and visualization.

A. MATLAB Code

This is the MATLAB code of the computation model. The code was written in MATLAB R2022a. For convenience, code was written across 6 scripts. The main mathematical model of transfer with the optimizer is saved in script 3) DeterModParams.m. All other scripts are supplemental scripts for data manipulation and figure creation.

1) ReadAllData

   This script reads in all the text file data from BIOPAC then saves a *.mat files in convenient column row format for future processing.

2) SaveAverageMetrics

   This script performs the peak finding steps and saves the average waveforms into a struct. It also computes a number of metrics such as SNR, and number of peaks, to determine waveform quality. It produces plots of the raw datasets, average waveforms and the spectrum of each dataset.

3) DeterModParams

   This script is the meat of the code which contains the optimizer which uses the SNR criteria to fit parameters across subjects for each electrode type.

4) MeanVsSimWaveform

   This script creates figures of measured versus simulated mean waveforms as well as figures of the bode plots.

5) ParameterVisualizer

   This script creates figures of the circuit parameters and impedance terms versus the manufacturing parameters.

6) Leave1Out

   This script performs the LOOCV analysis and returns the RMSE table.

ReadAllData.m

```
% (1) This script saves all ECG data into a matlab cell variable.
% it takes a file location and a data size as inputs
% and it produces a mat file as an output which has header data and raw
% data saved as workspace variables.

%Load in all data into a cell
startpath = pwd;
datapath = 'C:\Users\peter\Documents\School\Fall2021\ASEN6950_MSThesis\data';
% delim = sprintf('\r\n');    %newline delimiter
numsubject = 10;        %Number of human Subjects
numdata = 17;           %Number of datasets
dataset = cell(numsubject,numdata); %Preallocate data size
headerset = cell(numsubject,numdata); %Preallocate data size
for hh = 1:10   %ii is the human subject
    dirname = sprintf('sub%d',hh);
    folder = [datapath,'\',dirname];
    file = dir(folder);
    for kk = 1:17
        fname = file(kk+2).name
        [data,header] = readECGtxt([folder,'\',fname]);
        headerset{hh,kk} = header;
        dataset{hh,kk} = data;
    end

end

savefile = 'rawdataset.mat';
save(savefile, 'headerset','dataset');

function [data,header] = readECGtxt(fname)
    header_rows=7;  %Number of header Rows in the data text file
    header = cell(header_rows,1);
    fid = fopen(fname);
    for kk = 1:header_rows
        header{kk} = fgets(fid);
    end
    datacell = textscan(fid,'%f%f','Headerlines',0);
    if contains(header{6},'min')
        datacell{1} = datacell{1}*60;
        header{6}(1:3) = 'sec';
    end
    data = [datacell{1},datacell{2}];
    fclose(fid);
end
```

SaveAverageMetrics.m

```
% (2) This Script Loads all the data sets and creates a average ECG waveform for
%each electrode for each subject.

%% Begin Script
clc;close all;
clearvars -except dataset headerset
if ~exist('dataset','var')
    load('rawdataset.mat')
end
numee = [1:17];
numss = [1:10];
```

```
%% Inputs
makeplots = 1;      %Save to create the figures
saveplots = 0;      %flag just to save plots or not

savename = 'ECG_Metrics6.mat';
saveMeans = 0;      %Save the mean waveform data in the savename type

%% Initialize Vairables
ECGdata = struct('Vmean',cell(10,17),'Tmean',cell(10,17),...
    'Vstd',cell(10,17),'numpks',zeros(1,1),'RRint',zeros(1,1));
SNR = nan(10,17);
numpks = nan(10,17);
%
cc = 1;         %Sub plot counter
%% Loop through entire data set
% Start with Electrode first, to get all Adhesives first

for ee = numee                  %Electrode index 1 is Adhesive
    for ss = numss              %Subject of interest
%         close all;
        fprintf('Subject %d, Electrode ID %d\n',ss,ee); %For troubleshooting
        header = headerset{ss,ee};  %Headerdata
        t = dataset{ss,ee}(:,1);                %(sec) Time Vector
        vraw = dataset{ss,ee}(:,2);                %(mV) Voltage Vector
        dt = 1/round(1/mean(diff(t)));         %(sec) time step
        t = [0:length(t)-1]*dt;     %Make Monotonically increasing

        %% Filter the ECG data using the circuitry of the BIOPAC system
        [v] = filter1ECG(vraw,t);

        %% Identify Peaks V and T positions
        %If it is adhesive data, the typical findpeaks() is sufficient
        %but if it is textile data, then a more rigorous peakfinder is
        %required. CrossCorrelatePeaks, uses the know shape and spacing of
        % the adhesive waveform to search for textile waveforms
        if ee == 1
            [Rpks,Tpks] = IdentifyPeaks(v,t,.5);
            RRint(ss,ee) = checkRR(Tpks);    %Find RR Interval
        else
            RRint(ss,ee) = ECGdata(ss,1).RRint;
            Vadh = ECGdata(ss,1).Vmean;
            Tadh = ECGdata(ss,1).Tmean;
            [Rpks,Tpks] = CrossCorrelatePeaks(v,t,Vadh,Tadh,RRint(ss,ee),3/4,3/4);
        end

        %Obtain index locations for each peak
        locs = floor(Tpks/dt)+1;        %Location of Peak in t Vector
        numpks(ss,ee) = length(Rpks);          %Number of peaks detected
        if numpks(ss,ee) < 20
            warning('Subj %d, Elec %d contains < 20 viable peaks',ss,ee)
        end
        numsamp = floor(RRint(ss,ee)/dt);%Number of samples in an average waveform

        %Snip and Stack waveforms by their peak
        Vwave = zeros(numsamp,numpks(ss,ee));  %Initialize V and T vectors
        Twave = zeros(numsamp,numpks(ss,ee));
        for kk = 1:numpks(ss,ee)               %Loops through each peak
            ix = (1:numsamp).'-floor(numsamp/2)+locs(kk); %Selects the indices around the peak
            if min(ix) < 1 || max(ix) > length(v)
                continue
            end
```

```
            Vwave(:,kk) = v(ix);        %Saves that waveform
            Twave(:,kk) = t(ix)-Tpks(kk);   %These should be basically identical
        end

        Tmean = median(Twave.').';        %somewhat redundant with Twave(:,1)
        Vmean = mean(Vwave.').';        %Finds the Average Waveform
        Vstd = std(Vwave.').';          %Finds the standard deviation of waveforms
        Vstd2p = Vmean+2*Vstd;
        Vstd2n = Vmean-2*Vstd;
        SNR(ss,ee) = snr(Vmean,Vstd);       %Signal to Noise Ratio

        %% Store Metrics in a struct for access later
        ECGdata(ss,ee).Vmean = [Vmean];             %Voltage Vector
        ECGdata(ss,ee).Tmean = [Tmean];             %Time Vector
        ECGdata(ss,ee).Vstd = [Vstd];               %# Vector
        ECGdata(ss,ee).RRint = RRint(ss,ee); %sec R to R interval
        ECGdata(ss,ee).numpks = numpks(ss,ee);             %Number of used Peaks
        ECGdata(ss,ee).SNR = SNR(ss,ee);

        %% Make Plots
        if makeplots
            set(0,'defaultAxesFontSize',14);
            f1 = figure;
            subplot(3,1,1)
            plot(t,v,Tpks,Rpks,'or')
            grid on;
            xlim([0,max(t)])
            headerstr = header{1}(10:end-6);
            headerstr(headerstr == '_') = ' ';
            titlestr = sprintf('ECG for %s data',headerstr);
            title(titlestr);ylim(round([-max(Rpks),max(Rpks)]*1.3,2))
            xlabel('Time (sec)');ylabel('Voltage (mV)');
            legend('ECG Waveform','Rpeaks','location','sw')
            subplot(3,1,2)
            grid on; hold on
            plot(Tmean,Vmean,'k','Linewidth',2)
            plot(Tmean,Vstd2p,':k','Linewidth',1.5)
            plot(Tmean,Vstd2n,':k','Linewidth',1.5)
            plot(Twave,Vwave,':')
            plot(Tmean,Vmean,'k','Linewidth',2)
            xlabel('Time (sec)');ylabel('Voltage (mV)');
            tname = sprintf('Peak Aligned Waveforms, SNR=%2.1f,
numPks=%d',SNR(ss,ee),numpks(ss,ee));
            title(tname);
            legend('Mean ECG Waveform','+/- 2 standard Devations','location','Sw')

            [f,P1,phi] = MakeSpectrum(t,v);
            subplot(3,1,3)
            plot(f,P1);
            axis([0,100,0,max(P1)])
            xlabel('Frequency (Hz)');ylabel('Amplitude (mV)');
            title('Magnitude of Signal in Frequency Spectrum');
            grid on
            f1.Position = [200,100,700,900];

            if saveplots
                figname = sprintf('MeanECG_Sub%d_ID%d',ss,ee);
                savepath = [pwd,'\Figures\',savename(1:end-4)];
                saveas(f1,[savepath,'\',figname],'jpg')
            end
        end
```

```
        cc = cc+1;
    end
end

%% Extract Criteria for Good/Bad Data
totSNR = sum(sum(SNR>0))
numNanSNR = sum(sum(isnan(SNR)))
totpks = sum(sum(numpks>30))

if saveMeans
    save(savename,'ECGdata','SNR','numpks')
    fprintf('DataSaved!\n')
end


%% ======================== FUNCTION LIST ========================

% This function will use the waveform measured from a clean (Adhesive)
% dataset to perform a convolution (Cross correlation) on the noisy dataset
% in order to identify the actual ECG waveform peaks through the noise.
function [Rpks,Tpks] = CrossCorrelatePeaks(v,t,Vadh,Tadh,RRint,alpha,beta)
    %1) Find the peaks on the raw data This will have a high number of
    %false positives, but a low number of false negatives
    [R1,T1] = findpeaks(v,t,'MinPeakDistance',RRint);
    R1p5 = rmoutliers(R1);
    RR = .75*median(RRint);          %Find the spacing between peaks for fine tuning
    [Rmid] = checkMid(R1p5);               %Find Average Peak Height

    Vfilt = Vadh/max(Vadh)*Rmid;        %Scale the amplitude of the known good waveform
    ynorm = sum(Vfilt.^2);              %Normalize convolution result
    y = conv(v,flipud(Vfilt),'same')/ynorm;   %Convolution of dataset with Adhesive Waveform
    [R2,T2] = findpeaks(y,t,'MinPeakDistance',RR,'MinPeakHeight',.5);

    [R3,T3] = rmvPeaks(R2,T2,1+alpha,1-alpha,1);      %Remove outlier peaks in convolution

    % Since the convoluted waveform is not the same, we need to find the
    % peaks on the original t and v, that correspond to the peaks in the
    % convoluted y.
    ix = zeros(size(T3));
    for kk = 1:length(T3)
        ix(kk) = find(T3(kk)==t);
    end
    R4 = v(ix);
    T4 = t(ix);

    [Rmid] = checkMid(R4);

    Rpks = R4(~isoutlier(R4));
    Tpks = T4(~isoutlier(R4));
end


% This function wil remove peaks larger than Rmax and less than Rmin, and
% it will also remove peaks adjacent to the offending peak.
function [Rpk,Tpk] = rmvPeaks(Rpk1,Tpk1,Rmax,Rmin,win)
    IdPks = find(Rpk1>Rmax | Rpk1<Rmin);
%     IdPks = isoutlier(Rpk1) | < Rpk1 < Rmin;
%Removebad peaks and the adjacent peaks aswell
    if ~isempty(IdPks)
        badpks = [];
        for kk = 1:length(IdPks)
```

```
            badpks = [badpks,IdPks(kk)+[-win:win]];
        end
        badpks(badpks <= 0) = [];
        badpks(badpks >= length(Rpk1)) = [];
        Rpk1(unique(badpks)) = [];
        Tpk1(unique(badpks)) = [];
    end
    Rpk = Rpk1;
    Tpk = Tpk1;
end

% This function filters the ECG data with a 60Hz notch, a 2nd order LPF and
% a 2nd order HPF.
function [v] = filter1ECG(vraw,t)

        w0 = 60*2*pi;               % Center Frequency of Notch
        wc = 1.5*2*pi;              % Bandwith of Notch filter
        Notch = tf([1,0,w0^2],[1,wc,w0^2]);

        wlow = 2*pi*35;            %LPF Cutoff Frequency
        d = 1;                      %Damping Factor
%         LPF = tf([0,1],[1/wlow,1]); %Single pole Low Pass Filter
        LPF = tf([0,0,wlow^2],[1,2*d*wlow,wlow^2]); %Double pole LPF

        whigh = 2*pi*1;             %HPF Cutoff Frequency
%         HPF = tf([1/whigh,0],[1/whigh,1]);  %Single pole High pass filter
        HPF = tf([1,0,0],[1,2*d*whigh,whigh^2]); %Double Pole LPF
        v = lsim(Notch*LPF*HPF,vraw,t); %Does the filtering without the Gain
end

% This function will scan through the v and t data identifying the R-peaks
% and remove the outliers. This function uses findpeaks() and then removes
% outlier peaks
function [Rpks,Tpks] = IdentifyPeaks(v,t)

    [R1,T1] = findpeaks(v,t,'MinPeakDistance',.5);    %Find Peaks preliminary1
    RRint = median(diff(T1));       %Median RR Interval
    % Bound RR interval
    if RRint > 1.5
        warning('Median RRinterval > 1.5sec')
    elseif RRint < .5
        warning('Median RRinterval < 0.5 sec')
    end

    Rpks = R1(~isoutlier(R1));
    Tpks = T1(~isoutlier(R1));

end
```

DeterModParams.m

```
% (3) This script will run through the methodology for a single subject and electrode

clc;clear;close all;

%% Load in Mean Measured Waveforms
load('ECG_Metrics6.mat')
valfitname = 'valsfit7_op5.mat';
makeplot = 0;         %Flag for making plots
optmcnt =5;           %Optimizer Count limit
```

```
subjs = [1,2,4,6,8,9];    %Subjects of interest (excluded 3,5,7,10)
ea = 1;             %Adhesive Electrode index

%% Make Adhesive Transfer Function
% "Detrmination of the parameters of the skin-electrode Impedance Model for ECG Measurement"
% "By: Assambo, Baba, Dozio and Burke".
Ce = 0.9e-6;        %(F) Capacitance of Epidermis
Re = 35.2e3;        %(Ohm) Resistance of Epidermis
Rop = 1e6;          %(Ohm) Impedance of Opamp (ECG100C Specification) 2Mohm/2
R3 = 3.6e3;         %(Ohms) Rs+Rl+Ru, DC impedance Term
Rs = 1e3;           %(ohm) Impedance of Electrolyte (Approximation)
R2 = R3-Rs;         %(Ohms) DC term without Electrolyte
Cd = 5.8e-6;        %(F) Capacitance of Electrode
Rd = 25.9e3;        %(Ohm) Resistance of Electrode

skinparams = [Ce,Re,Rop,R2];    %Skin Parameters
elecparams = [Cd,Rd,Rs];        %[Farads, Ohms, Ohms] Electrode Parameters
TFadh = GenTFdouble(elecparams,skinparams); %Adhesive Transfer function

%% Make ECG transfer function with Adhesive Electrode
Gain = 2000;        %(Linear) Gain of Amplifier Biodomadix
Amp  = tf(Gain,1);  %Transfer Function of Amplifier

TFecgA = Amp*TFadh;  %Transfer function of Adhesive ECG system
iTFecgA = 1/TFecgA;   %Inverse Transfer Function of Adhesive ECG system

%% Start For Loop
valsfit = zeros(17,4);  %Initialize Variable to save optimized Parameters
for ee = 2:17           %Loop through Each textile Electrode
    fprintf('Subject FIT, Electrode ID %d\n',ee); %For troubleshooting

    %% Run Optimizer to find the unknown parameters of Electrode
    %Since Capacitance is on the order of uFarads, and resistance is on the
    %order of MOhms, the units are changed here in order to allow the
    %optimizer to optimize around similar 'magnitude' parameters.

    %set up upper and lower bounds for uknowns put into single matrix [Cd,Rd,Rs];
    Cmax = .1;                   %uFarads
    Rdmax = 50;                 %Mohms
    Rsmax = 50;                 %Mohms
    ub = [Cmax,Rdmax,Rsmax];    %uFarad,MOhm,MOhm [Upper Boudns]
    lb = 1e-4*[Cd/1e-6,Rd/1e6,Rs/1e6]; %lower bound is .1% of adhesive Values
    cc = 0;
    Cost = 1e10;
     fminopt = optimoptions("fmincon","Display",'none');
    while cc<optmcnt
        %Set up initial conditions for Electrode Parameters
        init_ukn = rand(1,3).*(ub-lb)+lb;       %random starting variable
        kno = skinparams;

        ukn = fmincon(@(ukn)
ErrFuncXsub(ukn,kno,ee,subjs,iTFecgA,ECGdata),init_ukn,[],[],[],[],lb,ub,[],fminopt);
        cc = cc+1;
        Cost(cc) = ErrFuncXsub(ukn,kno,ee,subjs,iTFecgA,ECGdata);
        if cc == 1
            uknbest = ukn;
        elseif Cost(cc) < min(Cost(1:end-1))
            uknbest = ukn;
        end
    end
```

```
    valsfit(ee,:) = [uknbest,min(Cost)];
    [Cdfit,Rdfit,Rsfit] = deal(valsfit(ee,1),valsfit(ee,2),valsfit(ee,3));

end
if exist(valfitname,'file')
    warning('Did not Overwrite filename. DATA NOT SAVED.')
else
    save(valfitname,'valsfit')
    fprintf('DATA SAVED in %s\n',valfitname)
end

fprintf('\n DeterModParams Complete! \n')

%% ------------------ Functions --------------------

%Error Function that finds the error between a simulated and measured
%signal
function Error = ErrFunc(ukn,kno,Vsig,Vmeas,t)
    ukn = ukn.*[1e-6,1e6,1e6];  %Convert from uF & Mohm to F and Ohm.
    Gain = 2000;        %(Linear) Gain of Amplifier Biodomadix
    Amp  = tf(Gain,1);  %Transfer Function of Amplifier
    TFelec = GenTFdouble(ukn,kno);   %Generate electrode Transfer Function

    TFecg = Amp*TFelec;  %Transfer function of ECG system

    Vsim = lsim(TFecg,Vsig,t);   %Create a Simulated Waveform
%     Error = sum(abs(Vmeas-Vsim).^2);
    Error = sum(abs(Vmeas/max(Vmeas)-Vsim/(max(Vmeas))).^2);
end

% Error Function Across Subjects for Doubletime model
function Error = ErrFuncXsub(ukn,kno,ee,subjs,iTFecgA,ECGdata)
ea = 1;
cc=1;
for ss = subjs
    ex = [9,9,9,8;12,9,6,4].';            %Manual Exclusion
    flag1 = ECGdata(ss,ee).numpks> 30;      %keep criteria
    flag2 = ~any(ss == ex(:,1) & ee == ex(:,2)); %Not a manual exclude
    if flag1 && flag2
        ixsub(cc) = ss;
        cc=cc+1;
    end

end

err = zeros(1,10);

for ss = ixsub
    Va = ECGdata(ss,ea).Vmean;         %mV Mean ECG Measured Adhesive
    tA = ECGdata(ss,ea).Tmean;              %sec Time Vector Adhesive
    Ve = ECGdata(ss,ee).Vmean;         %mV Mean ECG Measured Textile
    tE = ECGdata(ss,ee).Tmean;              %sec Time Vector Textile
    [Va,Ve,t] = TrimVectors(Va,Ve,tA,tE);

    Vsig = lsim(iTFecgA,Va,t);  %In Body Signal
    err(ss) = ErrFunc(ukn,kno,Vsig,Ve,t);   %Individual Errors
end
Error = sum(err);   %The fit error is the sum of the individual errors
end

% Generates the transfer function when no variables are known
```

```
function TFelec = GenTF(ukn)
ord = length(ukn)/2;
if isodd(length(ukn))
    error('ukn must be even number length');
end
num = ukn(1:ord);
den = ukn(ord+1:end);
TFelec = tf(num,den);
end

% Trims lengths so they are the same
function [Va,Ve,t] = TrimVectors(Va,Ve,tA,tE)
    % ========= Adjust Vector Lengths to be same length =============
    % Trim the longer one so it is as long as the shorter one.
    lenvA = length(Va);         %# Length of Adhesive datasete
    lenvE = length(Ve);         %# Length of Textile datasete

    if lenvA > lenvE            %Adhesive Vector is longer than Textile
        %trim Adhesive Data
        if isodd(lenvE)         %is The Textile Vector odd length?
            lenvE = lenvE -1;   %make it even length
        end
        rmv = floor((lenvA-lenvE)/2);  %Number of indeces to remove
        Va = Va(rmv+1:lenvE+rmv);
        Ve = Ve(1:lenvE);
        t = tE(1:lenvE)-min(tE);
    elseif lenvE > lenvA
        % trim Textile Data
        if isodd(lenvA)
            lenvA = lenvA - 1;      %If its odd subtract one from index
        end
        rmv = floor((lenvE-lenvA)/2);       %Number of indeces to remove
        Ve = Ve(rmv+1:lenvA+rmv);
        Va = Va(1:lenvA);
        t = tA(1:lenvA)-min(tA);
    else
        %Same length Dont need to remove anything
        t = tA-min(tA);
        if mean(diff(tE))-mean(diff(tA)) > 1e-10
            warning('Time Vectors are not equal')
        end
    end
end
```

MeanVsSimWaveform.m

```
% (4) This script creates makes all Sim vs Meas Plots

clc;clear;close all

saveplots = 0;
makebodeplot = 0;
makeplots = 0;
makeworst = 2;  % 1 for worst, 2 for best, 0 for no plots
makeSweep = 0;

fname1 = 'valsfit7_op5.mat'
load(fname1)

if ~exist('ECGdata','var')
    load('ECG_Metrics6.mat')
```

```
end

for ss = 1:10
    for ee = 1:17
        numpks(ss,ee) = ECGdata(ss,ee).numpks;
        SNR(ss,ee) = ECGdata(ss,ee).SNR;
    end
end
Label2 = {'Adhesive';'Area1';'1Si'; '1St';...
     'Area2';'2Si';'2St';...
     'Area3';'3Si'; '3St';'Area4';...
     '4Si'; '4St';'Area5';'Area6';'Area7';'Area8'};

%% ========== Adhesive Values ==========
[Cdfit,Rdfit,Rsfit,costfit] = deal(valsfit(:,1),valsfit(:,2),valsfit(:,3),valsfit(:,4));
% Adhesive Values
Rs = 1e3;               %(ohm) Impedance of Electrolyte (Approximation)
Cd = 5.8e-6;            %(F) Capacitance of Electrode
Rd = 25.9e3;            %(Ohm) Resistance of Electrode
Ce = 0.9e-6;            %(F) Capacitance of Epidermis
Re = 35.2e3;            %(Ohm) Resistance of Epidermis
Rop = 1e6;              %(Ohm) Impedance of Opamp (ECG100C Specification) 2Mohm/2
R2 = 2.6e3;             %(Ohms) DC term without Electrolyte Approximation Rlead+Ru


Cdfit1 = Cdfit/1e6;     %Convert CdFit from uF to F
Rdfit1 = Rdfit*1e6;     %Convert Rdfit from MOhms to Ohms
Rsfit1 = Rsfit*1e6;     %Convert Rsfit from MOhmz to Ohms
Cdfit1(1) = Cd;         %Adding Adhesive to List
Rdfit1(1) = Rd;         %Adding Adhesive to List
Rsfit1(1) = Rs;         %Adding Adhesive to List
R3 = R2+Rsfit1;         %(Ohms) Rs+Rl+Ru, DC impedance Term

%% ================== Meas vs Sim'd Plots ======================
skinparams = [Ce,Re,Rop,R2];
elecparams = [Cdfit1,Rdfit1,Rsfit1];
Error = zeros(10,17);
RMSE = zeros(10,17);
set(0,'defaultAxesFontSize',14);
subjs = [1,2,4,6,8,9];

TFadh = GenTFdouble(elecparams(1,:),skinparams);    %Adhesive Transfer Function
Amp = tf(2000,1);
TFecgA = TFadh*Amp;
iTFecgA = 1/TFecgA;
ECGTFs(1) = TFecgA;

%% ================== Save Simm'd metrics ========================
for ee = 2:17

    TFelec = GenTFdouble(elecparams(ee,:),skinparams);  %The Electrodes Transferfunction

    TFecgE = TFelec*Amp;
    ECGTFs(ee) = TFecgE;        %Save all ECGs for Bode Plots

    for ss = subjs

        Vmeas = ECGdata(ss,ee).Vmean;      %Measured ECG signal
        Tmeas = ECGdata(ss,ee).Tmean;
        Vadh = ECGdata(ss,1).Vmean;
        Tadh = ECGdata(ss,1).Tmean;
```

```
        t = Tadh-min(Tadh);

        Vsig = lsim(iTFecgA,Vadh,t);       %inbody Signal


        Vsim = lsim(TFecgE,Vsig,t);         %Simulated Signal
        ECGdata(ss,ee).Vsim = Vsim;
        ECGdata(ss,ee).Vsig = Vsig;
        ECGdata(ss,ee).vals = elecparams(ee,:);
    end
end

for ee = 2:17
    cc = 1;
    if makeplots
        f1 = figure(100+ee);
    end
    for ss = subjs
        Vmeas = ECGdata(ss,ee).Vmean;      %Measured ECG signal
        Tadh = ECGdata(ss,1).Tmean;
        t = Tadh-min(Tadh);
        Vsim = ECGdata(ss,ee).Vsim;
        if SNR(ss,ee) >0 %&& numpks(ss,ee) > 30
            RMSE(ss,ee) = sqrt(mean((Vmeas-Vsim).^2));
        end
        if makeplots
            subplot(length(subjs)/2,2,cc)
            grid on;hold on;
            plot(t,Vmeas,'DisplayName','Measured Signal','Linewidth',2)
            plot(t,Vsim,'-.','DisplayName','Simulated Signal','Linewidth',2)
            legend('Show','Location','southeast')
            title(sprintf('Sub %d, %s, SNR=%2.1f, Pks=%2.0f
',ss,Label2{ee},SNR(ss,ee),numpks(ss,ee)))
            if isodd(cc)
                ylabel('Voltage (mV)')
            end
            if any(cc==[length(subjs)-1,length(subjs)])
                xlabel('time (sec)')
            end
        end
        cc= cc+1;
    end

    if saveplots && makeplots
        f1.Position = [1921 47 1280 907];
        tmp = split(fname1,'_');
        figname = sprintf('MeasVSim_%s_v%s',Label2{ee},tmp{1}(end));
        savepath = [pwd,'\Figures\MeasVsSim\',figname];
        saveas(f1,[savepath],'jpg')
    end
end

%% ================ Area\Pattern sweep Plots ======================
if makeSweep
area_ids = [2,5,8,11,14,15,16,17];
patt_ids = [3,4,6,7,9,10,12,13];
plot_ids = area_ids;
for ss = subjs
    cc = 1;
    Vadh = ECGdata(ss,1).Vmean;
    Tadh = ECGdata(ss,1).Tmean;
```

```
    t = Tadh-min(Tadh);
%     Vsig = lsim(iTFecgA,Vadh,t);       %inbody Signal
    f2 = figure(200+ss);
    for ee = plot_ids
        Vmeas = ECGdata(ss,ee).Vmean;      %Measured ECG signal
        Tmeas = ECGdata(ss,ee).Tmean;
        Vsim = ECGdata(ss,ee).Vsim;
        subplot(length(plot_ids)/2,2,cc)
        grid on;hold on;
        plot(t,Vmeas,'DisplayName','Measured Signal','Linewidth',2)
        plot(t,Vsim,'-.','DisplayName','Simulated Signal','Linewidth',2)
        legend('Show','Location','southeast')
        title(sprintf('Sub %d, %s, SNR=%2.1f, Pks=%2.0f
',ss,Label2{ee},SNR(ss,ee),numpks(ss,ee)))
        if cc>ceil(length(plot_ids)/2)
            xlabel('time (sec)')
        end
        if any(cc==[1,length(plot_ids)/2+1])
            ylabel('Voltage (mV)')
        end
        cc=cc+1;
    end
    if saveplots
        f2.Position = [1921 47 1280 907];
        tmp = split(fname1,'_');
        figname = sprintf('AreaSwp_MeasVSim_Sub%d_v%s',ss,tmp{1}(end));
        savepath = [pwd,'\Figures\MeasVsSim\AreaSwp\',figname];
        saveas(f2,[savepath],'jpg')

    end
end

%% ==================== RPeaks vs Area ====================
for ss = 1:10
    for ee = 1:17
        Vmeas = ECGdata(ss,ee).Vmean;      %Measured ECG signal
        Rmax(ss,ee) = max(Vmeas);
    end
end
ymax = round(max(max(Rmax(subjs,[1,area_ids])))*1.1,2)
f22 = figure(200+22);
for si = 1:6
    ss = subjs(si);
%     subplot(6,1,si);
    grid on; hold on;
    ylabel('Voltage (mV)');ylim([0,ymax]);

%     legend(sprintf('Sub%d',ss))
    plot(0:8,Rmax(ss,[1,area_ids]),'-o')

end
xlabel('Area (Label)');
title('Rpeaks of Measured ECG Waveforms')
tmp = split(sprintf('subj%d_',subjs),'_');

legend(tmp(1:length(subjs)),'location','best')
end


%% ================ best/worst ======================
if makeworst ~= 0
```

```
% make rows so the sort rows, can track which ID is the worst onces
topX = 6;      %How many extreme to plot ones
sub = 1:10;
ele = [1:17].';
[S,E] = meshgrid(sub,ele);
sub = reshape(S,numel(S),1);
ele = reshape(E,numel(E),1);
err = reshape(RMSE.',numel(RMSE),1);
sortedErr = flipud(sortrows([err,sub,ele]));
worstSubs = sortedErr(1:topX,2);
worstElec = sortedErr(1:topX,3);
ix = find(sortedErr(:,1)==0,1);
BestSubs = sortedErr(ix-topX:ix-1,2);
BestElec = sortedErr(ix-topX:ix-1,3);

f3 = figure(300);
for cc = 1:topX
    if makeworst == 1
        ee = worstElec(cc);
        ss = worstSubs(cc);
    else
        ee = BestElec(cc);
        ss = BestSubs(cc);
    end
    TFelec = GenTFdouble(elecparams(ee,:),skinparams);  %The Electrodes Transferfunction

    TFecgE = TFelec*Amp;
    ECGTFs(ee) = TFecgE;        %Save all ECGs for Bode Plots

    Vmeas = ECGdata(ss,ee).Vmean;      %Measured ECG signal
    Tmeas = ECGdata(ss,ee).Tmean;
    Vadh = ECGdata(ss,1).Vmean;
    Tadh = ECGdata(ss,1).Tmean;
    t = Tadh-min(Tadh);

    Vsig = lsim(iTFecgA,Vadh,t);       %inbody Signal
    Vsim = lsim(TFecgE,Vsig,t);         %Simulated Signal
    s(cc) = subplot(ceil(topX/2),2,cc);
    grid on;hold on;

    plot(t,Vmeas,'DisplayName','Measured Signal','Linewidth',2)
    plot(t,Vsim,'-.','DisplayName','Simulated Signal','Linewidth',2)
    legend('Show','Location','southeast')
    title(sprintf('Sub %d, %s, RMSE=%2.3fmV',ss,Label2{ee},RMSE(ss,ee)))

    if isodd(cc)
        ylabel('Voltage (mV)')
    end
    if any(cc==[topX,topX-1])
        xlabel('Time (sec)')
    end
    cc= cc+1;
end
f3.Position = [1921 47 1280 907];
if saveplots && makeworst ~= 0
    tmp = split(fname1,'_');
    if makeworst == 1
        figname = sprintf('Top%d_Worstfit_v%s',topX,tmp{1}(end));
    else
        figname = sprintf('Top%d_Bestfit_v%s',topX,tmp{1}(end));
    end
```

```
    savepath = [pwd,'\Figures\MeasVsSim\',figname];
    saveas(f3,[savepath],'jpg')
end

end


%% ================= BODE PLOTS ===============
if makebodeplot
    area_ids = [2,5,8,11,14,15,16,17]
ixArea = [1,area_ids];        %Area Sweep Indexes
ixArea = 1;

wlow = 100;
whigh = 1;
w0 = 60
wc = 2;
d = 1;

LPF2 = tf([0,0,wlow^2],[1,2*d*wlow,wlow^2]);
LPF = tf([0,1],[1/wlow,1]);
HPF2 = tf([1,0,0],[1,2*d*whigh,whigh^2]);
HPF = tf([1/whigh,0],[[1/whigh,1]]);
Notch = tf([1,0,w0^2],[1,wc,w0^2]);
FilterStage = LPF*HPF*Notch;

col = jet(length(ixArea));
col = {'m','r','y','g','c','b','k','k--'};

f4 = figure(400);
f4.Position = [680   450   800   500]
cc = 0;
    for kk = 1:length(ixArea)

        bode(ECGTFs(ixArea(kk))*FilterStage,{1,100});
        sp = f4.Children(2);
        sm = f4.Children(3);
        grid on; hold on;
        tmp{kk} = Label2{ixArea(kk)};
    end
    title('Bode Plot for Adhesive ECG System TF')
    sm.Children(end).LineWidth = 2;
    sp.Children(end).LineWidth = 2;
    for kk = 1:length(ixArea)
        sp.Children(kk).Children.LineWidth = 2;
        sm.Children(kk).Children.LineWidth = 2;
    end

    legend(sp,tmp,'location','w')
    ylim(sm,[55,70])
    legend(sm,tmp,'location','w')
end
```

ParameterVisualizer.m

```
% (5) The script creates plots of parameters
clc;close all;
clearvars -except ECGdata
fname1 = 'valsfit7_op5.mat';
```

```
load(fname1)                            %Load the fit data
% Sort the data into variables
[Cdfit,Rdfit,Rsfit,costfit] = deal(valsfit(:,1),valsfit(:,2),valsfit(:,3),valsfit(:,4));
ixValid = [3,4,5];                       %Validaiton Test
ixArea = [2,5,8,11,14,15,16,17];        %Area Sweep Indexes
ixPatt = [3,4,6,7,9,10,12,13];          %Pattern Indexes

mkr = 'ok';
set(0,'defaultAxesFontSize',13);
%% ========== Manufacturing Parameters ==========

Radh = 5/2.54/2;    %(in) Radius of Adhesive Electrode
adh_area = pi*Radh^2;
Dsn_size =
[1,adh_area;1,1;2,2;2,2;4/3,4/3;2,2;2,2;5/3,5/3;2,2;2,2;2,2;2,2;2,2;7/3,7/3;8/3,8/3;3,3;10/3,1
0/3];
Dsn_area = prod(Dsn_size,2);        %Designed Area
Mfr_size =
[1,adh_area;1/2,1;2/3,4/3;2/3,4/3;1/2,4/3;2/3,4/3;2/3,4/3;1,5/3;2/3,4/3;2/3,4/3;1,2;2/3,4/3;2/
3,4/3;1,7/3;3/2,8/3;3/2,3;3/2,10/3];
Mfr_area = prod(Mfr_size,2);

Label = {'Adhesive';'Area1';'1Si'; '1St';...
     'Area2';'2Si';'2St';...
     'Area3';'3Si'; '3St';'Area4';...
     '4Si'; '4St';'Area5';'Area6';'Area7';'Area8'};
Yarnnames = {'Adhesive';'Steel';'Silver';'Steel';'Steel';'Silver';...
    'Steel';'Steel';'Silver';'Steel';'Steel';'Silver';...
    'Steel';'Steel';'Steel';'Steel';'Steel'};
Pattnames = {'Adhesive';'1/15 Sateen';'1/15 Sateen'; '1/15 Sateen';...
     '1/15 Sateen';'Broken Twill';'Broken Twill';'1/15 Sateen';...
     'Twill'; 'Twill';'1/15 Sateen';'Birdseye'; 'Birdseye';...
     '1/15 Sateen';'1/15 Sateen';'1/15 Sateen';'1/15 Sateen'};
Decoder = [Label,Yarnnames,Pattnames,num2cell(Dsn_area),num2cell(Mfr_area)];


Allnames = Label;

StichNum = 36*36;       %Number of Stiches in a square pattern
Yarnwidth = 1;        %~Ratio of yarn width to stich spacing, stitch density
AnchorNum = [0,80,80,80,80,162,162,80,216,216,80,283,283,80,80,80,80].';
FloatNum = StichNum - AnchorNum;
PatternRatio = Yarnwidth*FloatNum./StichNum;
Cnd_area = Mfr_area.*PatternRatio;      %Conductive Surface Area

%% ========== Adhesive Values ==========
% Adhesive Values
Rs = 1e3;               %(ohm) Impedance of Electrolyte (Approximation)
Cd = 5.8e-6;            %(F) Capacitance of Electrode
Rd = 25.9e3;            %(Ohm) Resistance of Electrode
Ce = 0.9e-6;            %(F) Capacitance of Epidermis
Re = 35.2e3;            %(Ohm) Resistance of Epidermis
Rop = 1e6;              %(Ohm) Impedance of Opamp (ECG100C Specification) 2Mohm/2
R2 = 2.6e3;             %(Ohms) DC term without Electrolyte Approximation Rlead+Ru


Cdfit1 = Cdfit/1e6;     %Convert CdFit from uF to F
Rdfit1 = Rdfit*1e6;     %Convert Rdfit from MOhms to Ohms
Rsfit1 = Rsfit*1e6;     %Convert Rsfit from MOhmz to Ohms
Cdfit1(1) = Cd;         %Adding Adhesive to List
Rdfit1(1) = Rd;         %Adding Adhesive to List
```

```
Rsfit1(1) = Rs;          %Adding Adhesive to List
R3 = R2+Rsfit1;          %(Ohms) Rs+Rl+Ru, DC impedance Term
w= 2*pi*25;              %Frequency of operation

a0 = ones(size(Rsfit1));
a1 = (Re.*Ce+Rdfit1.*Cdfit1);
a2 = Cdfit1.*Ce.*Rdfit1.*Re;
b0 = R3 + Rdfit1 + Re;
b1 = R3.*(Re.*Ce+Cdfit1.*Rdfit1)+Rdfit1.*Re.*(Cdfit1+Ce);
b2 = R3.*Cdfit1.*Ce.*Rdfit1.*Re;
num = [(1i*w)^2,1i*w,1].*[b2,b1,b0];
den = [(1i*w)^2,1i*w,1].*[a2,a1,a0];

Zfit = sum(num,2)./sum(den,2);

%% ========== Area Plot ==========
[Dsn_area(ixArea),Mfr_area(ixArea),Cnd_area(ixArea)];
ixPlot = ixArea;

tname = ' at 25Hz'
fig3 = figure(30);

subplot(1,2,1)
title(['Z_e Magnitude',tname])
ylabel('Resistance (MOhms)');
xlabel('Area (in^2)'); ylim([0,50])
grid on;hold on;
% plot(Dsn_area(ixPlot),abs(Zfit(ixPlot))/1e6,'xr','Linewidth',2,'DisplayName','Design area')
plot(Mfr_area(ixPlot),abs(Zfit(ixPlot))/1e6,mkr,'Linewidth',2,'DisplayName','No SNR')
% plot(Cnd_area(ixPlot),abs(Zfit(ixPlot))/1e6,'sb','Linewidth',2,'DisplayName','Conduc area')
% legend('show','Location','ne')

subplot(1,2,2)
title(['Z_e Phase',tname])
ylabel('Angle (deg)');xlabel('Area (in^2)')
grid on;hold on;ylim([-10,0])
% plot(Dsn_area(ixPlot),angle(Zfit(ixPlot))*180/pi,'xr','Linewidth',2,'DisplayName','Design
area')
plot(Mfr_area(ixPlot),angle(Zfit(ixPlot))*180/pi,mkr,'Linewidth',2,'DisplayName','Manufr
Area')
% plot(Cnd_area(ixPlot),angle(Zfit(ixPlot))*180/pi,'sb','Linewidth',2,'DisplayName','Conduc
area')
% legend('show','Location','ne')

fig3.Position = [220,400,1050,400];

%% ========== Area Plot CdRdRs ==========
xname = 'Area (in^2)';
fig31 = figure(31);
subplot(1,3,1)
title('Cd')
ylabel('Capacitance (nF)'); ylim([0,30])
grid on;hold on;
plot(Mfr_area(ixPlot),Cdfit(ixPlot)*1e3,mkr,'Linewidth',2)
xlabel(xname)
% set(gca,'xtick',xvar,'xticklabel',Allnames(ixPlot))
% xlim([0,length(ixPlot)+1])

subplot(1,3,2)
title('Rd')
ylabel('Resistance (MOhms)');ylim([0,50])
```

```
grid on;hold on;
plot(Mfr_area(ixPlot),Rdfit(ixPlot),mkr,'Linewidth',2)
xlabel(xname)
% set(gca,'xtick',xvar,'xticklabel',Allnames(ixPlot))
% xlim([0,length(ixPlot)+1])

subplot(1,3,3)
title('Rs')
ylabel('Resistance (MOhms)');ylim([0,50])
grid on;hold on;
plot(Mfr_area(ixPlot),Rsfit(ixPlot),mkr,'Linewidth',2)
xlabel(xname)
% set(gca,'xtick',xvar,'xticklabel',Allnames(ixPlot))
% xlim([0,length(ixPlot)+1])

fig31.Position = [220,400,1050,400]

%% ========== Pattern Plot ==========

tname = sprintf(' @ %dHz',w/2/pi);
xname = 'Conductive Area (in^2)';
ixPatt1 = [3,6,9,12];                    %Silver Pattern Indexes
ixPatt2 = [4,7,10,13];                   %Steel Pattern Indexes
iP = [ixPatt1,ixPatt2];
% symtyp = ['or';'ob';'xr';'xb';'sr';'sb';'dr';'db'];
symtyp = ['or';'xr';'sr';'dr';'ob';'xb';'sb';'db';'or'];
% symtyp = ['.b';'.b';'.b';'.b';'.b';'.b';'.b';'.b';'.b'];
fig40 = figure(40);
s1= subplot(1,2,1);
title(['Z_e Magnitude',tname])
ylabel('Resistance (MOhms)'); ylim([0,50])
grid on;hold on;
xlabel(xname); xlim([.65,0.85])
% legend('show','Location','ne')

s2 = subplot(1,2,2);
title(['Z_e Phase',tname])
ylabel('Angle (deg)'); ylim([-10,0])
grid on;hold on;
xlabel(xname); xlim([.65,0.9])

for kk = 1:length(iP)

plot(s1,Cnd_area(iP(kk)),abs(Zfit(iP(kk)))/1e6,symtyp(kk,:),'Linewidth',2,'DisplayName',Label{
iP(kk)})

plot(s2,Cnd_area(iP(kk)),angle(Zfit(iP(kk)))*180/pi,symtyp(kk,:),'Linewidth',2,'DisplayName',L
abel{iP(kk)})
end
legend(s1,'show','Location','ne')
legend(s2,'show','Location','ne')
fig40.Position = [220,400,1050,400]

%% ========== Pattern Plot CdRdRs ==========
ixPlot = iP;
fig41 = figure(41);
s1 = subplot(1,3,1);
title('Cd')
ylabel('Capacitance (nF)'); ylim([0,30])
grid on;hold on;
xlabel(xname); xlim([.65,0.9])
```

```
s2 = subplot(1,3,2);
title('Rd')
ylabel('Resistance (MOhms)');ylim([0,50])
grid on;hold on;
xlabel(xname); xlim([.65,0.9])

s3 = subplot(1,3,3);
title('Rs')
ylabel('Resistance (MOhms)');ylim([0,50])
grid on;hold on;
xlabel(xname); xlim([.65,0.9])

for kk = 1:length(iP)

plot(s1,Cnd_area(iP(kk)),Cdfit(iP(kk))*1e3,symtyp(kk,:),'Linewidth',2,'DisplayName',Label{iP(k
k)})

plot(s2,Cnd_area(iP(kk)),Rdfit(iP(kk)),symtyp(kk,:),'Linewidth',2,'DisplayName',Label{iP(kk)})

plot(s3,Cnd_area(iP(kk)),Rsfit(iP(kk)),symtyp(kk,:),'Linewidth',2,'DisplayName',Label{iP(kk)})
end
legend(s1,'show','Location','ne')
legend(s2,'off','Location','ne')
legend(s3,'show','Location','ne')
fig41.Position = [220,400,1050,400]
```

Leave1Out.m

```
% (6) This script will run through the methodology for a single subject and electrode

clc;clear;close all;
load('ECG_Metrics6.mat');
savefitname = 'Leave1out_1.mat';

subjs = [1,2,4,6,8,9];          %Subjects to be considered
RMSE = zeros(16,length(subjs));

%% Make Adhesive Transfer Function
% "Detrmination of the parameters of the skin-electrode Impedance Model for ECG Measurement"
% "By: Assambo, Baba, Dozio and Burke".
Ce = 0.9e-6;        %(F) Capacitance of Epidermis
Re = 35.2e3;        %(Ohm) Resistance of Epidermis
Rop = 1e6;          %(Ohm) Impedance of Opamp (ECG100C Specification) 2Mohm/2
R3 = 3.6e3;         %(Ohms) Rs+Rl+Ru, DC impedance Term
Rs = 1e3;           %(ohm) Impedance of Electrolyte (Approximation)
R2 = R3-Rs;         %(Ohms) DC term without Electrolyte
Cd = 5.8e-6;        %(F) Capacitance of Electrode
Rd = 25.9e3;        %(Ohm) Resistance of Electrode

skinparams = [Ce,Re,Rop,R2];    %Skin Parameters
elecparams = [Cd,Rd,Rs];        %[Farads, Ohms, Ohms] Electrode Parameters
TFadh = GenTFdouble(elecparams,skinparams); %Adhesive Transfer function

%% Make ECG transfer function with Adhesive Electrode
Gain = 2000;        %(Linear) Gain of Amplifier Biodomadix
Amp  = tf(Gain,1);  %Transfer Function of Amplifier

TFecgA = Amp*TFadh;  %Transfer function of Adhesive ECG system
iTFecgA = 1/TFecgA;   %Inverse Transfer Function of Adhesive ECG system

%% Optimizer Values
```

```
Cmax = .1;                  %uFarads
Rdmax = 50;                 %Mohms
Rsmax = 50;                 %Mohms
ub = [Cmax,Rdmax,Rsmax];    %uFarad,MOhm,MOhm [Upper Boudns]
lb = 1e-4*[Cd/1e-6,Rd/1e6,Rs/1e6]; %lower bound is .1% of adhesive Values
optmcnt = 10;               %Number of times to run the optimizer

valsfit = zeros(length(subjs),17,4);  %Initialize Variable to save optimized Parameters
tic
for nn = 1:length(subjs)            %Step through each subject
    subout = subjs(nn);             %subject left out, of the fit
    ixsubout = subjs(nn) == subjs;  %index of subjects left out
    subin = subjs(~ixsubout);       %The remaining subjects included
    for ee = 2:17
        fprintf('Fit for Electrode ID %d, Subout ID %d\n',ee,subout)
        %Determine the parameters for this electrode, fit across subjects
        [bestfit,cost] = DetermParams(optmcnt,ub,lb,skinparams,ee,subin,iTFecgA,ECGdata);
        valsfit(nn,ee,:) = [bestfit,cost];  %Save betsfits into a values matrix

        % ===== Calculate the RMS Error for the excluded subject =====
        TFelec = GenTFdouble(bestfit.*[1e-6,1e6,1e6],skinparams);   %Transfer Functio of
Electrode
        TFecgE = TFelec*Amp;
        Vmeas = ECGdata(subout,ee).Vmean;
        Vadh = ECGdata(subout,ee).Vmean;
        Tadh = ECGdata(subout,1).Tmean;
        t = Tadh-min(Tadh);
        Vsig = lsim(iTFecgA,Vadh,t);
        Vsim = lsim(TFecgE,Vsig,t);
        del = abs(Vmeas-Vsim);      % I dont think RMSE is what she wants
        RMSD(ee-1,nn) = sqrt(sum((mean(del)-del).^2)/length(del));
        RMSE(ee-1,nn) = sqrt(sum((Vmeas-Vsim).^2)/length(Vmeas));
    end
    fprintf('%d Done\n',subout)

end
Metric = sqrt(mean(RMSE,2));
save(savefitname,'Metric');
toc
```

B. Measured versus Simulated Waveforms

A depiction of the simulated waveforms overlayed with the measured waveforms is provided for all 96 waveforms. The simulated mean ECG waveforms were created using the best fit parameters across all subjects which passed the SNR criteria. The title of each subplot expresses the subject, the electrode type label, the SNR expressed in decibels and Pks representing the number of waveforms that went into generating the mean measured waveform.

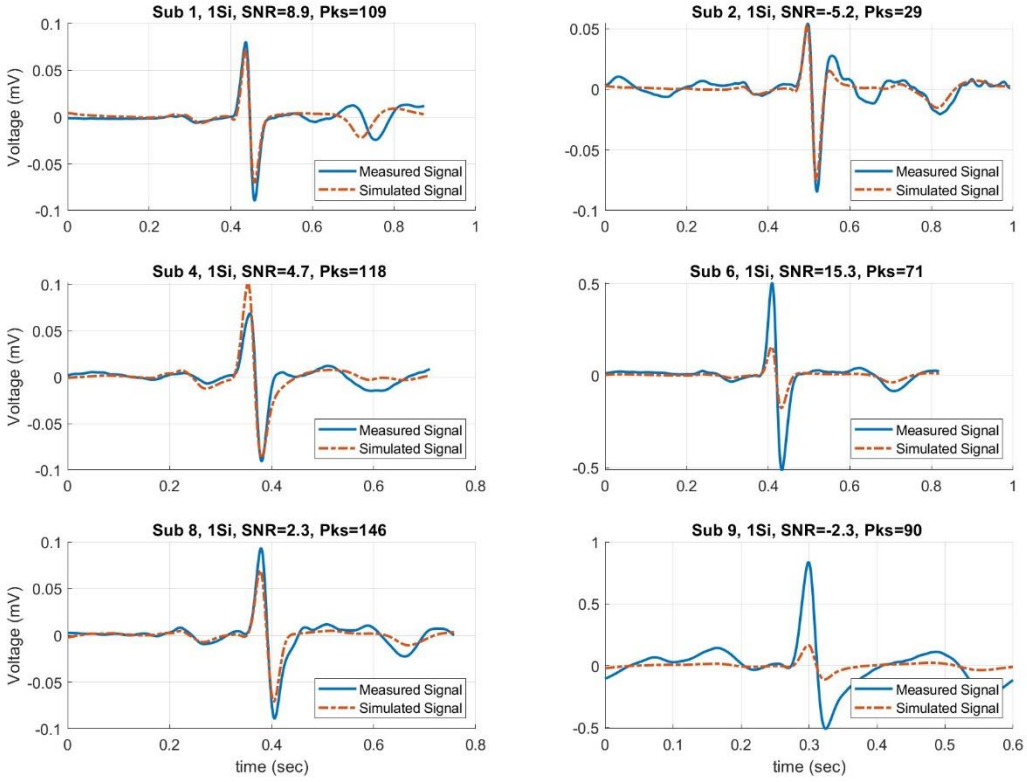
Sub 1, 1Si, SNR=8.9, Pks=109
Sub 2, 1Si, SNR=-5.2, Pks=29
Sub 4, 1Si, SNR=4.7, Pks=118
Sub 6, 1Si, SNR=15.3, Pks=71
Sub 8, 1Si, SNR=2.3, Pks=146
Sub 9, 1Si, SNR=-2.3, Pks=90
Voltage (mV)
time (sec)
Measured Signal
Simulated Signal

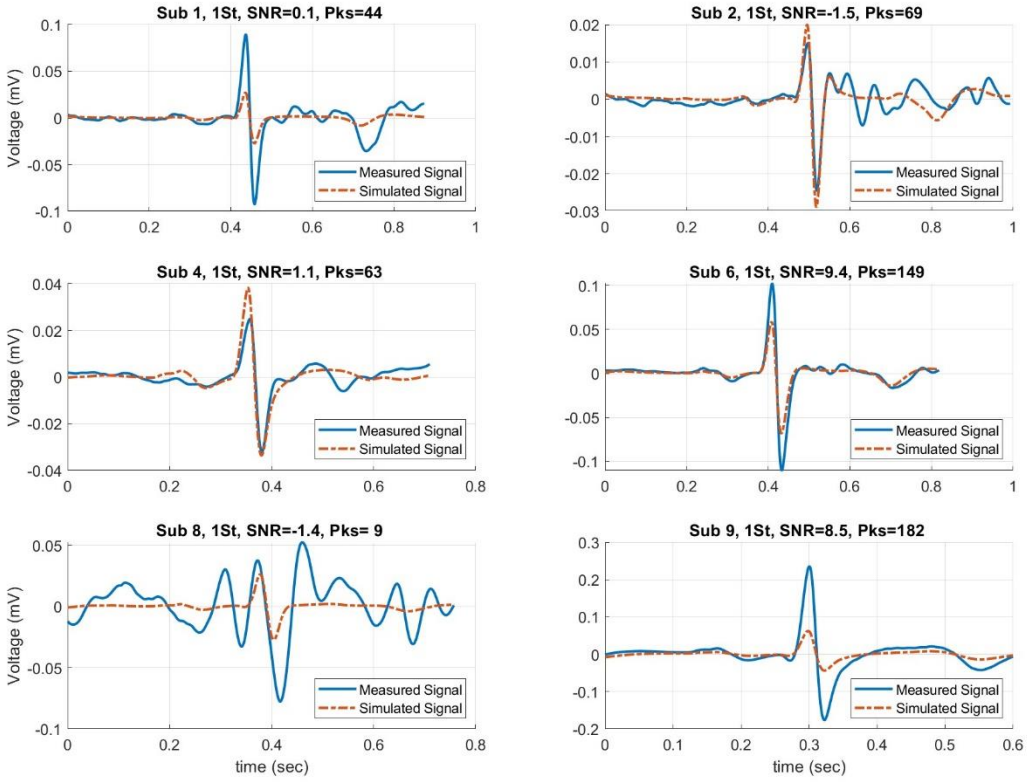
Sub 1, 1St, SNR=0.1, Pks=44
Sub 2, 1St, SNR=-1.5, Pks=69
Sub 4, 1St, SNR=1.1, Pks=63
Sub 6, 1St, SNR=9.4, Pks=149
Sub 8, 1St, SNR=-1.4, Pks= 9
Sub 9, 1St, SNR=8.5, Pks=182
Voltage (mV)
time (sec)
Measured Signal
Simulated Signal

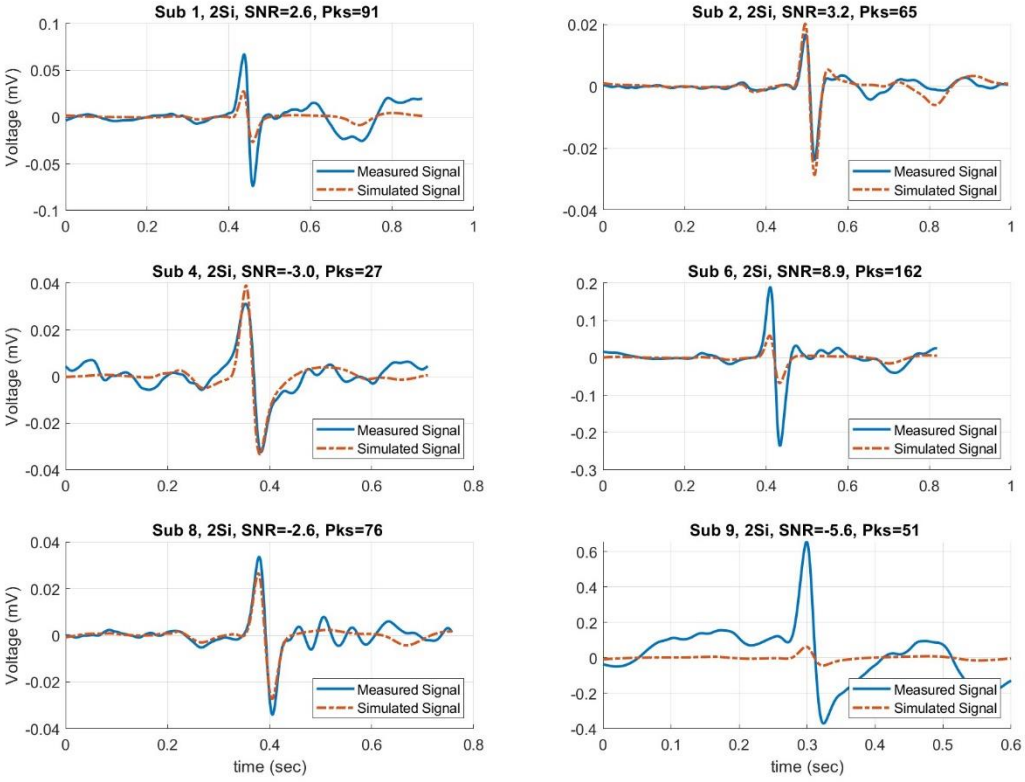
Sub 1, 2Si, SNR=2.6, Pks=91
Sub 2, 2Si, SNR=3.2, Pks=65
Sub 4, 2Si, SNR=-3.0, Pks=27
Sub 6, 2Si, SNR=8.9, Pks=162
Sub 8, 2Si, SNR=-2.6, Pks=76
Sub 9, 2Si, SNR=-5.6, Pks=51
Measured Signal
Simulated Signal
Voltage (mV)
time (sec)

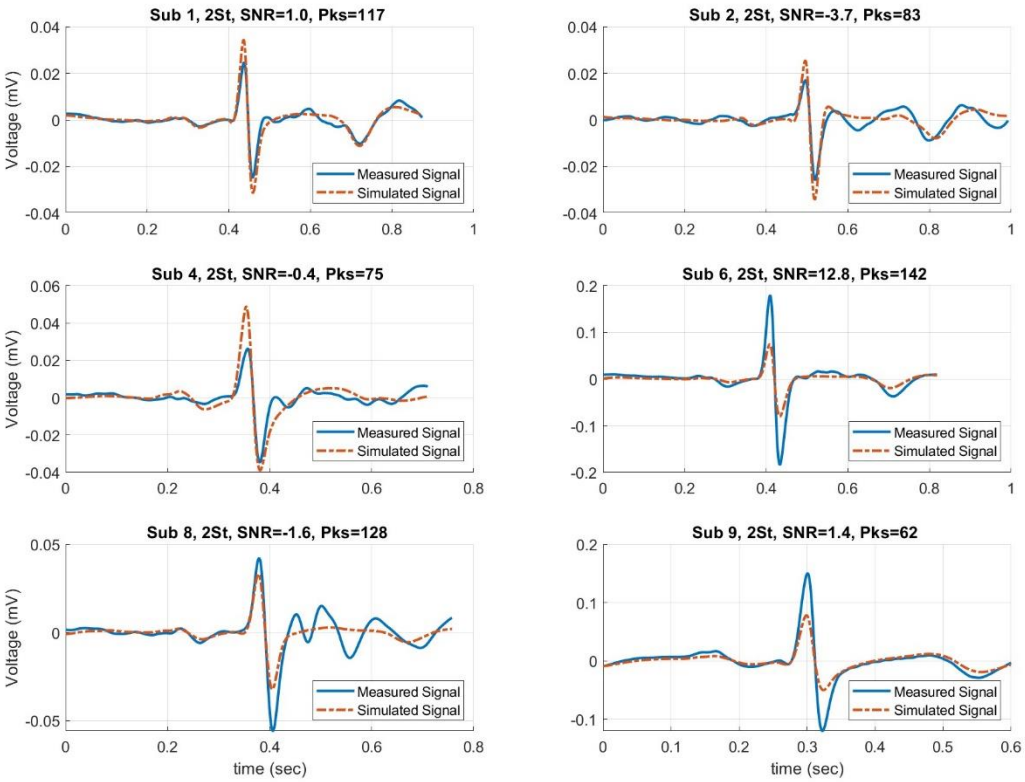
Sub 1, 2St, SNR=1.0, Pks=117
Sub 2, 2St, SNR=-3.7, Pks=83
Sub 4, 2St, SNR=-0.4, Pks=75
Sub 6, 2St, SNR=12.8, Pks=142
Sub 8, 2St, SNR=-1.6, Pks=128
Sub 9, 2St, SNR=1.4, Pks=62
Measured Signal
Simulated Signal
Voltage (mV)
time (sec)

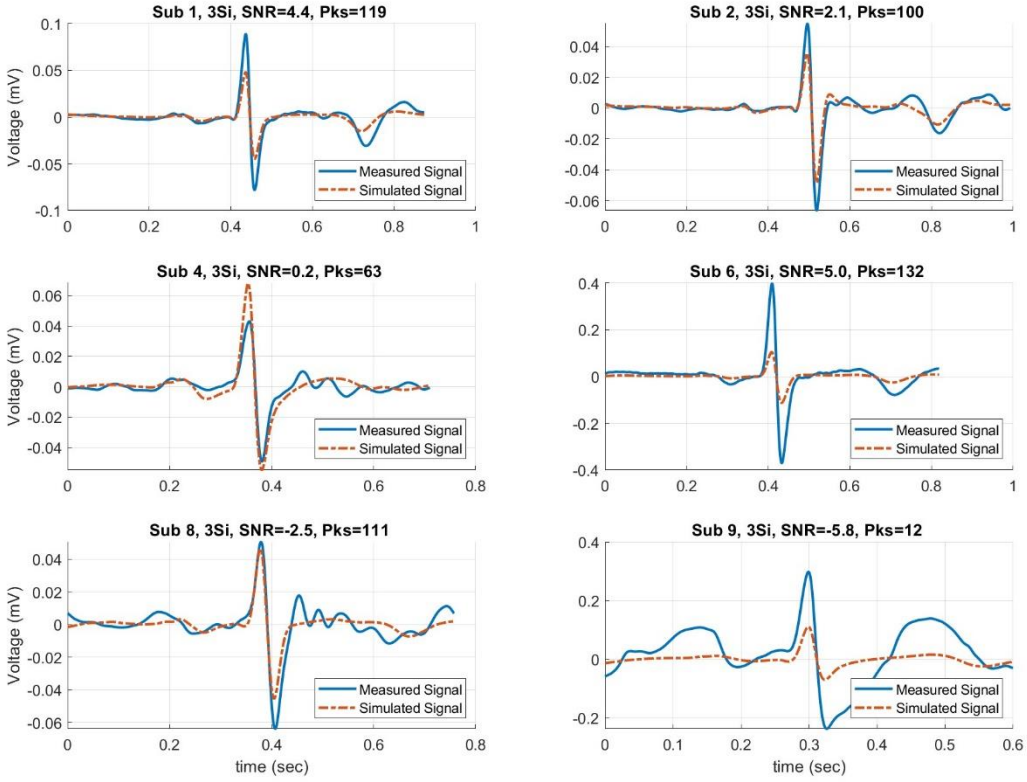
Sub 1, 3Si, SNR=4.4, Pks=119
Sub 2, 3Si, SNR=2.1, Pks=100
Sub 4, 3Si, SNR=0.2, Pks=63
Sub 6, 3Si, SNR=5.0, Pks=132
Sub 8, 3Si, SNR=-2.5, Pks=111
Sub 9, 3Si, SNR=-5.8, Pks=12
Measured Signal
Simulated Signal
Voltage (mV)
time (sec)

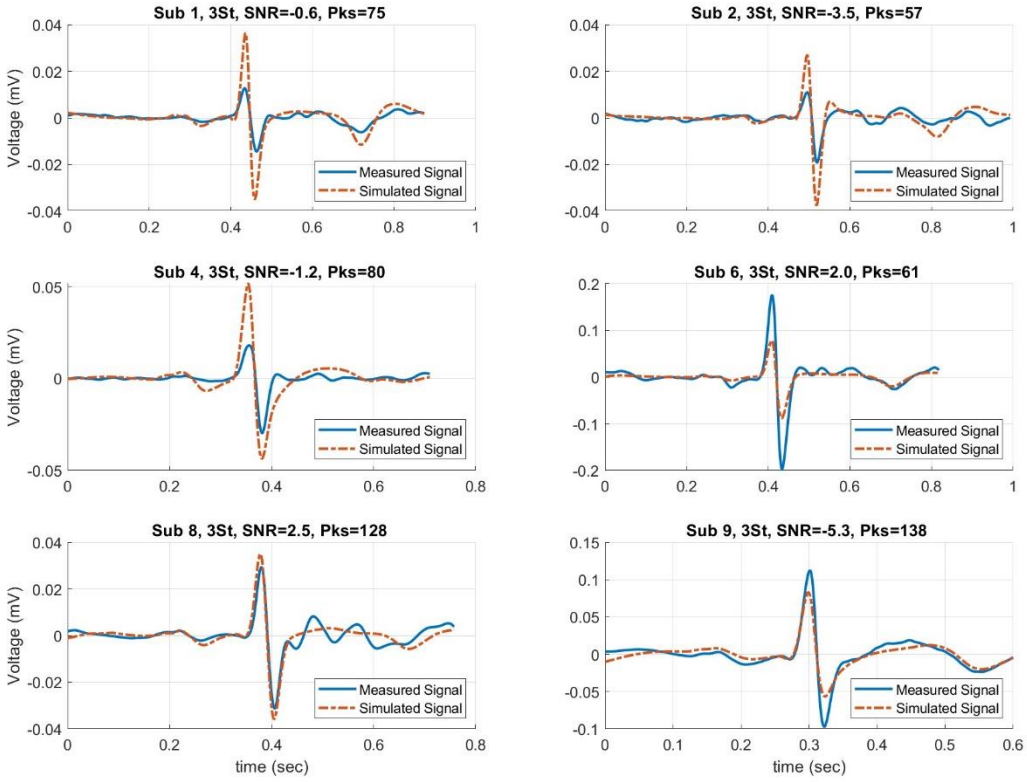
Sub 1, 3St, SNR=-0.6, Pks=75
Sub 2, 3St, SNR=-3.5, Pks=57
Sub 4, 3St, SNR=-1.2, Pks=80
Sub 6, 3St, SNR=2.0, Pks=61
Sub 8, 3St, SNR=2.5, Pks=128
Sub 9, 3St, SNR=-5.3, Pks=138
Measured Signal
Simulated Signal
Voltage (mV)
time (sec)

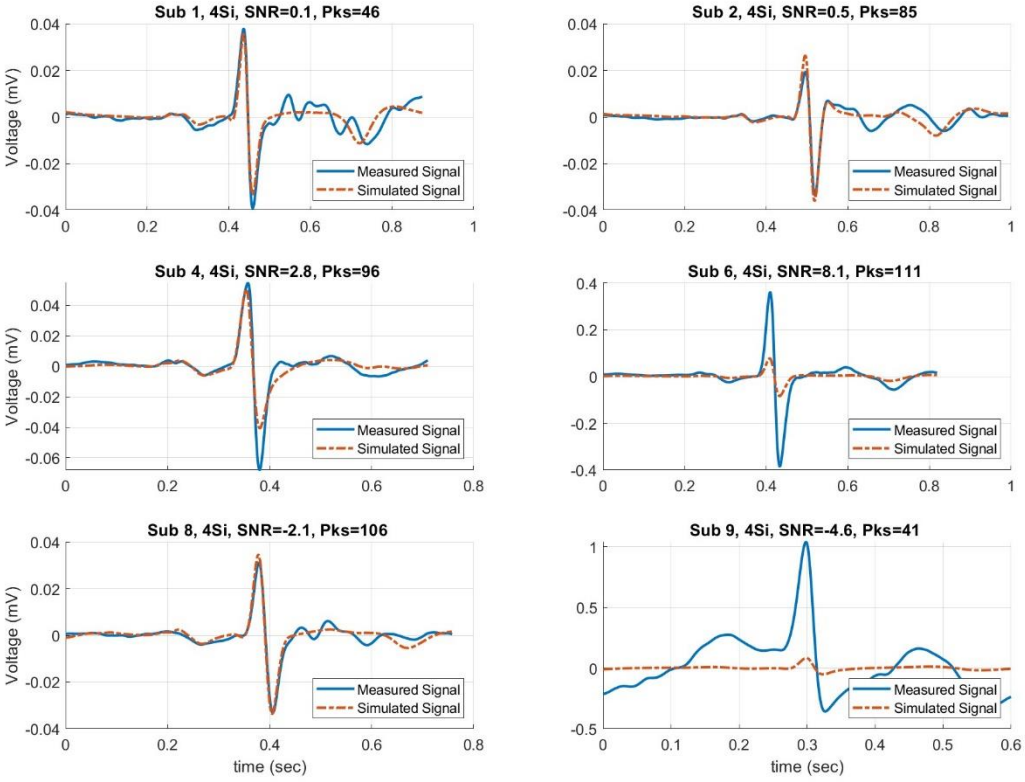
Sub 1, 4Si, SNR=0.1, Pks=46
Sub 2, 4Si, SNR=0.5, Pks=85
Sub 4, 4Si, SNR=2.8, Pks=96
Sub 6, 4Si, SNR=8.1, Pks=111
Sub 8, 4Si, SNR=-2.1, Pks=106
Sub 9, 4Si, SNR=-4.6, Pks=41
Voltage (mV)
time (sec)
Measured Signal
Simulated Signal

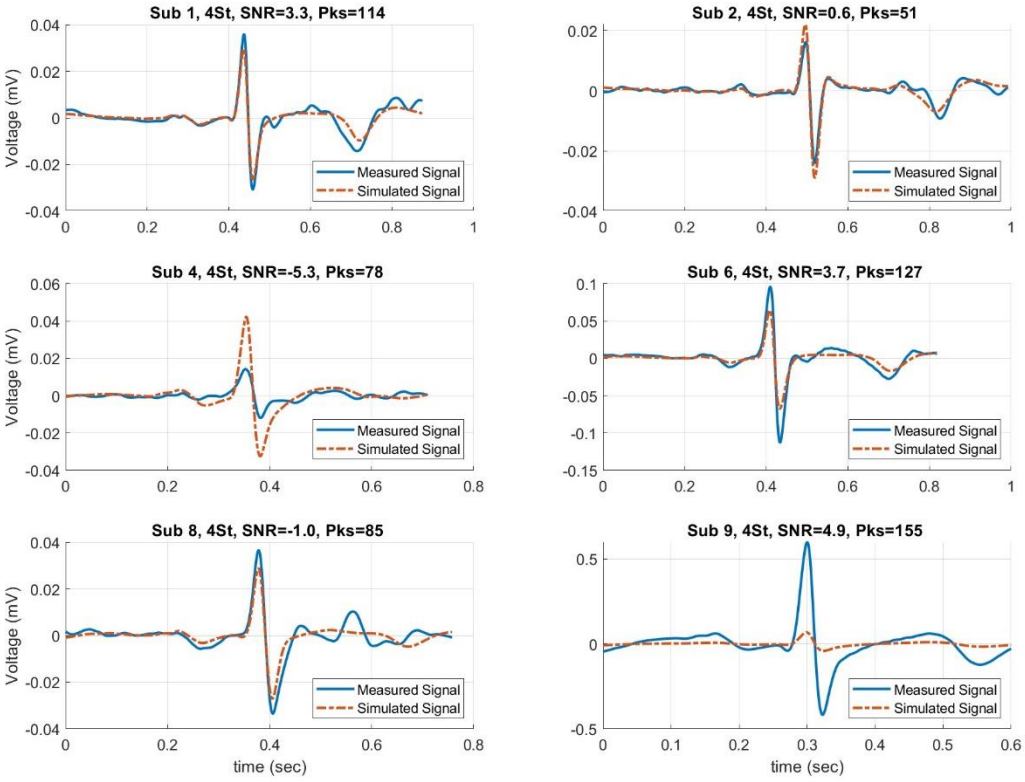
Sub 1, 4St, SNR=3.3, Pks=114
Sub 2, 4St, SNR=0.6, Pks=51
Sub 4, 4St, SNR=-5.3, Pks=78
Sub 6, 4St, SNR=3.7, Pks=127
Sub 8, 4St, SNR=-1.0, Pks=85
Sub 9, 4St, SNR=4.9, Pks=155
Voltage (mV)
time (sec)
Measured Signal
Simulated Signal

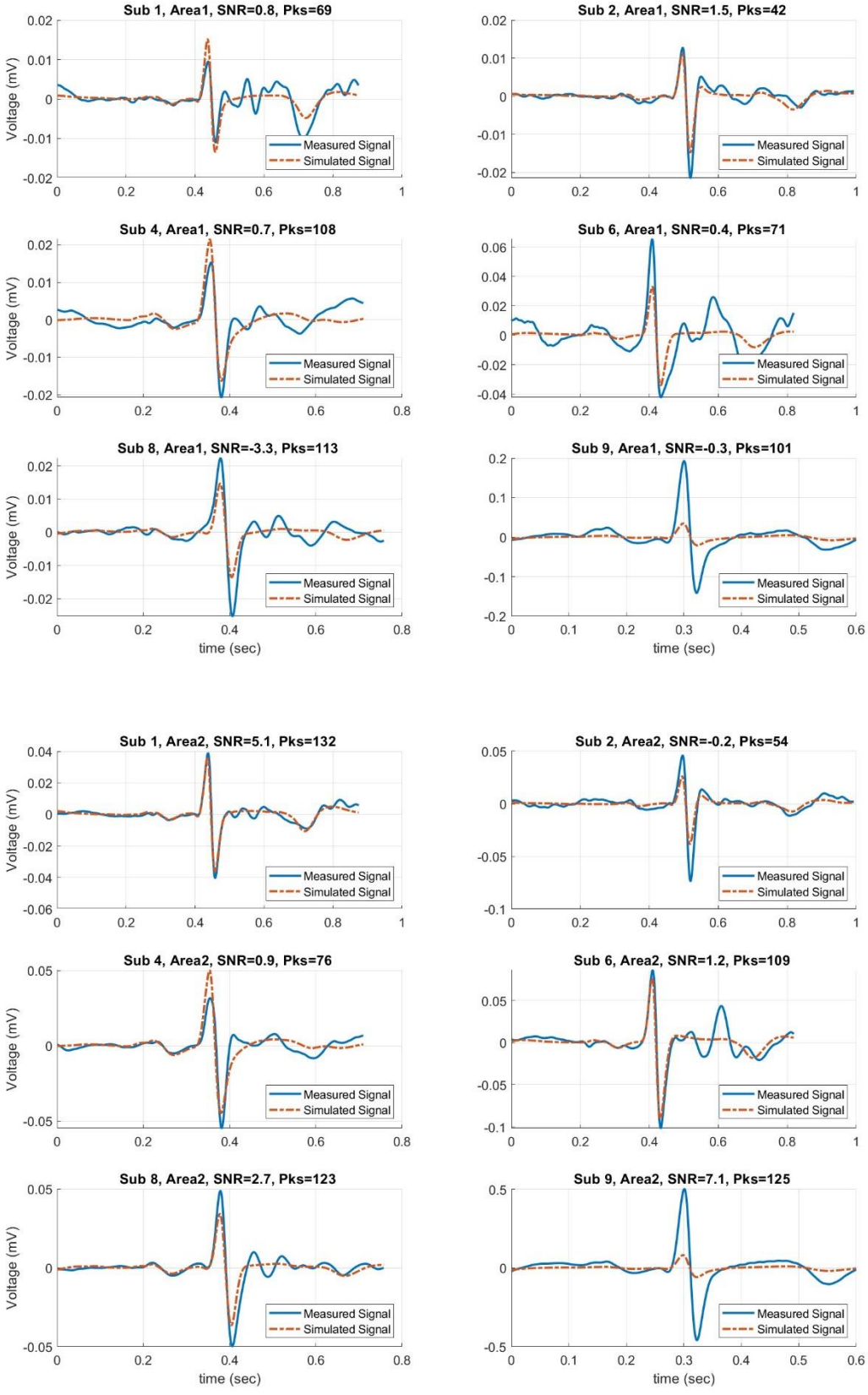
Sub 1, Area1, SNR=0.8, Pks=69
Sub 2, Area1, SNR=1.5, Pks=42
Sub 4, Area1, SNR=0.7, Pks=108
Sub 6, Area1, SNR=0.4, Pks=71
Sub 8, Area1, SNR=-3.3, Pks=113
Sub 9, Area1, SNR=-0.3, Pks=101
Sub 1, Area2, SNR=5.1, Pks=132
Sub 2, Area2, SNR=-0.2, Pks=54
Sub 4, Area2, SNR=0.9, Pks=76
Sub 6, Area2, SNR=1.2, Pks=109
Sub 8, Area2, SNR=2.7, Pks=123
Sub 9, Area2, SNR=7.1, Pks=125
Voltage (mV)
time (sec)
Measured Signal
Simulated Signal

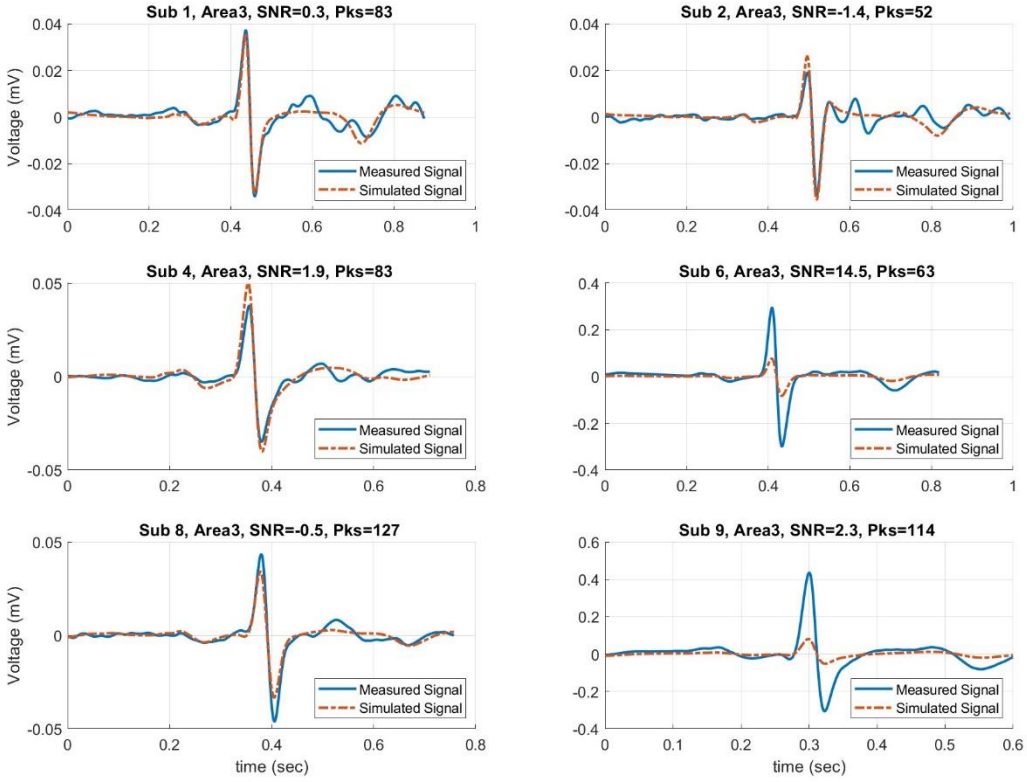
Sub 1, Area3, SNR=0.3, Pks=83
Sub 2, Area3, SNR=-1.4, Pks=52
Sub 4, Area3, SNR=1.9, Pks=83
Sub 6, Area3, SNR=14.5, Pks=63
Sub 8, Area3, SNR=-0.5, Pks=127
Sub 9, Area3, SNR=2.3, Pks=114
Voltage (mV)
time (sec)
Measured Signal
Simulated Signal

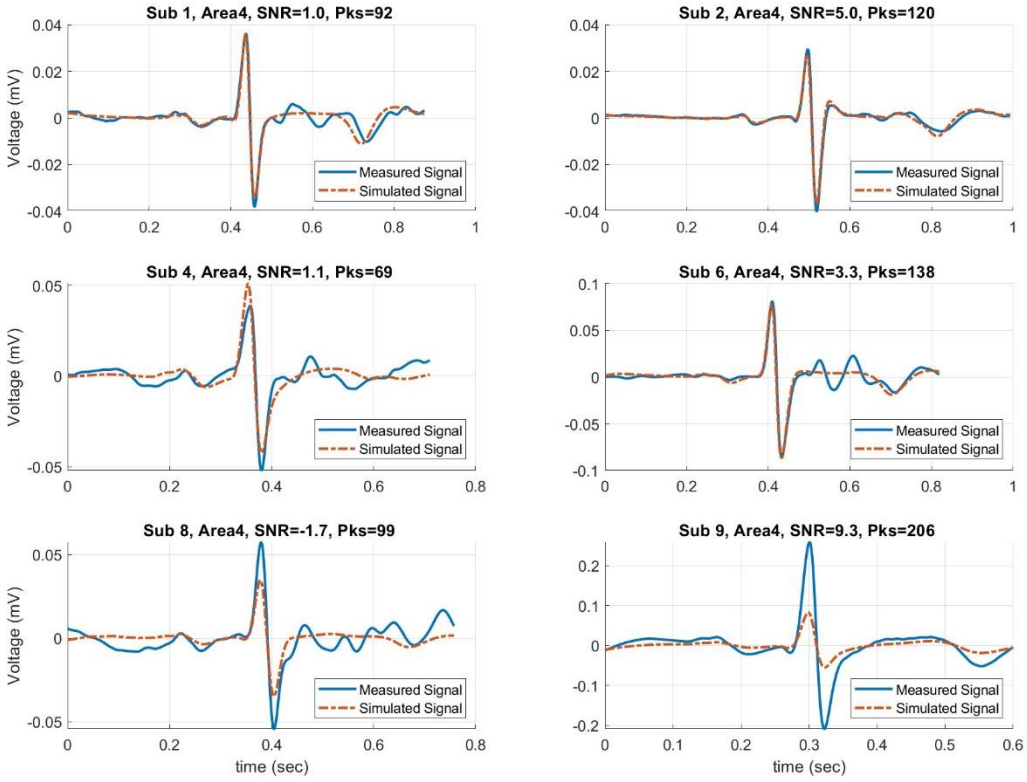
Sub 1, Area4, SNR=1.0, Pks=92
Sub 2, Area4, SNR=5.0, Pks=120
Sub 4, Area4, SNR=1.1, Pks=69
Sub 6, Area4, SNR=3.3, Pks=138
Sub 8, Area4, SNR=-1.7, Pks=99
Sub 9, Area4, SNR=9.3, Pks=206
Voltage (mV)
time (sec)
Measured Signal
Simulated Signal

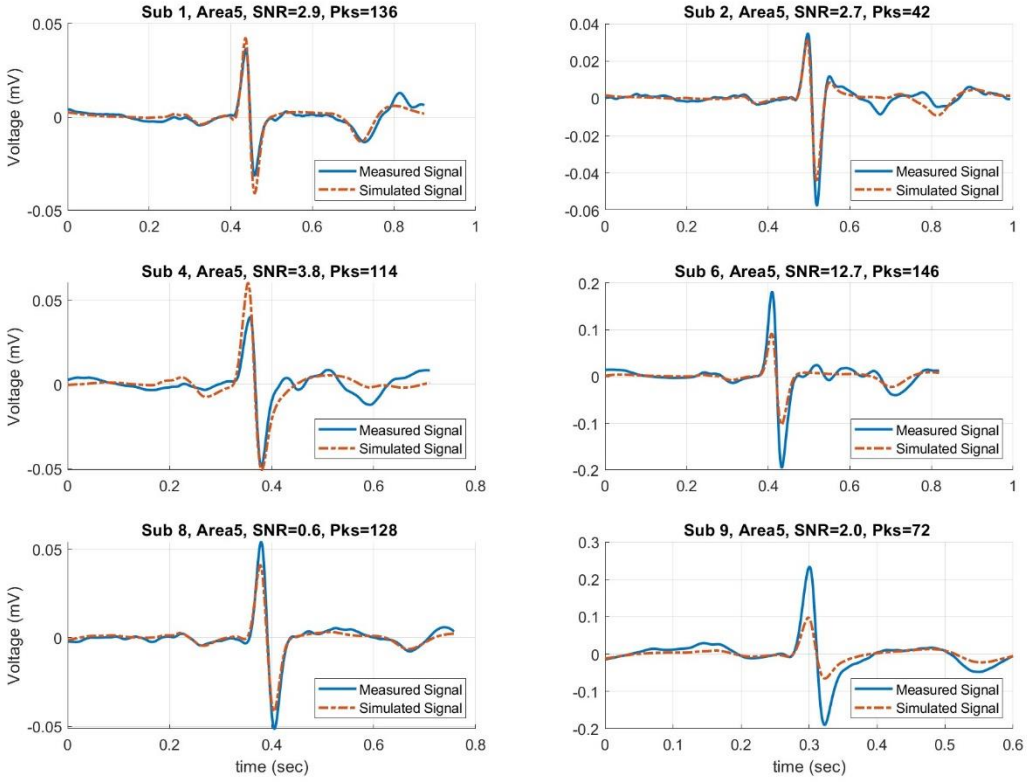
Sub 1, Area5, SNR=2.9, Pks=136
Sub 2, Area5, SNR=2.7, Pks=42
Sub 4, Area5, SNR=3.8, Pks=114
Sub 6, Area5, SNR=12.7, Pks=146
Sub 8, Area5, SNR=0.6, Pks=128
Sub 9, Area5, SNR=2.0, Pks=72
Voltage (mV)
time (sec)
Measured Signal
Simulated Signal

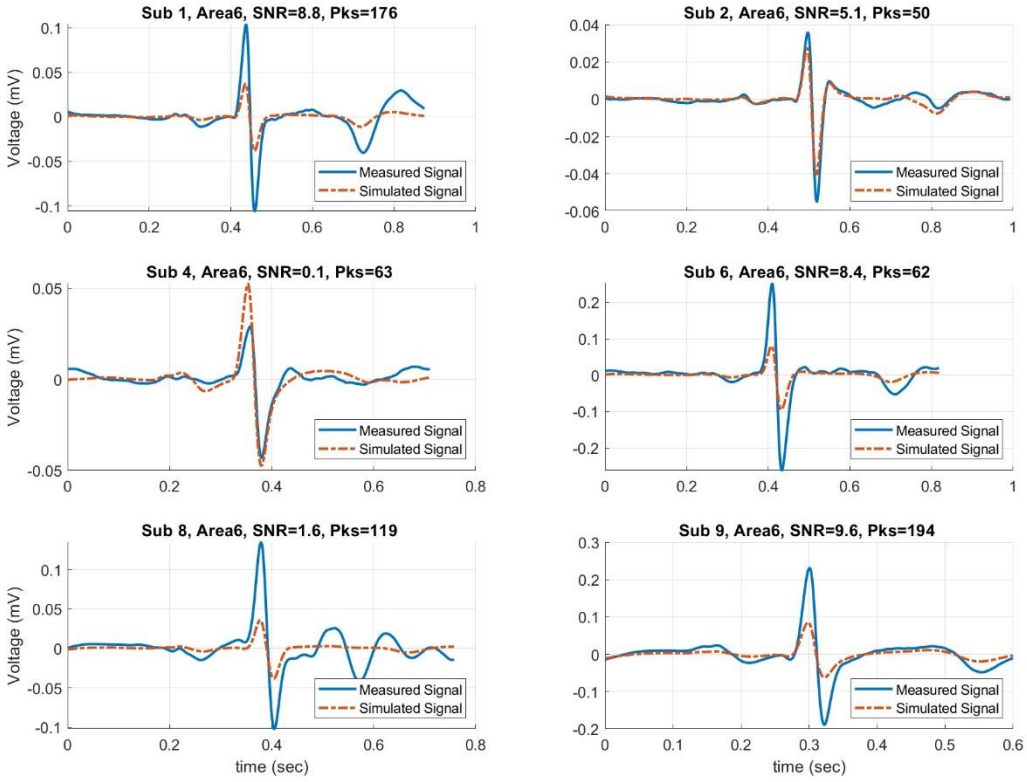
Sub 1, Area6, SNR=8.8, Pks=176
Sub 2, Area6, SNR=5.1, Pks=50
Sub 4, Area6, SNR=0.1, Pks=63
Sub 6, Area6, SNR=8.4, Pks=62
Sub 8, Area6, SNR=1.6, Pks=119
Sub 9, Area6, SNR=9.6, Pks=194
Voltage (mV)
time (sec)
Measured Signal
Simulated Signal

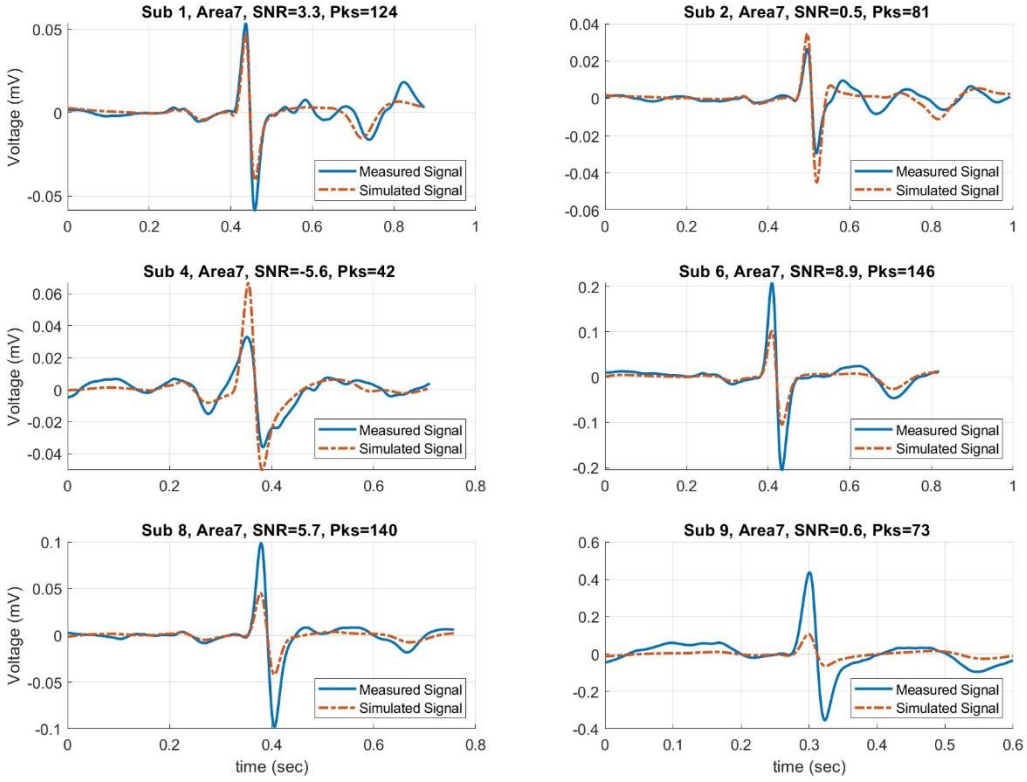
Sub 1, Area7, SNR=3.3, Pks=124
Sub 2, Area7, SNR=0.5, Pks=81
Sub 4, Area7, SNR=-5.6, Pks=42
Sub 6, Area7, SNR=8.9, Pks=146
Sub 8, Area7, SNR=5.7, Pks=140
Sub 9, Area7, SNR=0.6, Pks=73
Voltage (mV)
time (sec)
Measured Signal
Simulated Signal

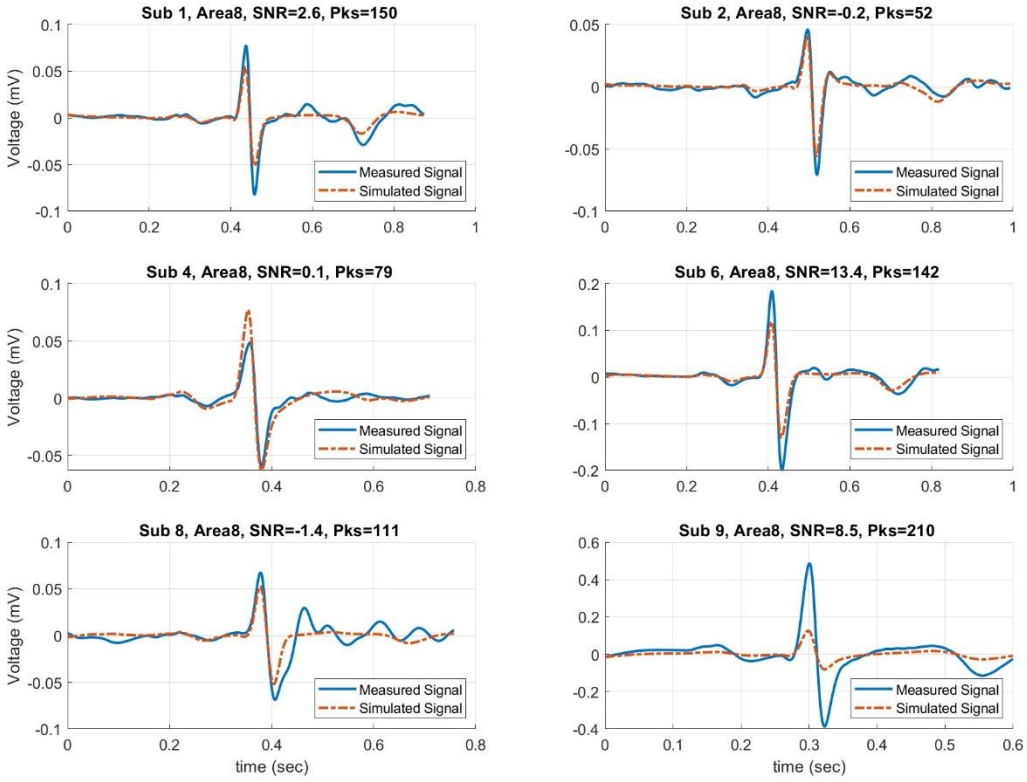
Sub 1, Area8, SNR=2.6, Pks=150
Sub 2, Area8, SNR=-0.2, Pks=52
Sub 4, Area8, SNR=0.1, Pks=79
Sub 6, Area8, SNR=13.4, Pks=142
Sub 8, Area8, SNR=-1.4, Pks=111
Sub 9, Area8, SNR=8.5, Pks=210
Voltage (mV)
time (sec)
Measured Signal
Simulated Signal

C. Bode Plots for ECG Systems with Woven Electrodes

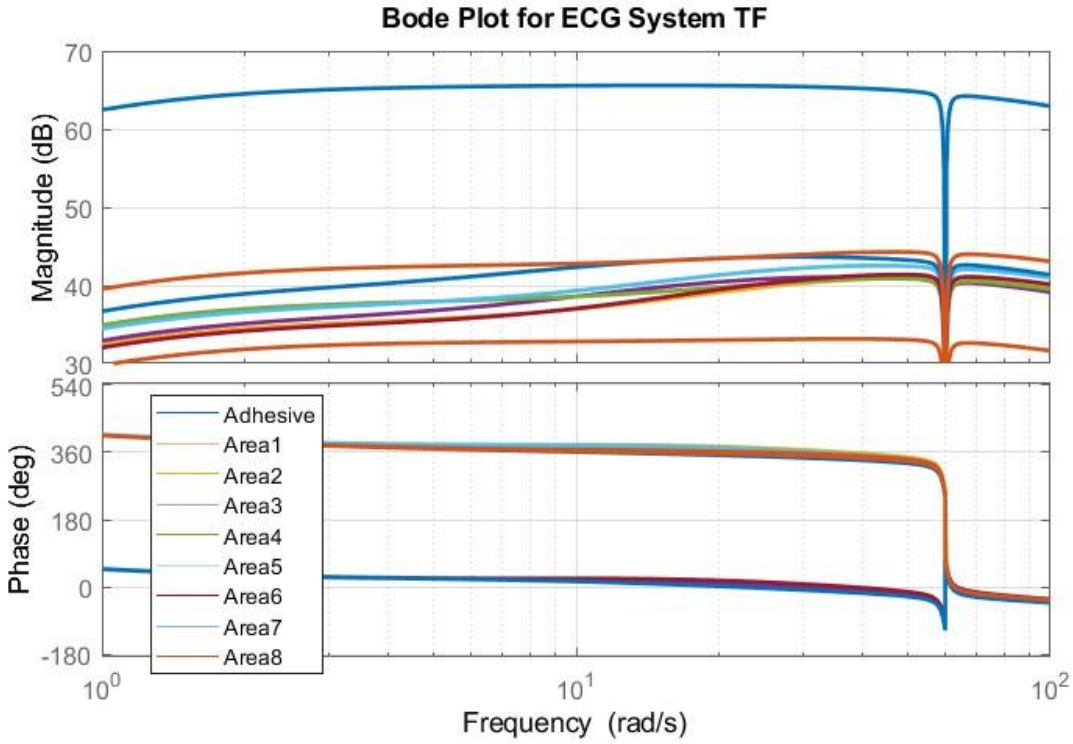

The magnitude of the ECG system has a slight high pass filtering behavior, but is overall dominated by approximately 30dB of attenuation relative to the adhesive electrode. There is also about 20 deg of phase delay between the input and output voltage at 25Hz. There is a 360-degree phase shift for a couple of the data sets, this is an artefact of MATLAB's plotting function failing to unwrap phase.

D. Circuit Parameters fit during the LOOCV

Below are the circuit parameters that were fit during the leave one out cross validation. Each highlighted cell represents the subjects which were not included in the fit. Since the subject was not included in the fit the circuit parameter is constant for a given row for those excluded subjects. The same criteria were used: SNR > 0dB and number of peaks > 30. The mean and standard deviation are given for each row of data.

Table 9: Parameter Cd fit during the LOOCV with the corresponding standard deviation and Mean

	Cd fit of excluded subject (nF)							
Label	1	2	4	6	8	9	Standard Deviation	Mean
Area1	1.9	6.7	13.6	2	2.6	2.6	4.624	4.900
Area2	3.7	4	9.2	3.4	3.5	3.9	2.257	4.617
Area3	5.7	7.6	14.7	6.7	7.6	7.5	3.222	8.300
Area4	5	4.5	7.7	4.5	5.1	4.9	1.211	5.283
Area5	5.5	6.5	11.6	5.8	6	6.2	2.311	6.933
Area6	3.7	3.8	12.4	3.7	3.8	3.9	3.520	5.217
Area7	18.2	22.7	17.9	14.2	18.9	17.9	2.715	18.300
Area8	6.2	7.1	22.3	5.7	7.1	6.8	6.441	9.200
1Si	8.8	9	20.7	8.1	6.9	9	5.101	10.417
2Si	3.5	17.4	4.5	3.8	4.5	4.5	5.422	6.367
3Si	6.6	6	75.8	6.9	7.7	7.7	28.103	18.450
4Si	5	6.6	7.6	5.6	6.1	6.1	0.887	6.167
1St	2.7	3.1	11.1	2.5	3.1	2.9	3.372	4.233
2St	11	8.9	8.9	7.3	8.9	9	1.176	9.000
3St	6.5	6.5	6.5	4.8	16.4	6.5	4.235	7.867
4St	9.4	11.6	9.7	9.5	9.7	9.5	0.841	9.900

Table 10: Parameter Rd fit during the LOOCV with the corresponding Standard Deviation and Mean

	Rd fit of excluded subject (MOhm)							
Label	1	2	4	6	8	9	Standard Deviation	Mean
Area1	28.49	50.00	50.00	13.47	10.20	10.20	19.013	27.062
Area2	21.51	19.93	8.76	38.98	21.86	20.38	9.702	21.904
Area3	11.43	16.67	11.64	29.14	16.67	19.37	6.502	17.487
Area4	13.75	13.94	6.06	11.35	10.90	10.95	2.850	11.158
Area5	16.19	16.17	11.65	18.29	14.70	14.87	2.205	15.311
Area6	26.47	24.78	9.41	27.30	25.47	23.96	6.712	22.900
Area7	6.51	3.65	8.80	14.17	8.43	8.35	3.452	8.318
Area8	7.44	5.40	2.57	6.85	5.40	5.62	1.684	5.546
1Si	13.51	6.15	1.61	7.65	6.79	6.15	3.831	6.976
2Si	34.21	50.00	44.46	50.00	44.46	44.46	5.768	44.600
3Si	8.33	9.41	1.05	7.41	5.98	5.98	2.925	6.359
4Si	12.66	6.32	5.88	9.54	8.81	8.81	2.450	8.669
1St	32.65	21.71	3.09	36.70	21.71	23.55	11.666	23.233
2St	3.81	50.00	50.00	50.00	50.00	50.00	18.858	42.301

3St	50.00	50.00	50.00	50.00	8.58	50.00	16.910	43.096
4St	11.65	50.00	21.34	22.24	21.34	21.72	13.023	24.714

Table 11: Parameter Rs fit during the LOOCV with the corresponding Standard Deviation and Mean

	Rs fit of excluded subject (MOhm)							
Label	1	2	4	6	8	9	Standard Deviation	Mean
Area1	31.67	39.84	34.19	35.74	34.69	34.69	2.676	35.137
Area2	13.32	13.17	11.26	13.52	13.70	13.51	0.909	13.081
Area3	14.37	14.48	10.46	15.99	14.48	15.24	1.922	14.169
Area4	13.55	13.56	12.97	13.26	13.50	14.01	0.347	13.472
Area5	10.71	12.03	9.93	12.06	11.70	11.88	0.868	11.385
Area6	13.22	13.27	6.96	13.20	12.92	13.04	2.523	12.101
Area7	11.79	6.21	11.06	12.05	11.98	11.60	2.268	10.783
Area8	9.41	8.49	5.12	9.28	8.49	8.97	1.602	8.296
1Si	6.43	6.14	4.59	6.64	6.37	6.14	0.739	6.051
2Si	20.86	5.65	18.28	20.70	18.28	18.28	5.697	17.006
3Si	10.95	11.02	5.92	10.76	10.03	10.03	1.945	9.785
4Si	14.33	10.53	14.92	14.62	13.99	13.99	1.610	13.730
1St	19.36	17.65	8.11	19.76	17.65	18.71	4.381	16.874
2St	6.44	15.11	15.11	17.21	15.11	16.68	3.945	14.276
3St	13.74	13.74	13.74	17.09	5.92	13.74	3.714	12.993
4St	18.74	12.25	17.89	19.76	17.89	18.28	2.651	17.468